NOAA Technical Report NESDIS 142-6

Regional Climate Trends and Scenarios for the U.S. National Climate Assessment

Part 6. Climate of the Northwest U.S.

Washington, D.C.
January 2013

U.S. DEPARTMENT OF COMMERCE
National Oceanic and Atmospheric Administration
National Environmental Satellite, Data, and Information Service

NOAA TECHNICAL REPORTS

National Environmental Satellite, Data, and Information Service

The National Environmental Satellite, Data, and Information Service (NESDIS) manages the Nation's civil Earth-observing satellite systems, as well as global national data bases for meteorology, oceanography, geophysics, and solar-terrestrial sciences. From these sources, it develops and disseminates environmental data and information products critical to the protection of life and property, national defense, the national economy, energy development and distribution, global food supplies, and the development of natural resources.

Publication in the NOAA Technical Report series does not preclude later publication in scientific journals in expanded or modified form. The NESDIS series of NOAA Technical Reports is a continuation of the former NESS and EDIS series of NOAA Technical Reports and the NESC and EDS series of Environmental Science Services Administration (ESSA) Technical Reports.

Copies of earlier reports may be available by contacting NESDIS Chief of Staff, NOAA/ NESDIS, 1335 East-West Highway, SSMC1, Silver Spring, MD 20910, (301) 713-3578.

NOAA Technical Report NESDIS 142-6

Regional Climate Trends and Scenarios for the U.S. National Climate Assessment

Part 6. Climate of the Northwest U.S.

Kenneth E. Kunkel, Laura E. Stevens, Scott E. Stevens, and Liqiang Sun
Cooperative Institute for Climate and Satellites (CICS), North Carolina State University and NOAA's National Climatic Data Center (NCDC)
Asheville, NC

Emily Janssen and Donald Wuebbles
University of Illinois at Urbana-Champaign
Champaign, IL

Kelly T. Redmond
Western Regional Climate Center, Desert Research Institute
Reno, NV

J. Greg Dobson
National Environmental Modeling and Analysis Center
University of North Carolina at Asheville
Asheville, NC

U.S. DEPARTMENT OF COMMERCE
Rebecca Blank, Acting Secretary

National Oceanic and Atmospheric Administration
Dr. Jane Lubchenco, Under Secretary of Commerce for Oceans and Atmosphere and NOAA Administrator

National Environmental Satellite, Data, and Information Service
Mary Kicza, Assistant Administrator

PREFACE

This document is one of series of regional climate descriptions designed to provide input that can be used in the development of the National Climate Assessment (NCA). As part of a sustained assessment approach, it is intended that these documents will be updated as new and well-vetted model results are available and as new climate scenario needs become clear. It is also hoped that these documents (and associated data and resources) are of direct benefit to decision makers and communities seeking to use this information in developing adaptation plans.

There are nine reports in this series, one each for eight regions defined by the NCA, and one for the contiguous U.S. The eight NCA regions are the Northeast, Southeast, Midwest, Great Plains, Northwest, Southwest, Alaska, and Hawai‘i/Pacific Islands.

These documents include a description of the observed historical climate conditions for each region and a set of climate scenarios as plausible futures – these components are described in more detail below.

While the datasets and simulations in these regional climate documents are not, by themselves, new, (they have been previously published in various sources), these documents represent a more complete and targeted synthesis of historical and plausible future climate conditions around the specific regions of the NCA.

There are two components of these descriptions. One component is a description of the historical climate conditions in the region. The other component is a description of the climate conditions associated with two future pathways of greenhouse gas emissions.

Historical Climate

The description of the historical climate conditions was based on an analysis of core climate data (the data sources are available and described in each document). However, to help understand, prioritize, and describe the importance and significance of different climate conditions, additional input was derived from climate experts in each region, some of whom are authors on these reports. In particular, input was sought from the NOAA Regional Climate Centers and from the American Association of State Climatologists. The historical climate conditions are meant to provide a perspective on what has been happening in each region and what types of extreme events have historically been noteworthy, to provide a context for assessment of future impacts.

Future Scenarios

The future climate scenarios are intended to provide an internally consistent set of climate conditions that can serve as inputs to analyses of potential impacts of climate change. The scenarios are not intended as projections as there are no established probabilities for their future realization. They simply represent an internally consistent climate picture using certain assumptions about the future pathway of greenhouse gas emissions. By “consistent” we mean that the relationships among different climate variables and the spatial patterns of these variables are derived directly from the same set of climate model simulations and are therefore physically plausible.

These future climate scenarios are based on well-established sources of information. No new climate model simulations or downscaled data sets were produced for use in these regional climate reports.

The use of the climate scenario information should take into account the following considerations:

1. All of the maps of climate variables contain information related to statistical significance of changes and model agreement. This information is crucial to appropriate application of the information. Three types of conditions are illustrated in these maps:
    a. The first condition is where most or all of the models simulate statistically significant changes and agree on the direction (whether increasing or decreasing) of the change. If this condition is present, then analyses of future impacts and vulnerabilities can more confidently incorporate this direction of change. It should be noted that the models may still produce a significant range of magnitude associated with the change, so the manner of incorporating these results into decision models will still depend to a large degree on the risk tolerance of the impacted system.
    b. The second condition is where the most or all of the models simulate changes that are too small to be statistically significant. If this condition is present, then assessment of impacts should be conducted on the basis that the future conditions could represent a small change from present or could be similar to current conditions and that the normal year-to-year fluctuations in climate dominate over any underlying long-term changes.
    c. The third condition is where most or all of the models simulate statistically significant changes but do not agree on the direction of the change, i.e. a sizeable fraction of the models simulate increases while another sizeable fraction simulate decreases. If this condition is present, there is little basis for a definitive assessment of impacts, and, separate assessments of potential impacts under an increasing scenario and under a decreasing scenario would be most prudent.
2. The range of conditions produced in climate model simulations is quite large. Several figures and tables provide quantification for this range. Impacts assessments should consider not only the mean changes, but also the range of these changes.
3. Several graphics compare historical observed mean temperature and total precipitation with model simulations for the same historical period. These should be examined since they provide one basis for assessing confidence in the model simulated future changes in climate.
    a. Temperature Changes: Magnitude. In most regions, the model simulations of the past century simulate the magnitude of change in temperature from observations; the southeast region being an exception where the lack of century-scale observed warming is not simulated in any model.
    b. Temperature Changes: Rate. The *rate* of warming over the last 40 years is well simulated in all regions.
    c. Precipitation Changes: Magnitude. Model simulations of precipitation generally simulate the overall observed trend but the observed decade-to-decade variations are greater than the model observations.

In general, for impacts assessments, this information suggests that the model simulations of temperature conditions for these scenarios are likely reliable, but users of precipitation simulations may want to consider the likelihood of decadal-scale variations larger than simulated by the models. It should also be noted that accompanying these documents will be a web-based resource with downloadable graphics, metadata about each, and more information and links to the datasets and overall descriptions of the process.

1. INTRODUCTION

The Global Change Research Act of 1990[1] mandated that national assessments of climate change be prepared not less frequently than every four years. The last national assessment was published in 2009 (Karl et al. 2009). To meet the requirements of the act, the Third National Climate Assessment (NCA) report is now being prepared. The National Climate Assessment Development and Advisory Committee (NCADAC), a federal advisory committee established in the spring of 2011, will produce the report. The NCADAC Scenarios Working Group (SWG) developed a set of specifications with regard to scenarios to provide a uniform framework for the chapter authors of the NCA report.

This climate document was prepared to provide a resource for authors of the Third National Climate Assessment report, pertinent to the states of Washington, Oregon, and Idaho; hereafter referred to collectively as the Northwest. The specifications of the NCADAC SWG, along with anticipated needs for historical information, guided the choices of information included in this description of Northwest climate. While guided by these specifications, the material herein is solely the responsibility of the authors and usage of this material is at the discretion of the 2013 NCA report authors.

This document has two main sections: one on historical conditions and trends, and the other on future conditions as simulated by climate models. The historical section concentrates on temperature and precipitation, primarily based on analyses of data from the National Weather Service's (NWS) Cooperative Observer Network, which has been in operation since the late 19th century. Additional climate features are discussed based on the availability of information. The future simulations section is exclusively focused on temperature and precipitation.

With regard to the future, the NCADAC, at its May 20, 2011 meeting, decided that scenarios should be prepared to provide an overall context for assessment of impacts, adaptation, and mitigation, and to coordinate any additional modeling used in synthesizing or analyzing the literature. Scenario information for climate, sea-level change, changes in other environmental factors (such as land cover), and changes in socioeconomic conditions (such as population growth and migration) have been prepared. This document provides an overall description of the climate information.

In order to complete this document in time for use by the NCA report authors, it was necessary to restrict its scope in the following ways. Firstly, this document does not include a comprehensive description of all climate aspects of relevance and interest to a national assessment. We restricted our discussion to climate conditions for which data were readily available. Secondly, the choice of climate model simulations was also restricted to readily available sources. Lastly, the document does not provide a comprehensive analysis of climate model performance for historical climate conditions, although a few selected analyses are included.

The NCADAC directed the "use of simulations forced by the A2 emissions scenario as the primary basis for the high climate future and by the B1 emissions scenario as the primary basis for the low climate future for the 2013 report" for climate scenarios. These emissions scenarios were generated by the Intergovernmental Panel on Climate Change (IPCC) and are described in the IPCC Special Report on Emissions Scenarios (SRES) (IPCC 2000). These scenarios were selected because they

[1] http://thomas.loc.gov/cgi-bin/bdquery/z?d101:SN00169:|TOM:/bss/d101query.html

incorporate much of the range of potential future human impacts on the climate system and because there is a large body of literature that uses climate and other scenarios based on them to evaluate potential impacts and adaptation options. These scenarios represent different narrative storylines about possible future social, economic, technological, and demographic developments. These SRES scenarios have internally consistent relationships that were used to describe future pathways of greenhouse gas emissions. The A2 scenario "describes a very heterogeneous world. The underlying theme is self-reliance and preservation of local identities. Fertility patterns across regions converge very slowly, which results in continuously increasing global population. Economic development is primarily regionally oriented and per capita economic growth and technological change are more fragmented and slower than in the other storylines" (IPCC 2000). The B1 scenario describes "a convergent world with…global population that peaks in mid-century and declines thereafter…but with rapid changes in economic structures toward a service and information economy, with reductions in material intensity, and the introduction of clean and resource-efficient technologies. The emphasis is on global solutions to economic, social, and environmental sustainability, including improved equity, but without additional climate initiatives" (IPCC 2000).

The temporal changes of emissions under these two scenarios are illustrated in Fig. 1 (left panel). Emissions under the A2 scenario continually rise during the 21st century from about 40 gigatons (Gt) CO_2-equivalent per year in the year 2000 to about 140 Gt CO_2-equivalent per year by 2100. By contrast, under the B1 scenario, emissions rise from about 40 Gt CO_2-equivalent per year in the year 2000 to a maximum of slightly more than 50 Gt CO_2-equivalent per year by mid-century, then falling to less than 30 Gt CO_2-equivalent per year by 2100. Under both scenarios, CO_2 concentrations rise throughout the 21st century. However, under the A2 scenario, there is an acceleration in concentration trends, and by 2100 the estimated concentration is above 800 ppm. Under the B1 scenario, the rate of increase gradually slows and concentrations level off at about 500 ppm by 2100. An increase of 1 ppm is equivalent to about 8 Gt of CO_2. The increase in concentration is considerably smaller than the rate of emissions because a sizeable fraction of the emitted CO_2 is absorbed by the oceans.

The projected CO_2 concentrations are used to estimate the effects on the earth's radiative energy budget, and this is the key forcing input used in global climate model simulations of the future. These simulations provide the primary source of information about how the future climate could evolve in response to the changing composition of the earth's atmosphere. A large number of modeling groups performed simulations of the 21st century in support of the IPCC's Fourth Assessment Report (AR4), using these two scenarios. The associated changes in global mean temperature by the year 2100 (relative to the average temperature during the late 20th century) are about +6.5°F (3.6°C) under the A2 scenario and +3.2°F (1.8°C) under the B1 scenario with considerable variations among models (Fig. 1, right panel).

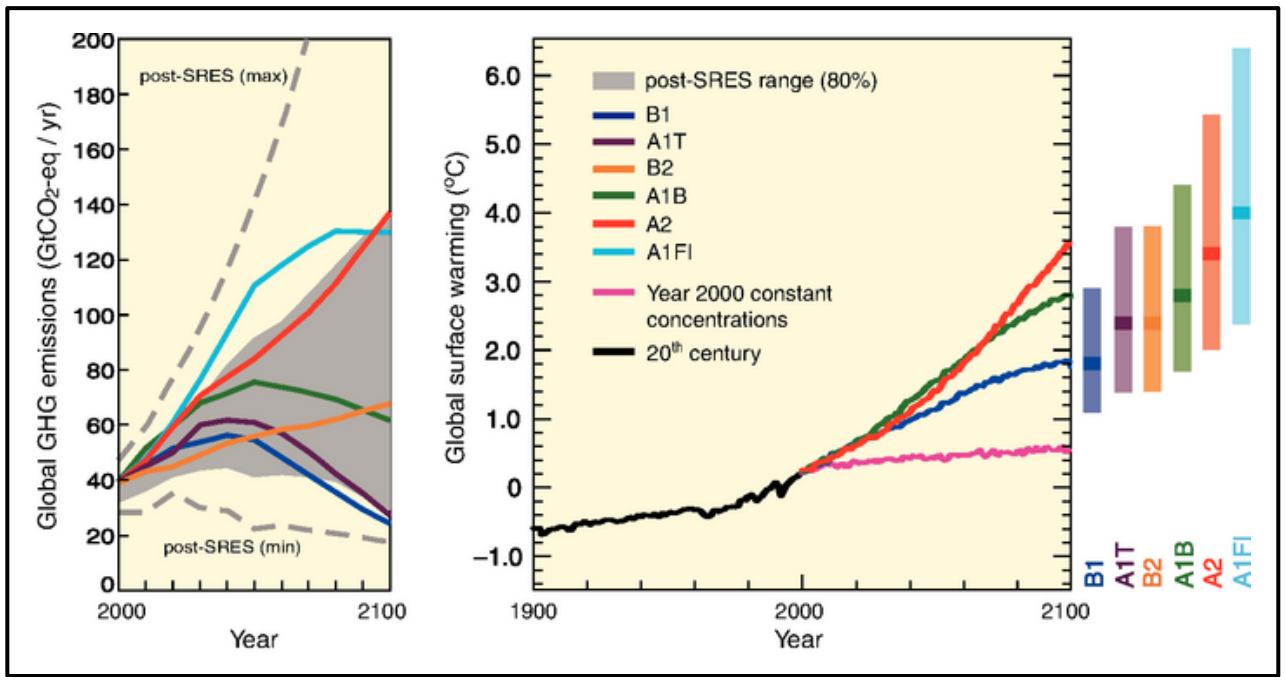

Figure 1. Left Panel: Global GHG emissions (in $GtCO_2$-eq) in the absence of climate policies: six illustrative SRES marker scenarios (colored lines) and the 80th percentile range of recent scenarios published since SRES (post-SRES) (gray shaded area). Dashed lines show the full range of post-SRES scenarios. The emissions include CO_2, CH_4, N_2O and F-gases. Right Panel: Solid lines are multi-model global averages of surface warming for scenarios A2, A1B and B1, shown as continuations of the 20th-century simulations. These projections also take into account emissions of short-lived GHGs and aerosols. The pink line is not a scenario, but is for Atmosphere-Ocean General Circulation Model (AOGCM) simulations where atmospheric concentrations are held constant at year 2000 values. The bars at the right of the figure indicate the best estimate (solid line within each bar) and the likely range assessed for the six SRES marker scenarios at 2090-2099. All temperatures are relative to the period 1980-1999. From IPCC AR4, Sections 3.1 and 3.2, Figures 3.1 and 3.2, IPCC (2007).

In addition to the direct output of the global climate model simulations, the NCADAC approved "the use of both statistically- and dynamically-downscaled data sets". "Downscaling" refers to the process of producing higher-resolution simulations of climate from the low-resolution outputs of the global models. The motivation for use of these types of data sets is the spatial resolution of global climate models. While the spatial resolution of available global climate model simulations varies widely, many models have resolutions in the range of 100-200 km (~60-120 miles). Such scales are very large compared to local and regional features important to many applications. For example, at these scales mountain ranges are not resolved sufficiently to provide a reasonably accurate representation of the sharp gradients in temperature, precipitation, and wind that typically exist in these areas.

Statistical downscaling achieves higher-resolution simulations through the development of statistical relationships between large-scale atmospheric features that are well-resolved by global models and the local climate conditions that are not well-resolved. The statistical relationships are developed by comparing observed local climate data with model simulations of the recent historical climate. These relationships are then applied to the simulations of the future to obtain local high-

resolution projections. Statistical downscaling approaches are relatively economical from a computational perspective, and thus they can be easily applied to many global climate model simulations. One underlying assumption is that the relationships between large-scale features and local climate conditions in the present climate will not change in the future (Wilby and Wigley 1997). Careful consideration must also be given when deciding how to choose the appropriate predictors because statistical downscaling is extremely sensitive to the choice of predictors (Norton et al. 2011).

Dynamical downscaling is much more computationally intensive but avoids assumptions about constant relationships between present and future. Dynamical downscaling uses a climate model, similar in most respects to the global climate models. However, the climate model is run at a much higher resolution but only for a small region of the earth (such as North America) and is termed a "regional climate model (RCM)". A global climate model simulation is needed to provide the boundary conditions (e.g., temperature, wind, pressure, and humidity) on the lateral boundaries of the region. Typically, the spatial resolution of an RCM is 3 or more times higher than the global model used to provide the boundary conditions. With this higher resolution, topographic features and smaller-scale weather phenomena are better represented. The major downside of dynamical downscaling is that a simulation for a region can take as much computer time as a global climate model simulation for the entire globe. As a result, the availability of such simulations is limited, both in terms of global models used for boundary conditions and time periods of the simulations (Hayhoe 2010).

Section 3 of this document (Future Regional Climate Scenarios) responds to the NCADAC directives by incorporating analyses from multiple sources. The core source is the set of global climate model simulations performed for the IPCC AR4, also referred to as the Climate Model Intercomparison Project phase 3 (CMIP3) suite. These have undergone extensive evaluation and analysis by many research groups. A second source is a set of statistically-downscaled data sets based on the CMIP3 simulations. A third source is a set of dynamically-downscaled simulations, driven by CMIP3 models. A new set of global climate model simulations is being generated for the IPCC Fifth Assessment Report (AR5). This new set of simulations is referred to as the Climate Model Intercomparison Project phase 5 (CMIP5). These scenarios do not incorporate any CMIP5 simulations as relatively few were available at the time the data analyses were initiated.
As noted earlier, the information included in this document is primarily concentrated around analyses of temperature and precipitation. This is explicitly the case for the future scenarios sections; due in large part to the short time frame and limited resources, we capitalized on the work of other groups on future climate simulations, and these groups have devoted a greater effort to the analysis of temperature and precipitation than other surface climate variables.

Climate models have generally exhibited a high level of ability to simulate the large-scale circulation patterns of the atmosphere. These include the seasonal progression of the position of the jet stream and associated storm tracks, the overall patterns of temperature and precipitation, the occasional occurrence of droughts and extreme temperature events, and the influence of geography on climatic patterns. There are also important processes that are less successfully simulated by models, as noted by the following selected examples.

Climate model simulation of clouds is problematic. Probably the greatest uncertainty in model simulations arises from clouds and their interactions with radiative energy fluxes (Dufresne and Bony 2008). Uncertainties related to clouds are largely responsible for the substantial range of

global temperature change in response to specified greenhouse gas forcing (Randall et al. 2007). Climate model simulation of precipitation shows considerable sensitivities to cloud parameterization schemes (Arakawa 2004). Cloud parameterizations remain inadequate in current GCMs. Consequently, climate models have large biases in simulating precipitation, particularly in the tropics. Models typically simulate too much light precipitation and too little heavy precipitation in both the tropics and middle latitudes, creating potential biases when studying extreme events (Bader et al. 2008).

Climate models also have biases in simulation of some important climate modes of variability. The El Niño-Southern Oscillation (ENSO) is a prominent example. In some parts of the U.S., El Niño and La Niña events make important contributions to year-to-year variations in conditions. Climate models have difficulty capturing the correct phase locking between the annual cycle and ENSO (AchutaRao and Sperber 2002). Some climate models also fail to represent the spatial and temporal structure of the El Niño - La Niña asymmetry (Monahan and Dai 2004). Climate simulations over the U.S. are affected adversely by these deficiencies in ENSO simulations.

The model biases listed above add additional layers of uncertainty to the information presented herein and should be kept in mind when using the climate information in this document.

The representation of the results of the suite of climate model simulations has been a subject of active discussion in the scientific literature. In many recent assessments, including AR4, the results of climate model simulations have been shown as multi-model mean maps (e.g., Figs. 10.8 and 10.9 in Meehl et al. 2007). Such maps give equal weight to all models, which is thought to better represent the present-day climate than any single model (Overland et al. 2011). However, models do not represent the current climate with equal fidelity. Knutti (2010) raises several issues about the multi-model mean approach. These include: (a) some model parameterizations may be tuned to observations, which reduces the spread of the results and may lead to underestimation of the true uncertainty; (b) many models share code and expertise and thus are not independent, leading to a reduction in the true number of independent simulations of the future climate; (c) all models have some processes that are not accurately simulated, and thus a greater number of models does not necessarily lead to a better projection of the future; and (d) there is no consensus on how to define a metric of model fidelity, and this is likely to depend on the application. Despite these issues, there is no clear superior alternative to the multi-model mean map presentation for general use. Tebaldi et al. (2011) propose a method for incorporating information about model variability and consensus. This method is adopted here where data availability make it possible. In this method, multi-model mean values at a grid point are put into one of three categories: (1) models agree on the statistical significance of changes and the sign of the changes; (2) models agree that the changes are not statistically significant; and (3) models agree that the changes are statistically significant but disagree on the sign of the changes. The details on specifying the categories are included in Section 3.

2. REGIONAL CLIMATE TRENDS AND IMPORTANT CLIMATE FACTORS

2.1. Description of Data Sources

One of the core data sets used in the United States for climate analysis is the National Weather Service's Cooperative Observer Network (COOP), which has been in operation since the late 19th century. The resulting data can be used to examine long-term trends. The typical COOP observer takes daily observations of various climate elements that might include precipitation, maximum temperature, minimum temperature, snowfall, and snow depth. While most observers are volunteers, standard equipment is provided by the National Weather Service (NWS), as well as training in standard observational practices. Diligent efforts are made by the NWS to find replacement volunteers when needed to ensure the continuity of stations whenever possible. Over a thousand of these stations have been in operation continuously for many decades (NOAA 2012a).

For examination of U.S. long-term trends in temperature and precipitation, the COOP data is the best available resource. Its central purpose is climate description (although it has many other applications as well); the number of stations is large, there have been relatively few changes in instrumentation and procedures, and it has been in existence for over 100 years. However, there are some sources of temporal inhomogeneities in station records, described as follows:

- One instrumental change is important. For much of the COOP history, the standard temperature system was a pair of liquid-in-glass (LIG) thermometers placed in a radiation shield known as the Cotton Region Shelter (CRS). In the 1980s, the NWS began replacing this system with an electronic maximum-minimum temperature system (MMTS). Inter-comparison experiments indicated that there is a systematic difference between these two instrument systems, with the newer electronic system recording lower daily maximum temperatures (T_{max}) and higher daily minimum temperatures (T_{min}) (Quayle et al. 1991; Hubbard and Lin 2006; Menne et al. 2009). Menne et al. (2009) estimate that the mean shift (going from CRS/LIG to MMTS) is -0.52K for T_{max} and +0.37K for T_{min}. Adjustments for these differences can be applied to monthly mean temperature to create homogeneous time series.
- Changes in the characteristics and/or locations of sites can introduce artificial shifts or trends in the data. In the COOP network, a station is generally not given a new name or identifier unless it moves at least 5 miles and/or changes elevation by at least 100 feet (NWS 1993). Site characteristics can change over time and affect a station's record, even if no move is involved (and even small moves << 5 miles can have substantial impacts). A common source of such changes is urbanization around the station, which will generally cause artificial warming, primarily in T_{min} (Karl et al. 1988), the magnitude of which can be several degrees in the largest urban areas. Most research suggests that the overall effect on national and global temperature trends is rather small because of the large number of rural stations included in such analyses (Karl et al. 1988; Jones et al. 1990) and because homogenization procedures reduce the urban signal (Menne et al. 2009).
- Station siting can cause biases. Recent research by Menne et al. (2010) and Fall et al. (2011) examined this issue in great detail. The effects on mean trends was found to be small in both studies, but Fall et al. (2011) found that stations with poor siting overestimate (underestimate) minimum (maximum) temperature trends.

- Changes in the time that observations are taken can also introduce artificial shifts or trends in the data (Karl et al. 1986; Vose et al. 2003). In the COOP network, typical observation times are early morning or late afternoon, near the usual times of the daily minimum and maximum temperatures. Because observations occur near the times of the daily extremes, a change in observation time can have a measurable effect on averages, irrespective of real changes. The study by Karl et al. (1986) indicates that the difference in monthly mean temperatures between early morning and late afternoon observers can be in excess of 2°C. There has, in fact, been a major shift from a preponderance of afternoon observers in the early and middle part of the 20th century to a preponderance of morning observers at the present time. In the 1930s, nearly 80% of the COOP stations were afternoon observers (Karl et al. 1986). By the early 2000s, the number of early morning observers was more than double the number of late afternoon observers (Menne et al. 2009). This shift tends to introduce an artificial cooling trend in the data.

A recent study by Williams et al. (2011) found that correction of known and estimated inhomogeneities lead to a larger warming trend in average temperature, principally arising from correction of the biases introduced by the changeover to the MMTS and from the biases introduced by the shift from mostly afternoon observers to mostly morning observers.

Much of the following analysis on temperature, precipitation, and snow is based on COOP data. For some of these analyses, a subset of COOP stations with long periods of record was used, specifically less than 10% missing data for the period of 1895-2011. The use of a consistent network is important when examining trends in order to minimize artificial shifts arising from a changing mix of stations.

2.2. General Description of Northwest Climate

The Northwest region is characterized by a highly diverse climate with large spatial variations. This is primarily caused by the interactions of the large-scale atmospheric circulation with the mountains, particularly the Coastal and Cascade Ranges. The location of this region in the heart of the mid-latitudes leads to a dominance of the mid-latitude westerlies on the climate characteristics of this region. Most of the weather is due to the west-to-east progression of extra-tropical cyclones. The north-south oriented mountain ranges cause an enhancement of precipitation on the west (upwind) side of the ranges but block the penetration of moisture into the interior of the region. The result is a very large difference in precipitation between western and eastern portions of the region. There is a strong seasonal cycle of precipitation with a prominent cool season maximum resulting from the seasonal north-south movement of the jet stream. The cool temperatures of the surface ocean waters moderate the warm season temperatures west of the Cascade Range. East of the range, which blocks the eastward movement of air affected by marine influence, summer temperatures can be much warmer. Western areas also experience moderate winter temperatures due to the effects of the ocean and blockage of Arctic air masses from the interior of Canada by the mountains to the east. Interior regions can experience much colder temperatures because of the shielding of the Cascades from the moderating marine air masses, but the Rocky Mountains shield interior regions from many of the Arctic air outbreaks that affect the northern plains. The cold season is characterized by very frequent extra-tropical cyclones, leading to many days with precipitation and cloudy conditions. The coastal regions are the wettest places in the coterminous U.S., and the

Cascade Range experiences some of the largest snowfall totals. Summers are quite dry. This region has the lowest frequency of convective storms in the coterminous U.S.

Temperatures in the Northwest are generally moderate, with mean annual values varying from near 30°F in higher mountain areas to slightly greater than 50°F in the lowland areas of the west. Large-scale patterns of annual mean temperature are shown in Fig. 2. In general, annual temperature decreases away from the coast, and upward from sea level. More detailed maps of long-term mean maximum and minimum temperature that accurately reflect topography at the 800-meter scale can be found at PRISM (2012).

Average annual precipitation (Fig. 3) exhibits an extremely large range, reflecting the effects of the western mountain ranges. Precipitation is much higher west of the crest of the Cascade Range, with peaks in the Coast Range and the west slopes of the Cascades separated by a lowland relative north-south oriented minimum. Rain is the defining feature of climate in this area, and deeply embedded in the regional culture. East of the Cascades, annual precipitation decreases very greatly and rapidly, with gradients of 5 inches per mile near Santiam Pass. Other moist areas occur in northeast Oregon (Wallowa Mountains), in the mountains of northern Idaho (about 100 inches on the Montana border), and in Montana in the Kootenai and Flathead River Basins. Low elevation values range from less than 10 inches per year in much of the eastern parts of the region to more than 150 inches per year in Washington's Olympic Peninsula. Daly et al. (2002) estimate that at least 275 inches of precipitation (and perhaps as much as 320 inches; Daly, pers. comm.) fall annually on the west slopes of Mount Olympus in Olympic National Park.

The driest areas are along the Columbia River in eastern interior Washington, with annual totals of 7-8 inches common for the recent 1981-2010 period (NCDC 2012b). High resolution maps (Fig. 3 and PRISM 2012) show the significant accentuation with elevation that occurs everywhere in the region. The seasonality of precipitation is also very notable, with the main belt of upper westerlies bringing a succession of storms in winter, and then lifting northward of the Canadian border to bring dry and pleasant, though short, summers. In more elevated terrain east of the Cascades, and in the valleys of mountainous Idaho and Montana, late spring and early summer also bring significant rain that is very beneficial for agriculture. Many locations west of the Cascades receive measurable rain on more than half the days of the year (about 200 at Astoria); east of the Cascades measurable precipitation occurs at least 70-80 days per year.

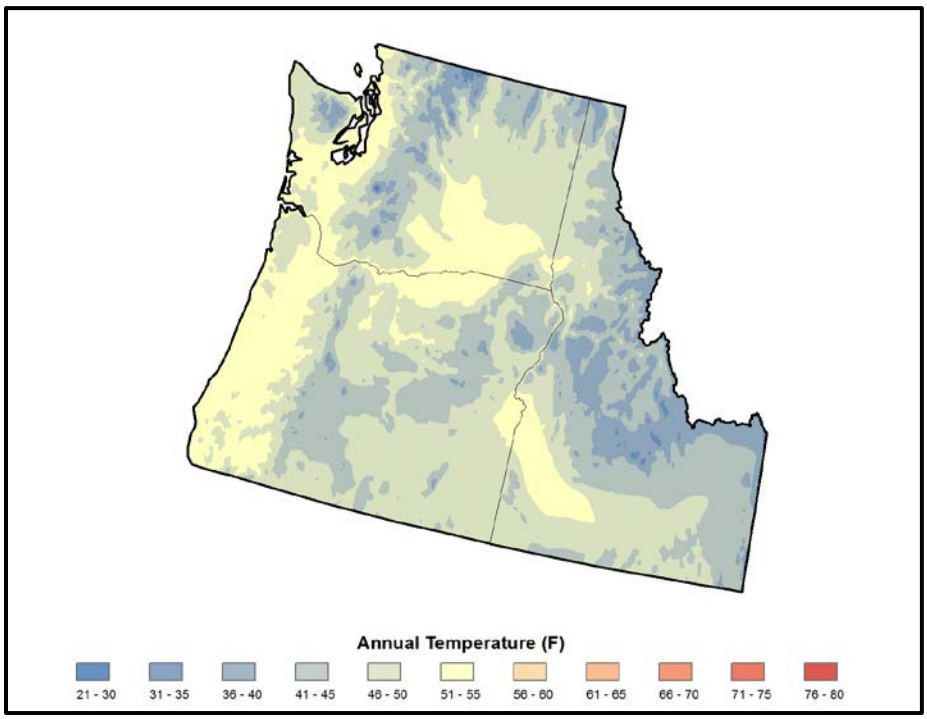

Figure 2. Average (1981-2010) annual temperature (°F) for the Northwest region. Based on a new gridded version of COOP data from the National Climatic Data Center, the CDDv2 data set (R. Vose, personal communication, July 27, 2012).

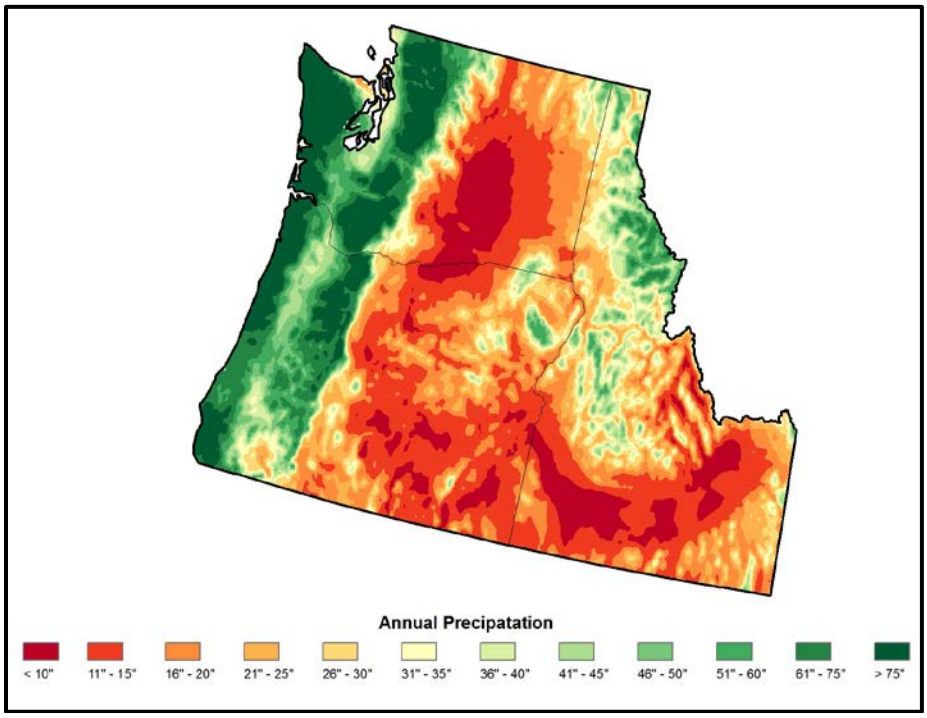

Figure 3. Average (1981-2010) annual precipitation (inches) for the Northwest region. Based on a new gridded version of COOP data from the National Climatic Data Center, the CDDv2 data set (R. Vose, personal communication, July 27, 2012).

Major urban centers in the region, ranked in the top 30 by population (U.S. Census Bureau 2011), include Seattle (#15), Portland (#23), and Boise (#85). Unlike major urban areas in other parts of the U.S., Portland and Seattle are rarely exposed to extreme temperatures and not well adapted to such events. However, extreme heat, when it occurs, is not accompanied by the high humidity typical of eastern U.S. heat waves. Severe storms in the winter result in major disruptions to surface and air transportation. Extreme rainfall causes a host of problems, including storm sewer overflow, flooding of homes and roadways, and contamination of municipal water supplies. Climate extremes combined with the urban pollution sources can create air quality conditions that are detrimental to human health.

Water resources are abundant in this region and, as a result, hydropower and irrigated agriculture represent important components of the region's economy. Agriculture is highly diverse, a result of the multiple climate conditions. Wheat production is very widespread in eastern areas, and fruit, vegetable, and turf grass production occur in the west. The steady supply of rain and mild growing conditions cause the temperate rain forests of the Pacific Northwest to be the most ecologically productive in the world (Schoonmaker et al. 1997).

2.3. Important Climate Factors

The Northwest region experiences a wide range of extreme weather and climate events that affect human society, ecosystems, and infrastructure. This discussion is meant to provide general information about these types of weather and climate phenomena. These include:

2.3.1. Winter Storms

At these latitudes the active storm belt brings numerous large-scale storms from about late October into March and April, often in close succession. The likelihood of precipitation rises rapidly during the second half of October, and the main season for significant storms is usually "in place" by the start of November. In western valleys, a stretch of 15 consecutive days of precipitation occurs about once a year. In contrast to the Sierra Nevada to the south, this region experiences many moderate and just a few large events, so that the wettest day of the year accounts for only about 4 percent of the annual precipitation in Astoria (compared with 10-15 percent in the southern Sierra Nevada). Occasionally these storms become large, deep, and powerful, bringing high winds over large areas, very significant precipitation (both rain and snow), and large waves.

In the Cascades the average winter (Dec-Feb) freezing level decreases from south to north: 5600 feet near Crater Lake, 4600 feet near Mount Hood, 4000 feet near Mount Rainier, and 3000 feet near Mount Baker. The average rain-snow line is typically 300-700 feet below this. In the Cascades, very heavy rain transitions to very heavy snow over a short vertical distance, so that very large accumulations of rain and snow are found in close proximity. The former U.S. seasonal snowfall record of 1122 inches in 1971-72, recorded at Mt. Rainier National Park, was exceeded in 1998-99 by an 1141" total at Mt. Baker in northern Washington. At the low elevations with the large population centers, snow is seldom seen, and typically averages 5-10 inches per year. On occasion, very cold systems move nearly due south or south-southwest near the coastline. Those with short over-water trajectories that pick up moisture but do not become too warm can drop very heavy snow on valley floors, greatly disrupting most economic sectors. In 1969, Eugene experienced an

exceptionally heavy snow, resulting in a depth of 34 inches on January 30, and not a single snow plow was owned by the city.

At times, cold air east of the Cascades, trapped by the Cascades, speeds westward through the major gap cut by the Columbia River, even as the upper air flow may be from the west over the Portland area. Warm rain overhead, falling into such cold air of just the right depth, will freeze on contact, and when such situations persist (as many as 3-4 days), major ice storms are possible. Some of these oscillate between freezing rain, sleet, and snow as the cold air varies in depth. Ice storms can also occur below the Fraser River Canyon and affect northwest Washington, and freezing rain does occur in the middle Columbia Basin, affecting Yakima, Richland, and Spokane.

Large windstorms typically follow recurving paths toward the north-northeast just off the coasts of Oregon and Washington, as shown by Mass (2008) for 8 major events since 1880. The Columbus Day Storm (Oct 12) of 1962 was probably the most powerful storm in the continental U.S. since the 1800s, with reliable reports of gusts to 130-175 mph, and extreme damage, including 11-15 billion board-feet (26-35 million cubic meters) of timber blown down. Many other wind storms are described by Mass (2008) and Taylor and Hatton (1999). Even on clear days, cold domes of high pressure east of the Cascades can force extremely strong and occasionally damaging winds westward through the deep and confined Columbia Gorge. When this cold air is deep enough to exceed pass elevations, downslope winds can also occur near gaps in the mountains, such as the destructive winds well over 100 mph at Enumclaw, WA, on December 24, 1983. Similar strong outflow winds from the Fraser River have been recorded over the San Juan Islands in Puget Sound, which recorded many gusts over 90 mph in December 1990. Deep Arctic outbreaks moving south into eastern Montana will also spill westward across the Continental Divide, notably near Glacier Park, with winds readily exceeding 100 mph at pass level.

2.3.2. Flood-Producing Extreme Precipitation

Winter cyclonic storms often produce heavy rain and snow in the Coast and Cascade Ranges. Some large storms (e.g., Columbus Day 1962) are remnant typhoons and tropical storms that have crossed the Pacific from near Asia. For cyclonic storms, typically, several adjoining basins flood at the same time. At times, an exceptionally long fetch and quasi-stationary pattern can tap subtropical moisture via the “Pineapple Express” or more recently identified Atmospheric Rivers (AR; Neiman et al. 2008). An atmospheric river in November 2006 produced 24-hour record precipitation in three different states along a straight line, in Oregon, Washington, and Idaho, and flooding of Many Glacier Lodge in Montana’s Glacier National Park.

The largest flood on record west of the Cascades was in the winter of 1861-62, a truly exceptional extended episode, when the Willamette River carried more than the typical Mississippi River flow. During the gauged period (1879 onward) the highest Columbia River flow at The Dalles was water year 1893-94 (313,600 cubic feet per second (cfs) on average), well above the next highest, 264,000 cfs in 1879-80 and 1996-97. In 1948, Vanport City, population 18,500, near Portland Airport, was destroyed on Memorial Day by a major snowmelt flood on the Columbia River, and never rebuilt. Heavy rain onto moderate snow pack can produce exceptional winter floods, such as in December 1964, at many locations still the flood of record. At times, rain on frozen ground can produce very rapid rises in runoff. The Columbia River Basin has become the most managed river system in the world, and flood peaks and damages have been greatly reduced.

Spring flooding from melting snows is common, but seldom can attain destructive levels unless combined with heavy rainfall events. During the warm season convective storms can produce localized flash flooding. Most notable in the Pacific Northwest is the June 1903 event in eastern Oregon at Heppner; converging tributaries of Willow Creek essentially destroyed the town and caused 247 deaths, the third-largest flood loss in U.S. history. Taylor and Hatton (1999) chronicle major floods in Oregon history.

2.3.3. Drought

The most widespread impacts of drought in the Pacific Northwest occur when precipitation is deficient in winter. Where precipitation is normally high, drought may not be as visually apparent, consisting of "less wet" conditions. Bumbaco and Mote (2010) describe effects of drought in other parts of the year. They discuss the strong role of temperature, especially in normal snow accumulation zones where the type (rain or snow) of precipitation matters greatly in leading to drought impacts in later months. East of the Cascades, where precipitation at lower elevations is not as concentrated into winter months, drought can also develop in other seasons, including summer. A dry winter lead-in to summer can set the stage for drought. One example is the 2001 drought on the Klamath River on the Oregon-California border, a basin that in a microcosm has almost all the possible dimensions of drought in a western setting (NRC 2004; 2008). In general, time series of various drought indices since 1900 (e.g., NCDC 2012a) sometimes show widespread regional coherence of drought, but do often show strong differences in drought status between the northern Rockies and the coastal areas, and among the Oregon high desert, the Snake River Plain, and the elevated areas of the Rockies along the Canada border.

The Columbia River above The Dalles drains 237,000 square miles, and annual streamflow is a useful areal integrator for drought. Low flow years were recorded in the mid-late 1920s, late 1930s, and early 1940s, with the lowest single years in 1926 and (slightly lower) in 2001. Gedalof et al. (2004) have reconstructed the streamflow history at The Dalles from 1750 onward, and find one drier period spanning the 1840s, and a few other episodes near 1776, 1804, and 1890.

Dry episodes have been associated with significant fires. Some have occurred with just modest precipitation reductions in normally dry months, and others have needed near-record dryness. Summer drought greatly facilitated the Montana-Idaho Great Burn of 1910, at 3 million acres the largest in U.S. history. Friction from a logging cable set off the 233,000 acre Tillamook Burn in Oregon in 1933, during normally dry August, but the event was fanned by strong easterly winds. The extreme drought preceding the Yellowstone fires of 1988 began with a dry winter, a wet April/May, and a very dry summer. About 36 percent (794,000 acres) of this national park burned until extinguished by September snow.

2.3.4. Heat and Cold Waves

State record temperatures for this region are either 118°F (WA, ID), or 119°F (OR), with Montana's record of 117°F in its far eastern plains. Because of ocean influences, heat episodes are longer east of the Cascades. Along the coast, most hot spells last just 1-3 days, and are almost always associated with offshore winds. Because fog and upwelling are more prevalent in summer, the warmest temperatures at the coast are mostly in early autumn.

Cold waves could be categorized into three types: coastal, interior valleys, and northern Great Plains. The coldest air masses of winter typically slide down the east side of the northern Rockies and, if deep enough, spill westward into Montana and Idaho. At times, these follow a trajectory more directly from the far north, to the west of the northern Rockies along the Fraser and Thompson Rivers and south into the Columbia River interior. These outbreaks tend to be not quite as cold as those to the east. A trajectory from the north to northeast, and a little farther west, can bring cold air to the coastal regions, assisted by river valleys draining from the interior. These air masses are more modified and are susceptible to ocean warming from any overwater portions of their trajectory. East of the Cascades, coldest temperatures are -54°F at Seneca and Ukiah, OR, -48°F at Mazama and Winthrop, WA, -60°F at Island Park Dam, ID, and -70°F at Rogers Pass, MT (unusually, just a few thousand feet west of the Continental Divide). Cold records west of the Cascades are generally in the -10 to -15°F range in Oregon, just above 0°F to single digits below 0°F in Washington, and episodes seldom last longer than a few days (Taylor and Hannan 1999; Taylor and Hatton 1999). Crater Lake, America's deepest, has been totally frozen over only in 1949 and January and December of 1985.

Although not likely with today's dams and reservoirs, the Columbia and Willamette Rivers have frozen over to such an extent that horse teams and automobiles were driven across these rivers during cold spells in the winters of 1861-62 (also the winter of the great flood), 1919, 1924, 1930, 1932, and 1937 (PNRBC 1969). Historical accounts of the frozen Columbia River (as both problem and advantage) are found in 1849 and on subsequent dates during the 19th century. Photos of planes using the frozen Columbia as a runway appeared in 1930.

2.3.5. Sea Level Rise

Sea level is affected by the amount of water in the ocean (ice cap and glacier effects, reservoir storage, and groundwater pumping), by its overall temperature averaged over depth, and by tectonic forces that are raising or lowering the earth's crust. The former effects are generally global in extent, but geological effects vary regionally. As a consequence, sea level rise is not uniform. The coasts of southern Oregon and of northern Washington are rising, with lowering in northern Oregon (Komar and Shih 1993; Allan and Komar 2006), as the subduction zones associated with the Gorda and Juan de Fuca tectonic plates push eastward under the continent. Occasional great earthquakes (the last one in 1700) relieve the accumulated strain, and the next large earthquake will likely lower the coast and provide an instantaneous adjustment. Incremental climate effects on sea level will add to this. In addition, short-term influences, such as El Niño or changes in wave height, are a further addition to the aforementioned changes.

2.4. Climatic Trends

The temperature and precipitation data sets used to examine trends were obtained from NOAA's National Climatic Data Center (NCDC). The NCDC data is based on NWS Cooperative Observer Network (COOP) observations, as descibed in Section 2.1. Some analyses use daily observations for selected stations from the COOP network. Other analyses use a new national gridded monthly data set at a resolution of 5 x 5 km, for the time period of 1895-2011. This gridded data set is derived from bias-corrected monthly station data and is named the "Climate Division Database version 2 beta" (CDDv2) and is scheduled for public release in January 2013 (R. Vose, NCDC, personal communication, July 27, 2012).

The COOP data were processed using 1901-1960 as the reference period to calculate anomalies. In Section 3, this period is used for comparing net warming between model simulations and observations. There were two considerations in choosing this period for this purpose. Firstly, while some gradually-increasing anthropogenic forcing was present in the early and middle part of the 20th century, there is a pronounced acceleration of the forcing after 1960 (Meehl et al. 2003). Thus, there is an expectation that the effects of that forcing on surface climate conditions should accelerate after 1960. This year was therefore chosen as the ending year of the reference period. Secondly, in order to average out the natural fluctuations in climate as much as possible, it is desirable to use the longest practical reference period. Both observational and climate model data are generally available starting around the turn of the 20th century, thus motivating the use of 1901 as the beginning year of the reference period. We use this period as the reference for historical time series appearing in this section in order to be consistent with related figures in Section 3.

2.4.1. Temperature

Figure 4 shows annual and seasonal time series of temperature anomalies for the period of 1895-2011, Temperatures have generally been above the long-term average for the last 25 years, both annually and for all four seasons. Annually, all but 2 years since 1986 have been above the 1901-1960 average. Two of the three warmest years on record, 1992 and 2003, have occurred during that period. The warmest year on record is 1934. Seasonal temperature behavior is similar to the annual behavior. Five of the nine warmest summers have occurred since 1998.

Table 1 shows temperature trends for the period of 1895-2011, calculated using the CDDv2 data set. Values are only displayed for trends that are statistically significant at the 95% confidence level. Temperature trends are statistically significant annually and for all seasons except spring, ranging from +0.10 to +0.20 °F/decade.

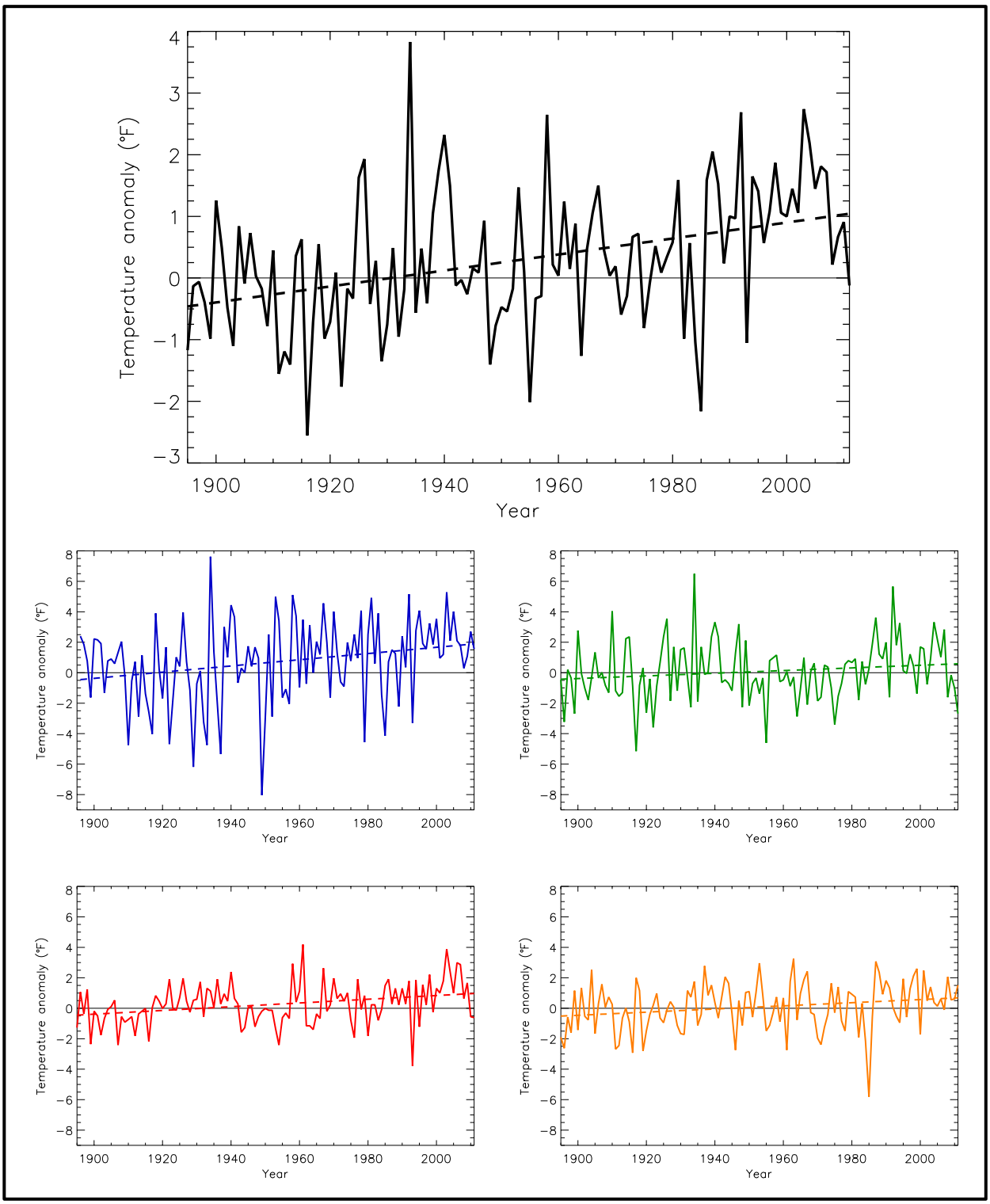

Figure 4. Temperature anomaly (deviations from the 1901-1960 average, °F) for annual (black), winter (blue), spring (green), summer (red), and fall (orange), for the Northwest U.S. Dashed lines indicate the best fit by minimizing the chi-square error statistic. Based on a new gridded version of COOP data from the National Climatic Data Center, the CDDv2 data set (R. Vose, personal communication, July 27, 2012). Note that the annual time series is on a unique scale. Trends are upward and statistically significant annually and for winter, summer, and fall.

Table 1. 1895-2011 trends in temperature anomaly (°F/decade) and precipitation anomaly (inches/decade) for the Northwest U.S., for each season as well as the year as a whole Based on a new gridded version of COOP data from the National Climatic Data Center, the CDDv2 data set (R. Vose, personal communication, July 27, 2012). Only values statistically significant at the 95% confidence level are displayed. Statistical significance of trends was assessed using Kendall's tau coefficient. The test using tau is a non-parametric hypothesis test.

Season	Temperature (°F/decade)	Precipitation (inches/decade)
Winter	+0.20	—
Spring	—	—
Summer	+0.12	—
Fall	+0.10	—
Annual	+0.13	—

See http://charts.srcc.lsu.edu/trends/ (LSU 2012) for a comparative seasonal or annual climate trend analysis of a specified from the Northwest, using National Climate Data Center (NCDC) monthly and annual temperature and precipitation datasets.

2.4.2. Precipitation

Figure 5 shows annual and seasonal time series of precipitation anomalies for the period of 1895-2011, again calculated using the CDDv2 data set. Annual precipitation has exhibited very high variability since 1976, compared to the previous 75 years. The most recent 35 years have included a few very wet years, including the wettest year on record in 1996. However, the majority of recent years have been below the 1901-1960 average, including the multi-year dry periods of 2007-2009 and 2000-2002. Seasonal behavior (Fig. 5) is generally similar. Winter is notable for the very high variability.

Trends in precipitation for the period of 1895-2011 can be seen in Table 1. Precipitation trends are not statistically significant for any season.

2.4.3. Extreme Heat and Cold

Large spatial variations in the temperature climatology of this region result in analogous spatial variations in the definition of "extreme temperature". We define here extremes as relative to a location's overall temperature climatology, in terms of local frequency of occurrence.

Figure 6 shows time series of an index intended to represent heat and cold wave events. This index specifically reflects the number of 4-day duration episodes with extreme hot and cold temperatures, exceeding a threshold for a 1 in 5-year recurrence interval, calculated using daily COOP data from long-term stations. Extreme events are first identified for each individual climate observing station. Then, annual values of the index are gridding the station values and averaging the grid box values.

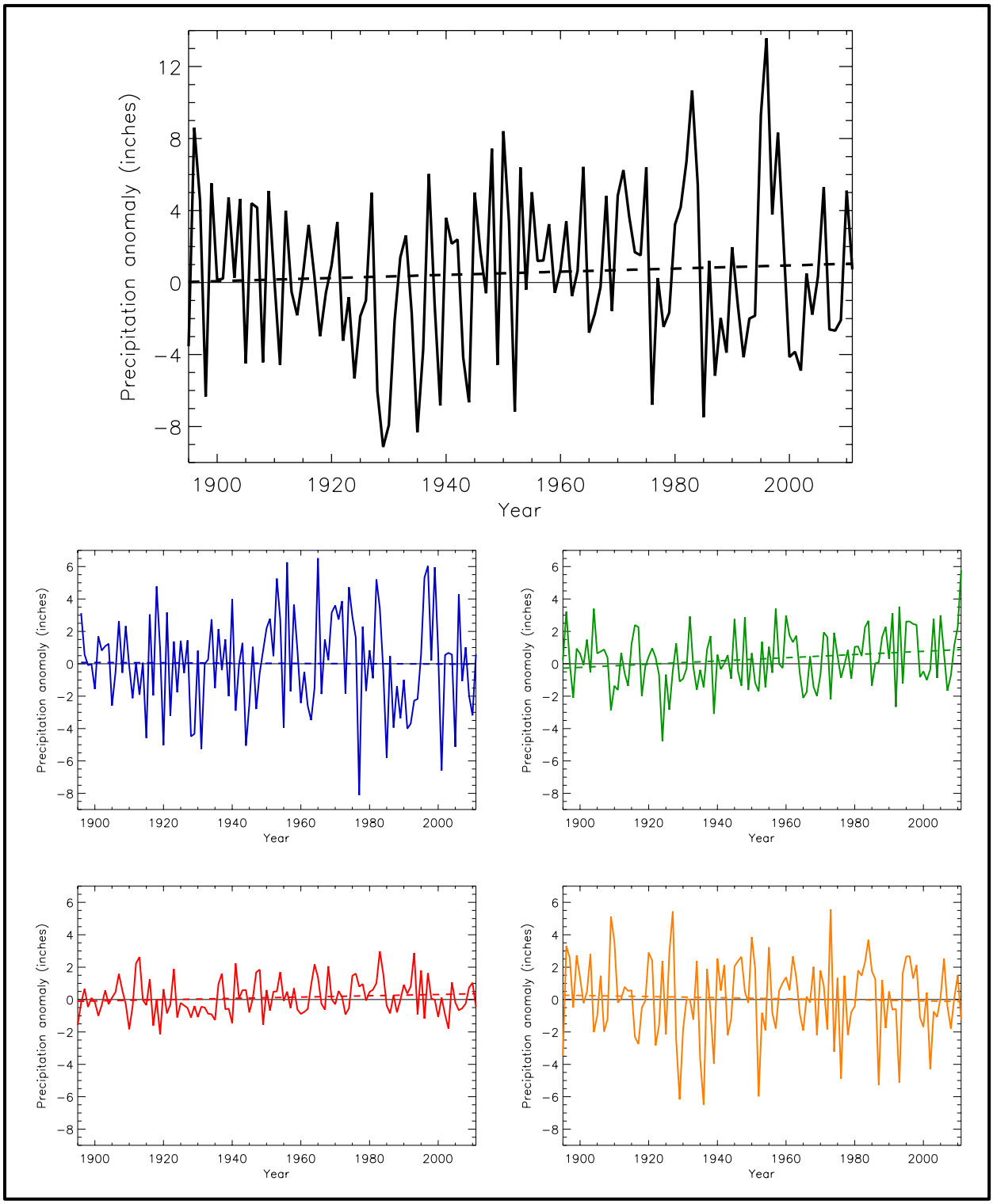

Figure 5. Precipitation anomaly (deviations from the 1901-1960 average, inches) for annual (black), winter (blue), spring (green), summer (red), and fall (orange), for the Northwest U.S. Dashed lines indicate the best fit by minimizing the chi-square error statistic. Based on a new gridded version of COOP data from the National Climatic Data Center, the CDDv2 data set (R. Vose, personal communication, July 27, 2012). Note that the annual time series is on a unique scale. Trends are not statistically significant for any season.

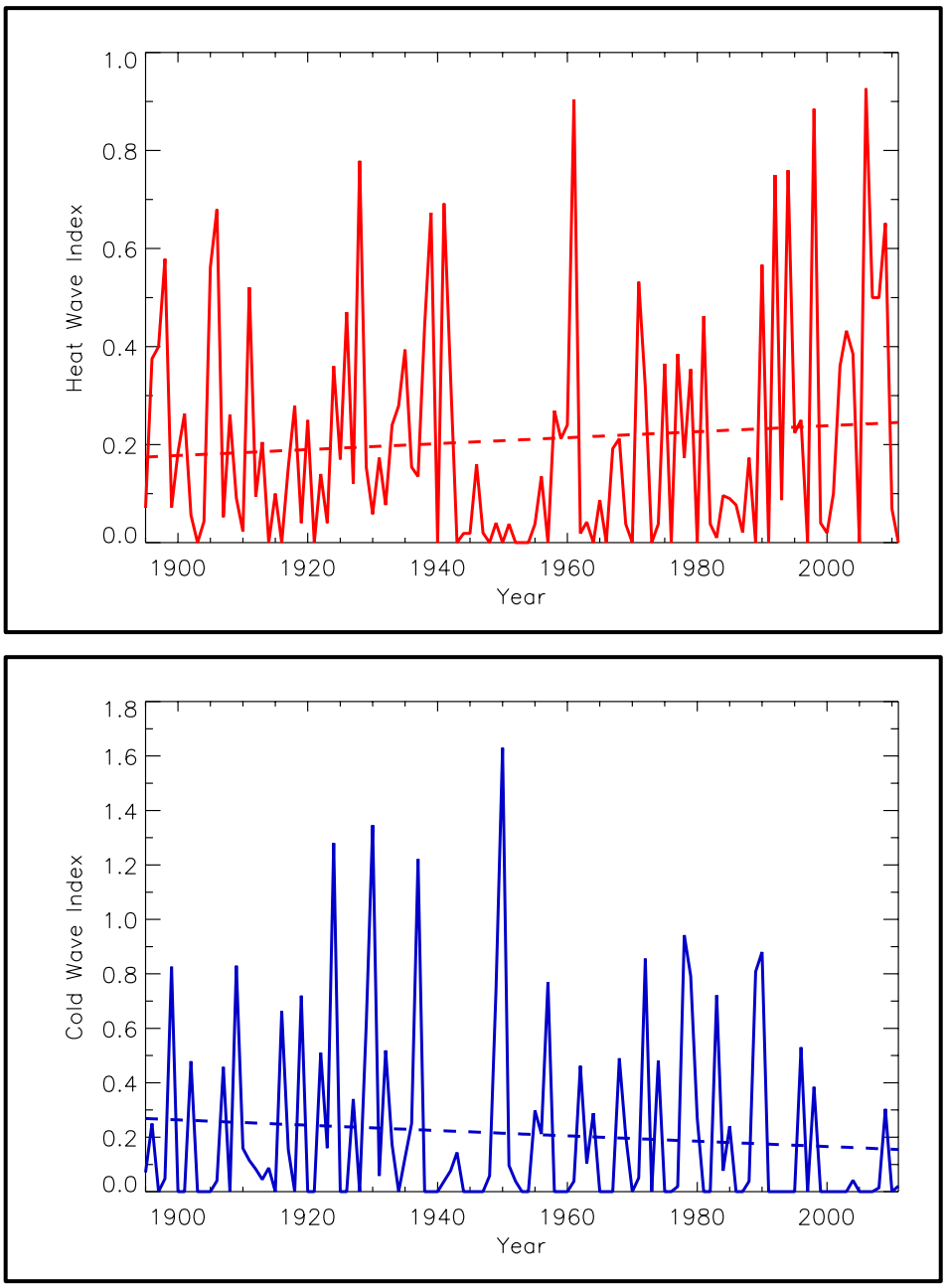

Figure 6. Time series of an index for the occurrence of heat waves (top) and cold waves (bottom), defined as 4-day periods that are hotter and colder, respectively, than the threshold for a 1 in 5-year recurrence, for the Northwest region. The dashed line is a linear fit. Based on daily COOP data from long-term stations in the National Climatic Data Center's Global Historical Climate Network data set. Only stations with less than 10% missing daily temperature data for the period 1895-2011 are used in this analysis. Events are first identified for each individual station by ranking all 4-day period mean temperature values and choosing the highest (heat waves) and lowest (cold waves) non-overlapping N/5 events, where N is the number of years of data for that particular station. Then, event numbers for each year are averaged for all stations in each 1x1° grid box. Finally, a regional average is determined by averaging the values for the individual grid boxes. This regional average is the index. The upward trend in heat waves is not statistically significant. The highest number of intense heat waves occurred in the 1930s and 2000s. The overall trend in cold waves is also not statistically significant. The number of intense cold wave events has been low during the last 15 years.

There is a large amount of interannual variability in extreme cold periods and extreme hot periods, reflecting the fact that, when they occur, such events affect large areas and thus large numbers of stations in the region simultaneously experience an extreme event exceeding the 1 in 5-year threshold.

The occurrence of heat waves, as illustrated by the heat wave index time series shown in Fig. 6 (top), has been high in the last 20 years. The number of intense heat episodes has been about 70% above the long-term average during the last 20 years. The highest number of intense heat waves occurred in 2006. Five of the top 10 years for intense heat occurred in the last 20 years.

The frequency of extreme cold periods (Fig. 6, bottom) has been generally low since 1990, with the exception of 1996, 1998, and 2009, when there were episodes of intense cold. All of the top ten years for intense cold occurred prior to 1991. The year with the highest value of this index was 1950.

2.4.4. Extreme Precipitation

There are many different metrics that have been used in research studies to examine temporal changes in extreme precipitation. Here, we define the threshold for an extreme event based on a recurrence interval. This type of definition is commonly used for design applications, for example, in the design of runoff control structures. The analysis was performed using daily COOP data from long-term stations for a range of recurrence intervals, from one to twenty years. The results were not very sensitive to the exact choice. Results are presented for the five-year threshold, as an intermediate value. The duration of the extreme event is another choice for a metric. A range of durations was analyzed, from one to ten days, but the results were also not very sensitive to the choice. Results are presented (Fig. 7) for 1-day duration events, which is the shortest duration possible because of the daily time resolution of the COOP data.

Compared to other regions, the interannual variability is relatively modest, probably reflecting the large number of winter storms that occur, providing multiple opportunities for extreme events to occur somewhere in the region. There was a period of high numbers of extreme events in the 1990s, but the numbers since then have been about the same as the prior records. There is no evidence of an overall trend. The year with the highest number of extreme events is 1996.

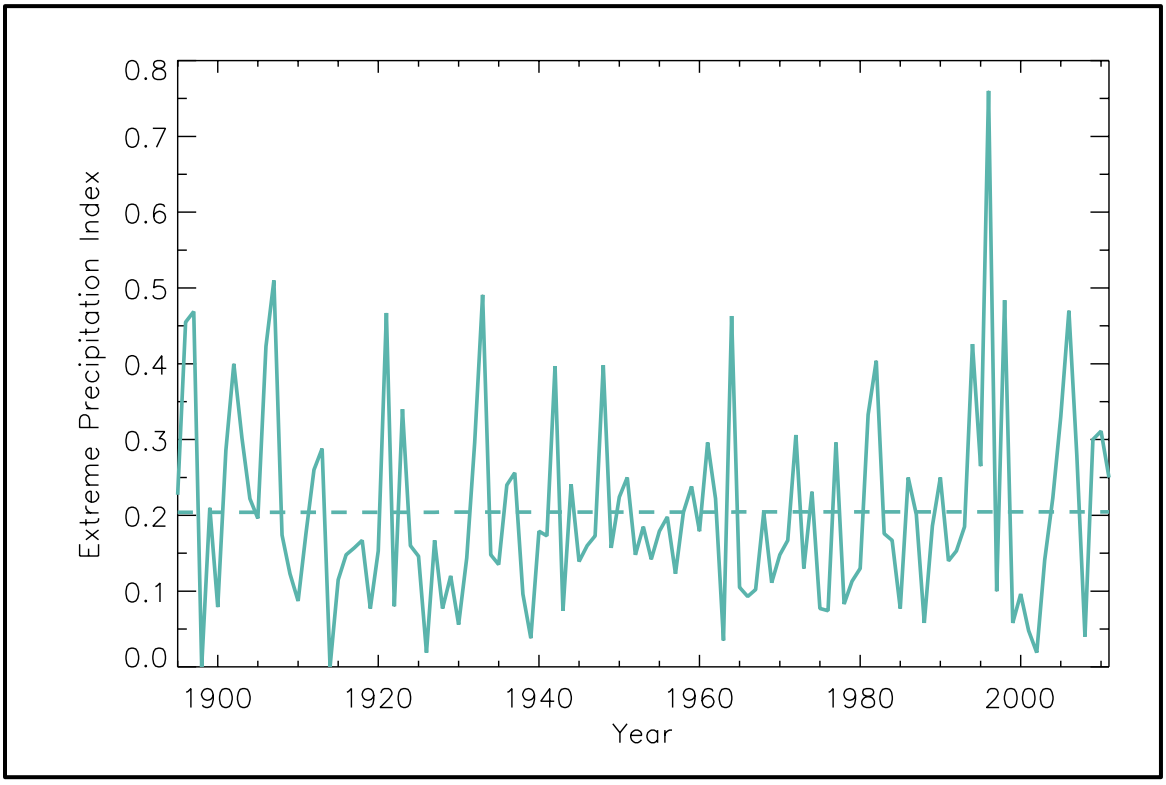

Figure 7. Time series of extreme precipitation index for the occurrence of 1-day, 1 in 5-year extreme precipitation, for the Northwest region. The dashed line is a linear fit. Based on daily COOP data from long-term stations in the National Climatic Data Center's Global Historical Climate Network data set. Only stations with less than 10% missing daily precipitation data for the period 1895-2011 are used in this analysis. Events are first identified for each individual station by ranking all daily precipitation values and choosing the top N/5 events, where N is the number of years of data for that particular station. Then, event numbers for each year are averaged for all stations in each 1x1° grid box. Finally, a regional average is determined by averaging the values for the individual grid boxes. This regional average is the extreme precipitation index. The highest number of extreme events occurred in 1996. There is no overall long-term trend.

2.4.5. Freeze-Free Season

Figure 8 shows a time series of freeze-free season length, calculated using daily COOP data from long-term stations. There is a statistically significant upward trend over the entire period (1895-2011). The time series can be characterized by four epochs: short seasons in the early part of the record, long seasons in the 1930s, moderately short seasons from the 1950s through the 1980s, and long seasons since about 1990. The season lengths during 1991-2010 average about 11 days longer than during 1961-1990. The last occurrence of 32°F in the spring has been occurring earlier and the first occurrence of 32°F in the fall has been happening later since 1990. The longest freeze-free season occurred in 1998.

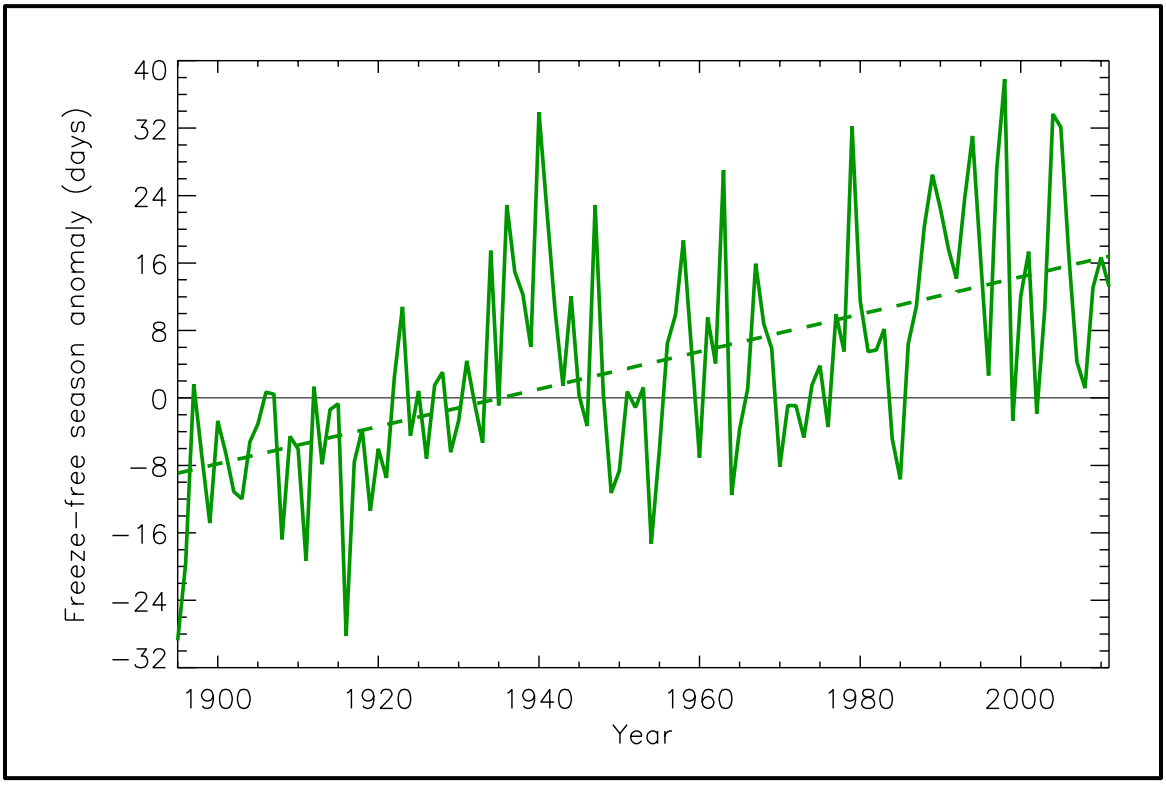

Figure 8. Time series of freeze-free season anomalies shown as the number of days per year, for the Northwest region. Length of the freeze-free season is defined as the period between the last occurrence of 32°F in the spring and first occurrence of 32°F in the fall. The dashed line is a linear fit. Based on daily COOP data from long-term stations in the National Climatic Data Center's Global Historical Climate Network data set. Only stations with less than 10% missing daily temperature data for the period 1895-2011 are used in this analysis. Freeze events are first identified for each individual station. Then, event dates for each year are averaged for 1x1° grid boxes. Finally, a regional average is determined by averaging the values for the individual grid boxes. There is an overall statistically significant upward trend.

3. FUTURE REGIONAL CLIMATE SCENARIOS

As noted above, the physical climate framework for the 2013 NCA report is based on climate model simulations of the future using the high (A2) and low (B1) SRES emissions scenarios. The resulting climate conditions are to be viewed as scenarios, not forecasts, and there are no explicit or implicit assumptions about the probability of occurrence of either scenario.

3.1. Description of Data Sources

This summary of future regional climate scenarios is based on the following model data sets:

- **Coupled Model Intercomparison Project phase 3 (CMIP3)** – Fifteen coupled Atmosphere-Ocean General Circulation Models (AOGCMs) from the World Climate Research Programme (WCRP) CMIP3 multi-model dataset (PCMDI 2012), as identified in the 2009 NCA report (Karl et al. 2009), were used (see Table 2). The spatial resolution of the great majority of these model simulations was 2-3° (a grid point spacing of approximately 100-200 miles), with a few slightly greater or smaller. All model data were re-gridded to a common resolution before processing (see below). The simulations from all of these models include:

  a) Simulations of the 20th century using best estimates of the temporal variations in external forcing factors (such as greenhouse gas concentrations, solar output, volcanic aerosol concentrations); and

  b) Simulations of the 21st century assuming changing greenhouse gas concentrations following both the A2 and B1 emissions scenarios. One of the fifteen models did not have a B1 simulation.

  These model simulations also serve as the basis for the following downscaled data set.

- **Downscaled CMIP3 (Daily_CMIP3)** – These temperature and precipitation data are at 1/8° (~8.6 miles latitude and ~6.0-7.5 miles longitude) resolution. The CMIP3 model data were initially downscaled on a monthly timescale using the bias-corrected spatial disaggregation (BCSD) method, for the period of 1961-2100. The starting point for this downscaling was an observationally-based gridded data set produced by Maurer et al. (2002). The climate model output was adjusted for biases through a comparison between this observational gridded data set and the model's simulation of the 20th century. Then, high-resolution gridded data for the future were obtained by applying change factors calculated as the difference between the model's present and future simulations (the so-called "delta" method).

  Daily statistically-downscaled data were then created by randomly sampling historical months and adjusting the values using the "delta" method (Hayhoe et al. 2004; 2008). Eight models with complete data for 1961-2100 were available and used in the Daily_CMIP3 analyses (Table 2).

- **North American Regional Climate Change Assessment Program (NARCCAP)** – This multi-institutional program is producing regional climate model (RCM) simulations in a coordinated experimental approach (NARCCAP 2012). At the time that this data analysis was initiated, simulations were available for 9 different combinations of an RCM driven by a general circulation model (GCM); during the development of these documents, two additional simulations became available and were incorporated into selected products. These 11 combinations involved four different GCMs and six different RCMs (see Table 3). The mean temperature and precipitation maps include all 11 combinations. For calculations and graphics

involving the distribution of NARCCAP models, analyses of only the original 9 model combinations were used. For graphics of the number of days exceeding thresholds and the number of degree days, the values were obtained from the Northeast Regional Climate Center, where only 8 of the model combinations were analyzed.

Each GCM-RCM combination performed simulations for the periods of 1971-2000, 1979-2004 and 2041-2070 for the high (A2) emissions scenario only. These simulations are at a resolution of approximately 50 km (~30 miles), covering much of North America and adjacent ocean areas. The simulations for 1971-2000 and 2041-2070 are "driven" (time-dependent conditions on the lateral boundaries of the domain of the RCM are provided) by global climate model simulations. The 1979-2004 simulations are driven by the NCEP/DOE Reanalysis II data set, which is an estimate of the actual time-dependent state of the atmosphere using a model that incorporates observations; thus the resulting simulations are the RCM's representation of historical observations. From this 1979-2004 simulation, the interval of 1980-2000 was selected for analysis.

Table 2. Listing of the 15 models used for the CMIP3 simulations (left column). The 8 models used in the daily statistically-downscaled (Daily_CMIP3) analyses are indicated (right column).

CMIP3 Models	**Daily_CMIP3**
CCSM3	X
CGCM3.1 (T47)	X
CNRM-CM3	
CSIRO-Mk3.0	
ECHAM5/MPI-OM	X
ECHO-G	X
GFDL-CM2.0	
GFDL-CM2.1	
INM-CM3.0	
IPSL-CM4	X
MIROC3.2 (medres)	X
MRI-CGCM2.3.2	X
PCM	X
UKMO-HadCM3	
UKMO-HadGEM1[2]	

[2] Simulations from this model are for the A2 scenario only.

Table 3. Combinations of the 4 GCMs and 6 RCMs that make up the 11 NARCCAP dynamically-downscaled model simulations.

		GCMs			
		CCSM3	CGCM3.1	GFDL-CM2.1	UKMO-HadCM3
RCMs	CRCM	X	X		
	ECPC			X[3]	
	HRM3			X[4]	X
	MM5I	X			X[3]
	RCM3		X	X	
	WRFG	X	X		

3.2. Analyses

Analyses are provided for the periods of 2021-2050, 2041-2070, and 2070-2099, with changes calculated with respect to an historical climate reference period (either 1971-1999, 1971-2000, or 1980-2000). These future periods will sometimes be denoted in the text by their midpoints of 2035, 2055, and 2085, respectively.

As noted above, three different intervals are used as the reference period for the historical climatology. Although a uniform reference period would be ideal, there were variations in data availability and in the needs of the author teams. For the NARCCAP maps of mean temperature and precipitation, the 1971-2000 period was used as the reference because that represents the full historical simulation period. The 1971-1999 period (rather than 1971-2000) was used as the reference for CMIP3 maps because some of the CMIP3 models' 20th century simulations ended in 1999, but we wanted to keep the same starting date of 1971 for both CMIP3 and NARCCAP mean temperature and precipitation maps. The 1980-2000 period was used as the historical reference for some of the NARCCAP maps (days over thresholds and degree days) because this is the analyzed period of the reanalysis-driven simulation, and we were requested to provide maps of the actual values of these variables, for both the historical period and the future period, and not just a difference map. A U.S.-wide climatology based on actual observations was not readily available for all of these variables and we chose to use the reanalysis-driven model simulation as an alternative. Since the reanalysis data set approximates observations, the reanalysis-driven RCM simulation will be free from biases arising from a driving GCM. To produce the future climatology map of actual values, we added the (future minus historical) differences to the 1980-2000 map values. For consistency then, the differences between future and present were calculated using the 1980-2000 subset of the 1971-2000 GCM-driven simulation.

Three different types of analyses are represented, described as follows:

[3] Data from this model combination were not used for simulations of the number of days exceeding thresholds or degree days.

[4] Data from these model combinations were not used for simulations of the number of days exceeding thresholds or degree days, or calculations and graphics involving the distribution of NARCCAP models.

- **Multi-model mean maps** – Model simulations of future climate conditions typically exhibit considerable model-to-model variability. In most cases, the future climate scenario information is presented as multi-model mean maps. To produce these, each model's data is first re-gridded to a common grid of approximately 2.8° latitude (~190 miles) by 2.8° longitude (~130-170 miles). Then, each grid point value is calculated as the mean of all available model values at that grid point. Finally, the mean grid point values are mapped. This type of analysis weights all models equally. Although an equal weighting does not incorporate known differences among models in their fidelity in reproducing various climatic conditions, a number of research studies have found that the multi-model mean with equal weighting is superior to any single model in reproducing the present-day climate (Overland et al. 2011). In most cases, the multi-model mean maps include information about the variability of the model simulations. In addition, there are several graphs that show the variability of individual model results. These should be examined to gain an awareness of the magnitude of the uncertainties in each scenario's future values.
- **Spatially-averaged products** – To produce these, all the grid point values within the Northwest regional boundaries are averaged and represented as a single value. This is useful for general comparisons of different models, periods, and data sources. Because of the spatial aggregation, this product may not be suitable for many types of impacts analyses.
- **Probability density functions (pdfs)** – These are used here to illustrate the differences among models. To produce these, spatially-averaged values are calculated for each model simulation. Then, the distribution of these spatially-averaged values is displayed. This product provides an estimate of the uncertainty of future changes in a tabular form. As noted above, this information should be used as a complement to the multi-model mean maps.

3.3. Mean Temperature

Figure 9 shows the spatial distribution of multi-model mean simulated differences in average annual temperature for the three future time periods (2035, 2055, 2085) relative to the model reference period of 1971-1999, for both emissions scenarios, for the 14 (B1) or 15 (A2) CMIP3 models. The statistical significance regarding the change in temperature between each future time period and the model reference period was determined using a 2-sample *t*-test assuming unequal variances for those two samples. For each period (present and future climate), the mean and standard deviation were calculated using the 29 or 30 annual values. These were then used to calculate *t*. In order to assess the agreement between models, the following three categories were determined for each grid point, similar to that described in Tebaldi et al. (2011):

- *Category 1*: If less than 50% of the models indicate a statistically significant change then the multi-model mean is shown in color. Model results are in general agreement that simulated changes are within historical variations;
- *Category 2*: If more than 50% of the models indicate a statistically significant change, and less than 67% of the significant models agree on the sign of the change, then the grid points are masked out, indicating that the models are in disagreement about the direction of change;
- *Category 3*: If more than 50% of the models indicate a statistically significant change, and more than 67% of the significant models agree on the sign of the change, then the multi-model mean is shown in color with hatching. Model results are in agreement that simulated changes are statistically significant and in a particular direction.

It can be seen from Fig. 9 that all three future time periods indicate an increase in temperature with respect to the reference period of 1971-1999, which is a continuation of the climatological upward trend of the last 30 years. Spatial variations are relatively small, especially for the low (B1) emissions scenario, although temperature increases along the coast are generally less than those in inland areas. For the high (A2) emissions scenario the warming also tends to increase towards the southeastern part of the region, with the greatest temperature difference occurring in southeastern Idaho. This is consistent with global analyses that show relatively gradual spatial changes on a global scale (Meehl et al. 2007), a probable consequence of the generally high instantaneous spatial coherence of temperature and the smoothing effect of multi-model averaging. Changes are simulated to increase for each future time period, and the differences between the A2 and B1 scenarios are also simulated to increase over time. For 2035, values range between 1.5 and 3.5°F for both emissions scenarios. For 2055, warming ranges between 2.5 and 4.5°F for B1 and between 2.5 and 5.5°F for A2. By 2085, the simulated temperature increases are 3.5 to 5.5°F for B1 and 5.5 to 8.5°F for A2. The CMIP3 models indicate that temperature changes across the Northwest U.S., for all three future time periods and both emissions scenarios, are statistically significant. The models also agree on the sign of change, with all grid points satisfying category 3 above, i.e. the models are in agreement on temperature increases throughout the region for each future time period and scenario.

Figure 10 shows the multi-model mean simulated annual and seasonal 30-year average temperature changes between 2041-2070 and 1971-2000 for the high (A2) emissions scenario, for 11 NARCCAP regional climate model simulations. The simulated annual temperature increases are greatest in the southeastern portion of the region and least along the coast, ranging from 3.0 to 5.0°F across the entire region. Temperature changes in winter range from 3.0 to 5.0°F with the greatest warming occurring in southeastern Idaho. Differences in spring are less than those in winter, ranging from 2.5 to 4.5°F, with the area of least warming extending farther eastward. The greatest temperature increases occur in summer, ranging from 3.5 to 6.0°F, with a more pronounced north-south gradient away from the coast. Ranges in the fall season are between 3.0 and 5.5°F, with a spatial variation most similar to that of the annual mean. The agreement between models was again assessed using the three categories described in Fig. 9. The models agree on the sign of change, with all grid points satisfying category 3, annually, and for all seasons.

Figure 11 shows the simulated change in annual mean temperature for each future time period with respect to 1971-1999, for both emissions scenarios, averaged over the entire Northwest region for the 14 (B1) or 15 (A2) CMIP3 models. In addition, values for 9 of the NARCCAP simulations and the 4 GCMs used in the NARCCAP experiment are shown for 2055 (A2 scenario only) with respect to 1971-2000. Both the multi-model mean and individual model values are shown. For the high (A2) emissions scenario, the CMIP3 models simulate average multi-model mean temperature increases of 2.5°F by 2035, 4.1°F by 2055, and 7.1°F by 2085. The increases for the low (B1) emissions scenario are nearly as large in 2035 at 2.2°F, but by 2085 the increase of 4.2°F is almost 3°F smaller than that for the A2 scenario. For 2055, the average temperature change simulated by the NARCCAP models (3.9°F) is comparable to the mean of the CMIP3 GCMs for the A2 scenario.

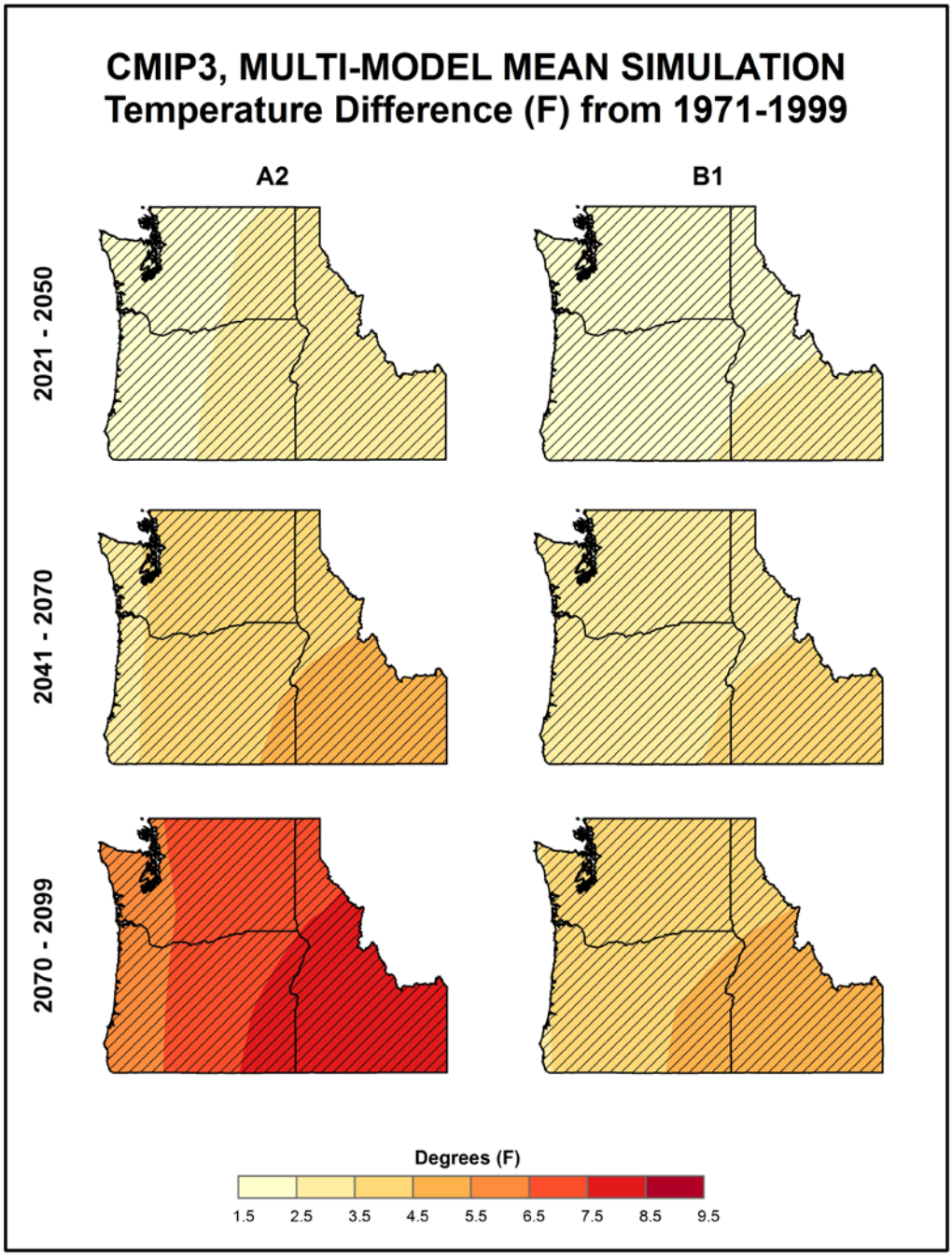

Figure 9. Simulated difference in annual mean temperature (°F) for the Northwest region, for each future time period (2021-2050, 2041-2070, and 2070-2099) with respect to the reference period of 1971-1999. These are multi-model means for the high (A2) and low (B1) emissions scenarios from the 14 (B1) or 15 (A2) CMIP3 global climate simulations. Color with hatching (category 3) indicates that more than 50% of the models show a statistically significant change in temperature, and more than 67% agree on the sign of the change (see text). Temperature changes increase throughout the 21st century, more rapidly for the high emissions scenario.

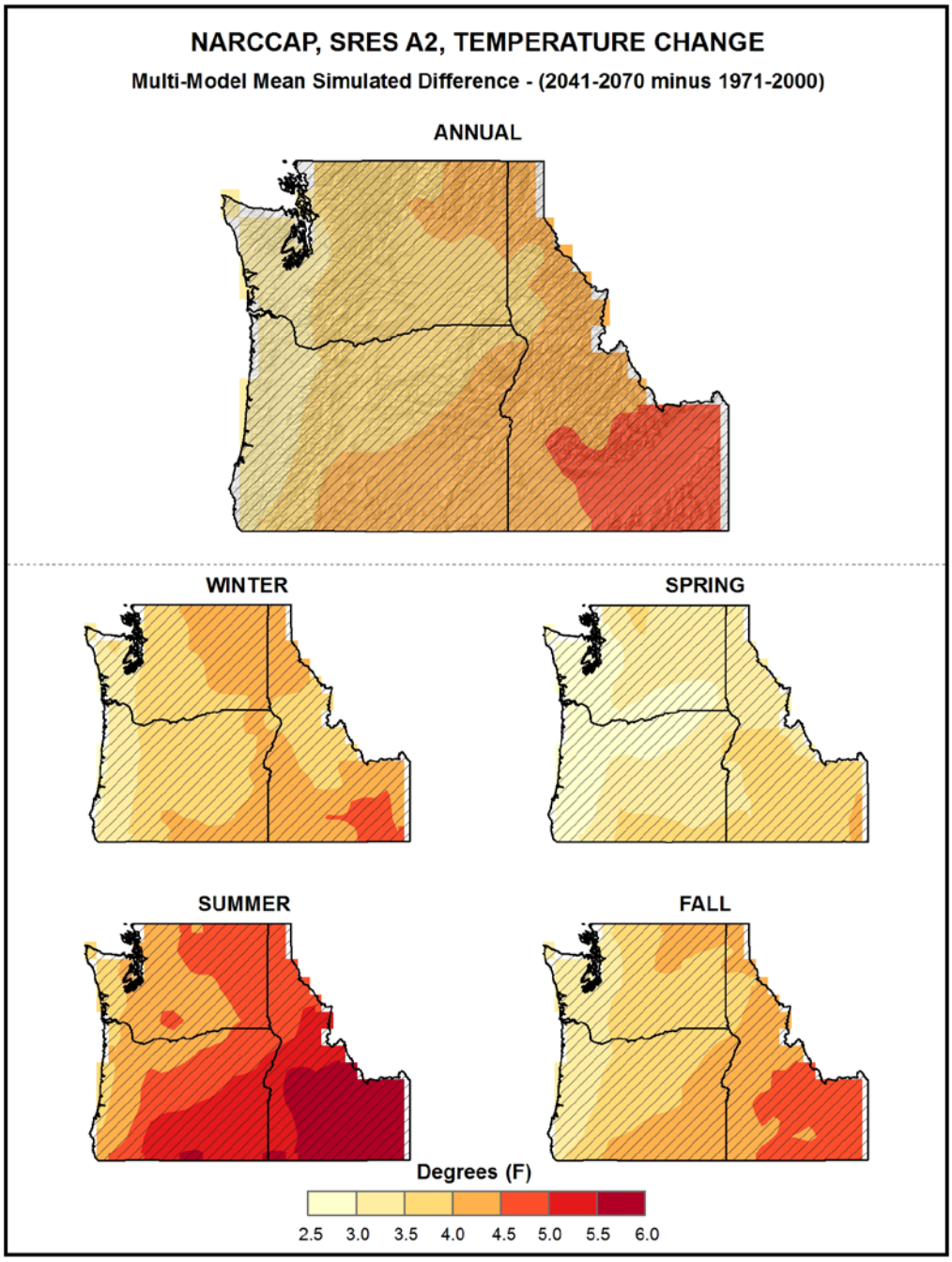

Figure 10. Simulated difference in annual and seasonal mean temperature (°F) for the Northwest region, for 2041-2070 with respect to the reference period of 1971-2000. These are multi-model means from 11 NARCCAP regional climate simulations for the high (A2) emissions scenario. Color with hatching (category 3) indicates that more than 50% of the models show a statistically significant change in temperature, and more than 67% agree on the sign of the change (see text). Note that the color scale is different from that of Fig. 9. Annual temperature changes for the NARCCAP simulations are similar to those for the CMIP3 global models (Fig. 9, middle left panel), but with greater warming in the southeastern portion of the region. Seasonal warming shows similar patterns in all seasons, with the greatest warming occurring in summer and winter.

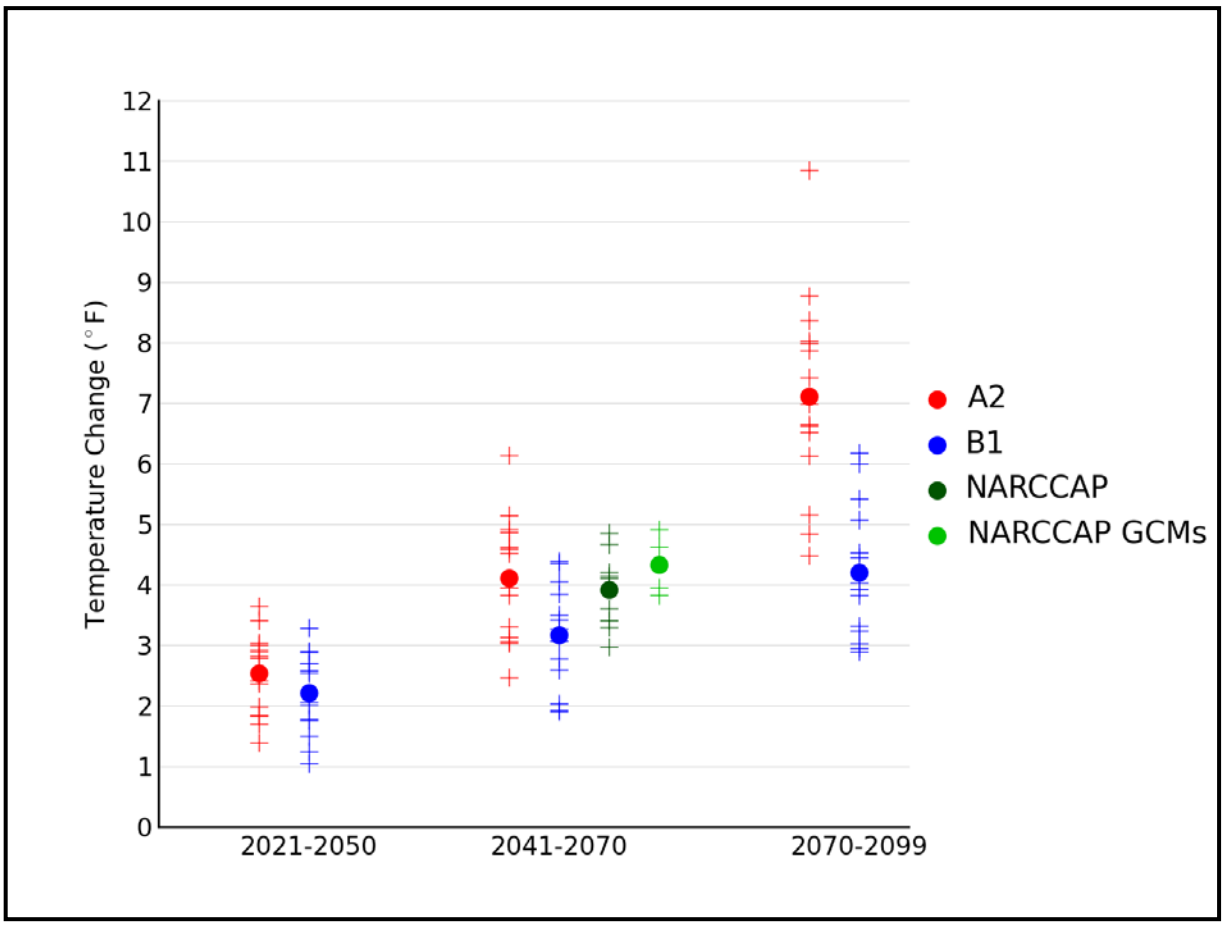

Figure 11. Simulated annual mean temperature change (°F) for the Northwest region, for each future time period (2021-2050, 2041-2070, and 2070-2099) with respect to the reference period of 1971-1999 for the CMIP3 models and 1971-2000 for the NARCCAP models. Values are given for the high (A2) and low (B1) emissions scenarios for the 14 (B1) or 15 (A2) CMIP3 models. Also shown for 2041-2070 (high emissions scenario only) are values for 9 NARCCAP models, as well as for the 4 GCMs used to drive the NARCCAP simulations. The small plus signs indicate each individual model and the circles depict the multi-model means. The range of model-simulated changes is large compared to the mean differences between A2 and B1 in the early and middle 21st century. By the end of the 21st century, the difference between A2 and B1 is comparable to the range of B1 simulations.

A key overall feature is that the simulated temperature changes are similar in value for the high and low emissions scenarios for 2035, but largely different for 2085. This indicates that early in the 21st century, the multi-model mean temperature changes are relatively insensitive to the emissions pathway, whereas late 21st century changes are quite sensitive to the emissions pathway. This arises because atmospheric CO_2 concentrations resulting from the two different emissions scenarios do not considerably diverge from one another until around 2050 (see Fig. 1). It can also be seen from Fig. 11 that the range of individual model changes is quite large, with considerable overlap between the A2 and B1 results, even for 2085. The range of temperature changes for the GCMs used to drive the NARCCAP simulations is small relative to the range for all CMIP3 models. This may be largely responsible for the relatively small range of the NARCCAP models.

Figure 12 shows the simulated change in seasonal mean temperature for each future time period with respect to 1971-1999 for the high (A2) emissions scenario, averaged over the entire Northwest region for the 15 CMIP3 models. Again, both the multi-model mean and individual model values are shown. Temperature increases are largest in the summertime, with values of just 3.4°F in 2035, 5.4°F in 2055, and 9.0°F in 2085. The spring season is simulated to experience the least amount of warming, from 2.0°F in 2035 to 5.7°F in 2085. The range of individual model temperature changes increases with each time period and is large relative to the differences between seasons and comparable to the differences between 2035 and 2085.

The distribution of simulated changes in annual mean temperature for each future time period with respect to 1971-1999 for both emissions scenarios among the 14 (B1) or 15 (A2) CMIP3 models is shown in Table 4. The distribution of 9 NARCCAP simulations (for 2055, A2 scenario only) is also shown for comparison, with respect to 1971-2000. Temperature changes simulated by the individual CMIP3 models vary from the lowest value of 1.1°F (in 2035 for the B1 scenario) to the highest value of 10.9°F (in 2085 for the A2 scenario). Although the inter-model range is seen to increase for each future time period, the interquartile range (the difference between the 75th and 25th percentiles) varies little, with values between 0.9 and 1.7°F across the three time periods. The NARCCAP simulated temperature changes have a smaller range than the comparable CMIP3 simulations, varying from 3.0°F to 4.9°F.

Table 4. Distribution of the simulated change in annual mean temperature (°F) from the 14 (B1) or 15 (A2) CMIP3 models for the Northwest region. The lowest, 25th percentile, median, 75th percentile and highest values are given for the high (A2) and low (B1) emissions scenarios, and for each future time period (2021-2050, 2041-2070, and 2070-2099) with respect to the reference period of 1971-1999. Also shown are values from the distribution of 9 NARCCAP models for 2041-2070, A2 only, with respect to 1971-2000.

Scenario	Period	Lowest	25th Percentile	Median	75th Percentile	Highest
A2	2021-2050	1.4	1.9	2.8	3.0	3.6
	2041-2070	2.5	3.2	4.1	4.8	6.1
	2070-2099	4.5	6.3	7.0	8.0	10.9
	NARCCAP (2041-2070)	3.0	3.4	4.1	4.2	4.9
B1	2021-2050	1.1	1.8	2.3	2.7	3.3
	2041-2070	1.9	2.6	3.2	3.8	4.4
	2070-2099	2.9	3.3	4.0	4.9	6.2

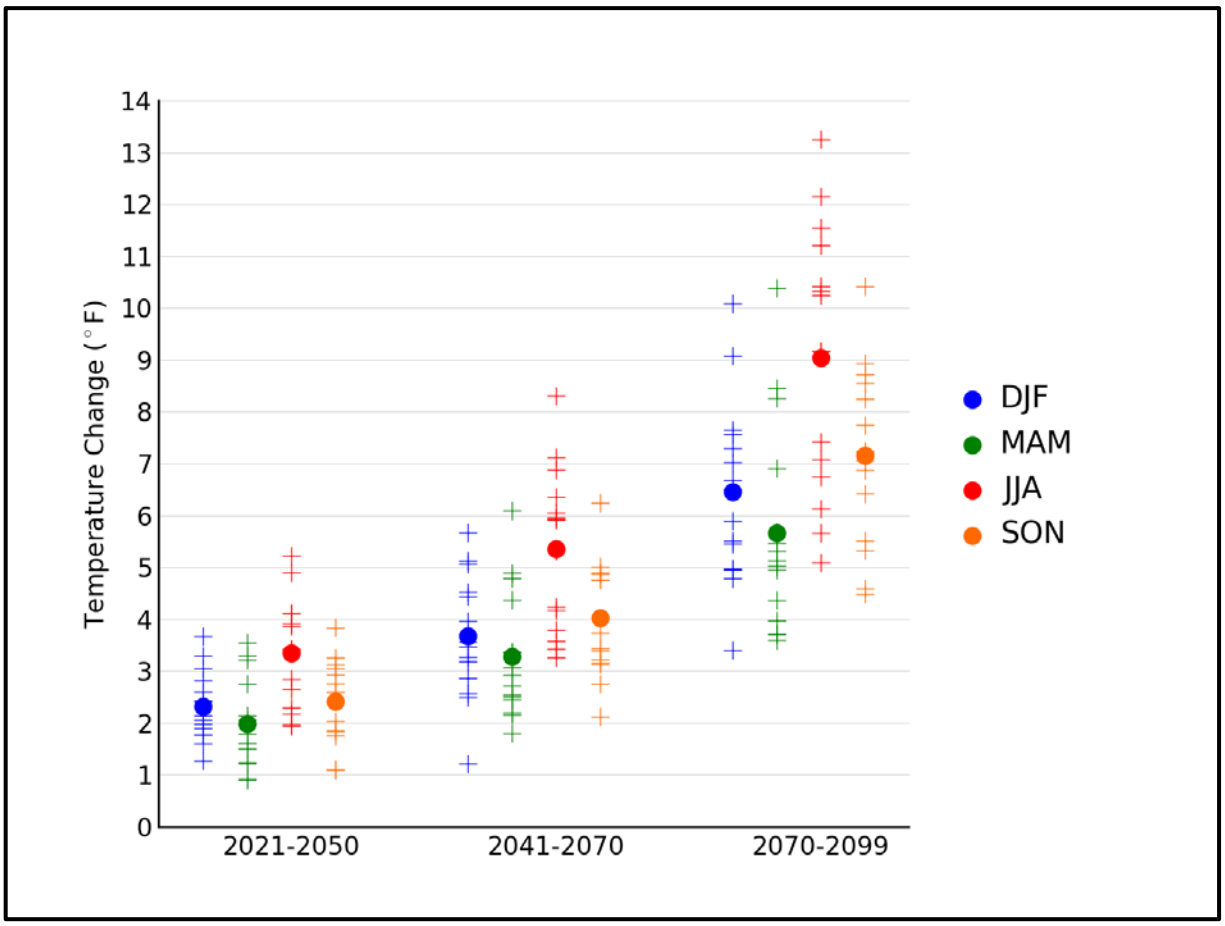

Figure 12. Simulated seasonal mean temperature change (°F) for the Northwest region, for each future time period (2021-2050, 2041-2070, and 2070-2099) with respect to the reference period of 1971-1999. Values are given for all 15 CMIP3 models for the high (A2) emissions scenario. The small plus signs indicate each individual model and the circles depict the multi-model means. Seasons are indicated as follows: winter (DJF, December-January-February), spring (MAM, March-April-May), summer (JJA, June-July-August), and fall (SON, September-October-November). The range of individual model-simulated changes is large compared to the differences among seasons and comparable to the differences between periods.

This table also illustrates the overall uncertainty arising from the combination of model differences and emission pathway. For 2035, the simulated changes range from 1.1°F to 3.6°F and are almost entirely due to differences in the models. By 2085, the simulated changes have an increased range of 2.9°F to 10.9°F, with roughly equal contributions from model differences and emission pathway uncertainties.

3.4. Extreme Temperature

A number of metrics of extreme temperatures were calculated from the NARCCAP dynamically-downscaled and CMIP3 daily statistically-downscaled (Daily_CMIP3) data sets. Maps of a few select variables and a table summarizing all of the results follow. Each figure of NARCCAP data includes three map panels and the calculations used in each panel require some explanation. One panel (top) shows the difference between the 2055 period (2041-2070) simulation for the high (A2) emissions scenario and the 1980-2000 subset of the 1971-2000 simulation driven by the GCM. Since biases in the RCM simulations can arise from biases either in the driving global climate model or in the RCM, these two simulations include both sources of biases. It is usually assumed that such biases will be similar for historical and future periods. When taking the difference of these, the biases should at least partially cancel. As noted above, we were requested to include actual values of the variables, not just the future minus historical differences. We decided that the best model representation of the present-day values is the 1980-2000 simulation because it is driven by reanalysis data (NOAA 2012b) and thus will not include biases from a driving global climate model (although the reanalysis data used to drive the RCM is not a perfect representation of the actual state of the atmosphere). Any biases should be largely from the RCM. Thus, the lower left panel in the following figures shows the actual values from the 1980-2000 simulation. The lower right panel shows the actual values for the future period, calculated by adding the differences (the 2041-2070 simulation minus the 1980-2000 subset of the 1971-2000 simulation) to the 1980-2000 simulation. If our assumption that the differencing of present and future at least partially cancels out model biases is true, then the predominant source of biases in the future values in the lower right hand panel is from the RCM simulation of the present-day, 1980-2000. The agreement among models was once again assessed using the three categories described in Fig. 9.

The selection of threshold temperatures to calculate extremes metrics is somewhat arbitrary because impacts-relevant thresholds are highly variable due to the very diverse climate of the U.S., with the exception of the freezing temperature, which is a universal physical threshold. In terms of high temperature thresholds, the values of 90°F, 95°F, and 100°F have been utilized in various studies of heat stress, although it is obvious that these thresholds have very different implications for the impacts on northern, cooler regions compared to southern, warmer regions. The threshold of 95°F has physiological relevance for maize production because the efficiency of pollination drops above that threshold. The low temperature thresholds of 10°F and 0°F also have varying relevance on impacts related to the background climate of a region. Fortunately, our analysis results are not qualitatively sensitive to the chosen thresholds. Thus, the results for these somewhat arbitrary choices nevertheless provide general guidance into scenarios of future changes.

Figure 13 shows the spatial distribution of the multi-model mean change in the average annual number of days with a maximum temperature exceeding 95°F, between 2055 and the model reference period of 1980-2000, for the high (A2) emissions scenario, for 8 NARCCAP regional climate model simulations. The largest increases of more than 12 days can be seen in the southeast

of the region, with increases of up to 18 days in southern Idaho. The smallest increases of less than 3 days occur in areas with a presently low number of 95°F days, including the high elevation areas of the Cascades and Rocky Mountains, where the general increase in temperature is not large enough to increase the chances for such warm days. The NARCCAP models indicate that the changes in the number of 95°F days across the majority of the Northwest are statistically significant. The models also agree on the sign of change, with these grid points satisfying category 3, i.e. the models are in agreement that the number of days above 95°F will increase throughout the region under this emissions scenario. For portions of western Washington and Idaho where the number of days is near zero in both the historical and future periods, the changes are not statistically significant for most models (category 1). In these areas where the historical number of days is very small, the models are in agreement that the increases in temperature are not sufficiently large to substantially increase the number of such days under this scenario.

Figure 14 shows the NARCCAP multi-model mean change in the average annual number of days with a minimum temperature below 10°F between 2055 and the model reference period of 1980-2000, for the high (A2) emissions scenario. Inland areas are simulated to experience a relatively large decrease in the number of days. The largest decreases occur in central Idaho, with the number of days below 10°F decreasing by up to 30 in some areas. The smallest decreases of between 0 and 5 days occur in coastal areas where the number of occurrences in the present-day climate is already near zero. The majority of grid points satisfy category 3, with the models indicating that the changes in the number days below 10°F across the Northwest are statistically significant. The models also agree on the sign of change, i.e. they are in agreement that the number of days with a minimum temperature of less than 10°F will decrease throughout the region under this emissions scenario. In western Oregon, the changes are not statistically significant (category 1), because the number of days in both the historical and future periods is zero or near zero.

Figure 15 shows the NARCCAP multi-model mean change in the average annual number of days with a minimum temperature of less than 32°F between 2055 and the model reference period of 1980-2000, for the high (A2) emissions scenario. Model simulated decreases are largest (decreases of more than 40 days) in high elevation areas. The least amount of change is simulated along the Pacific coast, where the number of freezes in the historical period is low. The NARCCAP models indicate that the changes in the number of days below freezing are statistically significant across the entire Northwest. The models also agree on the sign of change, with all grid points satisfying category 3, i.e. the models are in agreement that the number of days below 32°F will decrease throughout the region under this emissions scenario.

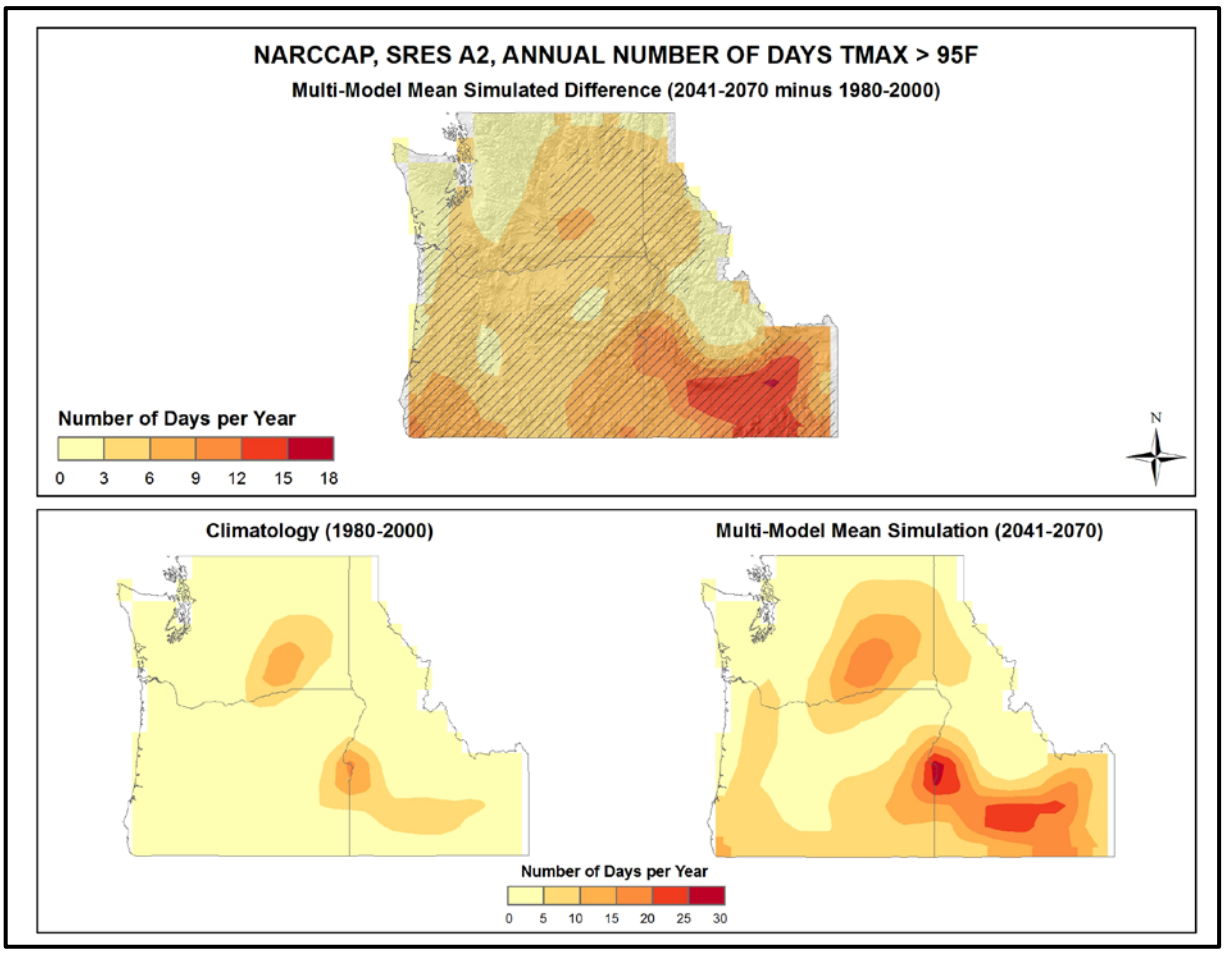

Figure 13. Simulated difference in the mean annual number of days with a maximum temperature greater than 95°F (T_{max} > 95°F) for the Northwest region, for the 2041-2070 time period with respect to the reference period of 1980-2000 (top). Color only (category 1) indicates that less than 50% of the models show a statistically significant change in the number of days. Color with hatching (category 3) indicates that more than 50% of the models show a statistically significant change in the number of days, and more than 67% agree on the sign of the change (see text). Mean annual number of days with T_{max} > 95°F for the 1980-2000 reference period (bottom left). Simulated mean annual number of days with T_{max} > 95°F for the 2041-2070 future time period (bottom right). These are multi-model means from 8 NARCCAP regional climate simulations for the high (A2) emissions scenario. Note that top and bottom color scales are different. Increases are smallest at high elevations and largest in the southeastern portion of the region.

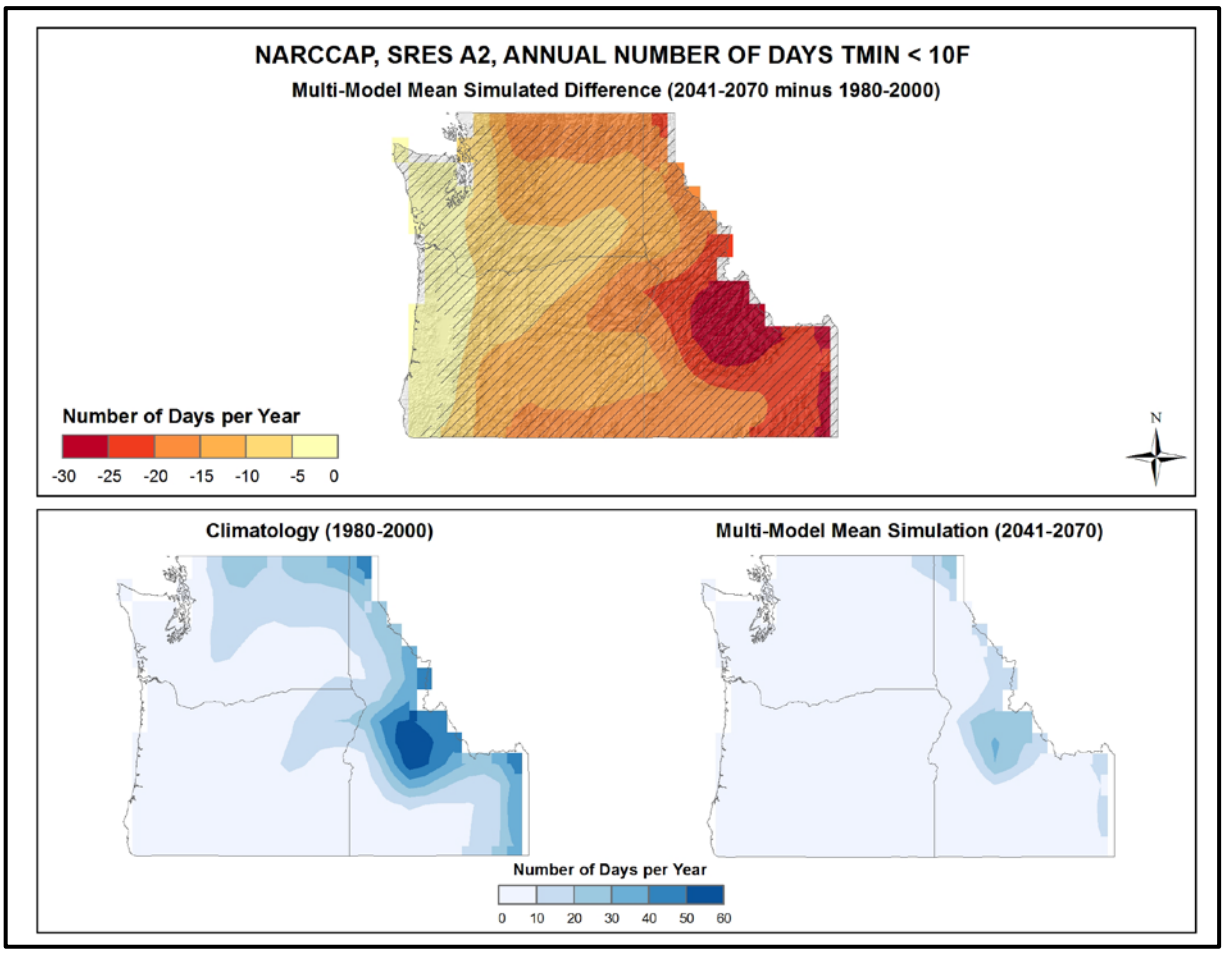

Figure 14. Simulated difference in the mean annual number of days with a minimum temperature less than 10°F (T_{min} < 10°F) for the Northwest region, for the 2041-2070 time period with respect to the reference period of 1980-2000 (top). Color only (category 1) indicates that less than 50% of the models show a statistically significant change in the number of days. Color with hatching (category 3) indicates that more than 50% of the models show a statistically significant change in the number of days, and more than 67% agree on the sign of the change (see text). Mean annual number of days with T_{min} < 10°F for the 1980-2000 reference period (bottom left). Simulated mean annual number of days with T_{min} < 10°F for the 2041-2070 future time period (bottom right). These are multi-model means from 8 NARCCAP regional climate simulations for the high (A2) emissions scenario. Decreases are largest for inland areas, while coastal regions are simulated to experience almost no change.

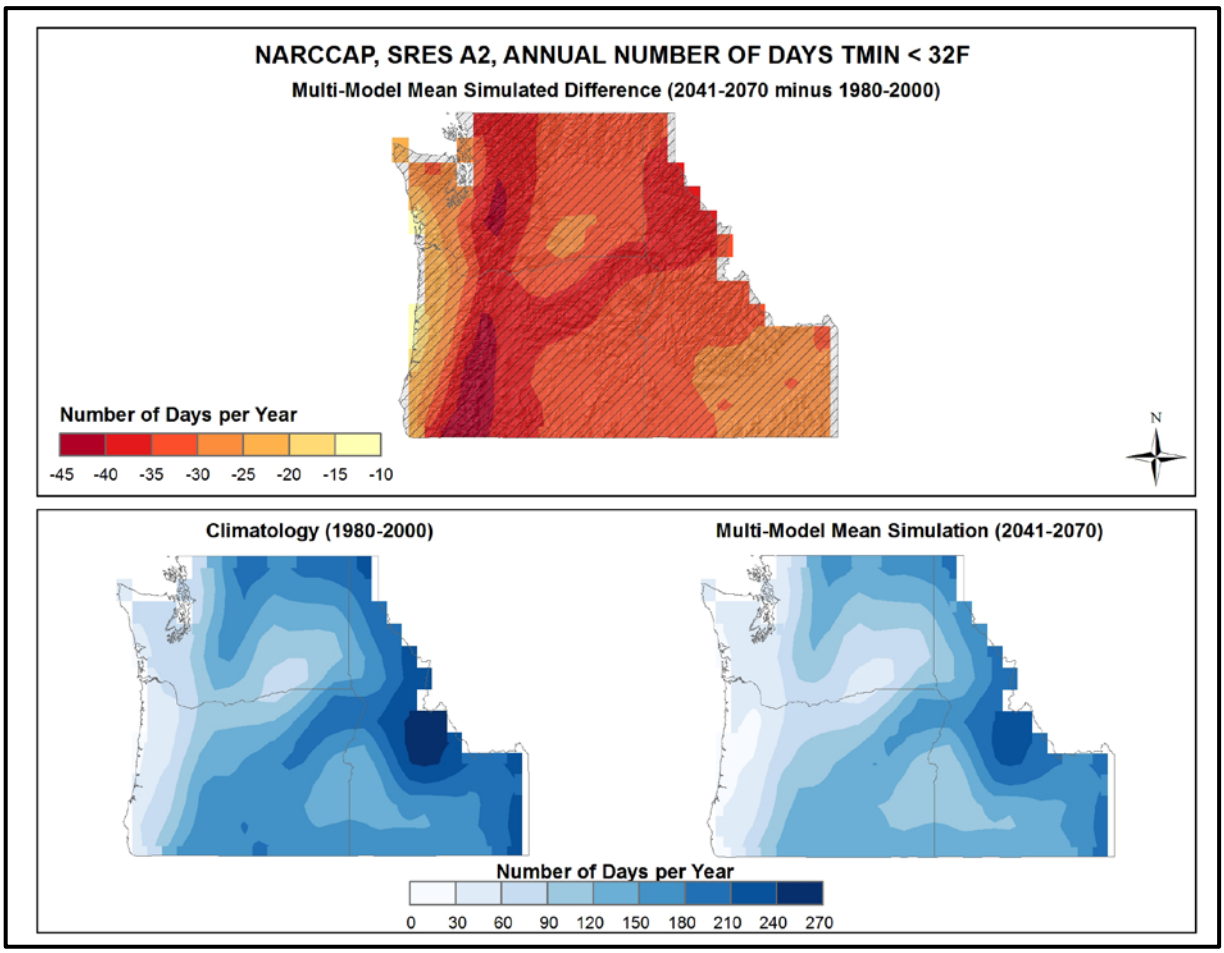

Figure 15. Simulated difference in the mean annual number of days with a minimum temperature less than 32°F (T_{min} < 32°F) for the Northwest region, for the 2041-2070 time period with respect to the reference period of 1980-2000 (top). Color with hatching (category 3) indicates that more than 50% of the models show a statistically significant change in the number of days, and more than 67% agree on the sign of the change (see text). Mean annual number of days with T_{min} < 32°F for the 1980-2000 reference period (bottom left). Simulated mean annual number of days with T_{min} < 32°F for the 2041-2070 future time period (bottom right). These are multi-model means from 8 NARCCAP regional climate simulations for the high (A2) emissions scenario. Decreases are largest for inland areas, while coastal regions are simulated to experience almost no change.

Consecutive warm days can have large impacts on a geographic area and its population, and are analyzed here as one metric of heat waves. Figure 16 shows the NARCCAP multi-model mean change in the average annual maximum number of consecutive days with maximum temperatures exceeding 95°F between 2055 and the model reference period of 1980-2000, for the high (A2) emissions scenario. The pattern is similar to the change in the total number of days exceeding 95°F for the difference map, as well as the climatological reference period. In southern Idaho the average annual longest string of days with such high temperatures is simulated to increase by up to 10 days. In the rest of the region, increases are generally in the range of 0-6 days. This continues the upward trend in heat waves seen in the region over the past 20 years (see Section 2.4.3). Changes in the number of consecutive days over 95°F are not statistically significant for portions of western Oregon. All other grid points satisfy category 3, however, with the models indicating that changes across the Northwest are statistically significant. The models also agree on the sign of change, i.e. the models are in agreement that the number of consecutive days above 95°F will increase throughout the region under this emissions scenario.

3.5. Other Temperature Variables

The spatial distribution of the NARCCAP multi-model mean change in the average length of the freeze-free season between 2055 and the model reference period of 1980-2000, for the high (A2) scenario, is shown in Fig. 17. The freeze-free season is defined as the period of time between the last spring freeze (a daily minimum temperature of less than 32°F) and the first fall freeze. There are increases of at least 20 more days in the annual freeze-free season throughout the region, continuing the marked upward trend of the past century (see Section 2.4.5). The largest simulated increases are in areas west of the Cascades, with values of greater than 40 days. Areas in the central part of the region are simulated to experience increases of a month or more, while an increase of less than 25 days is simulated for central Idaho. All grid points satisfy category 3, with the models indicating that the changes in the length of the freeze-free season across the Northwest are statistically significant. The models also agree on the sign of change, i.e. the models are in agreement that the freeze-free season length will increase throughout the region under this emissions scenario.

Cooling and heating degree days are accumulative metrics related to energy use, more specifically regarding the cooling and heating of buildings, with a base temperature of 65°F, assumed to be the threshold below which heating is required and above which cooling is required. Heating degree days provide a measure of the extent (in degrees), and duration (in days), that the daily mean temperature is below the base temperature. Cooling degree days measure the extent and duration that the daily mean temperature is above the base temperature.

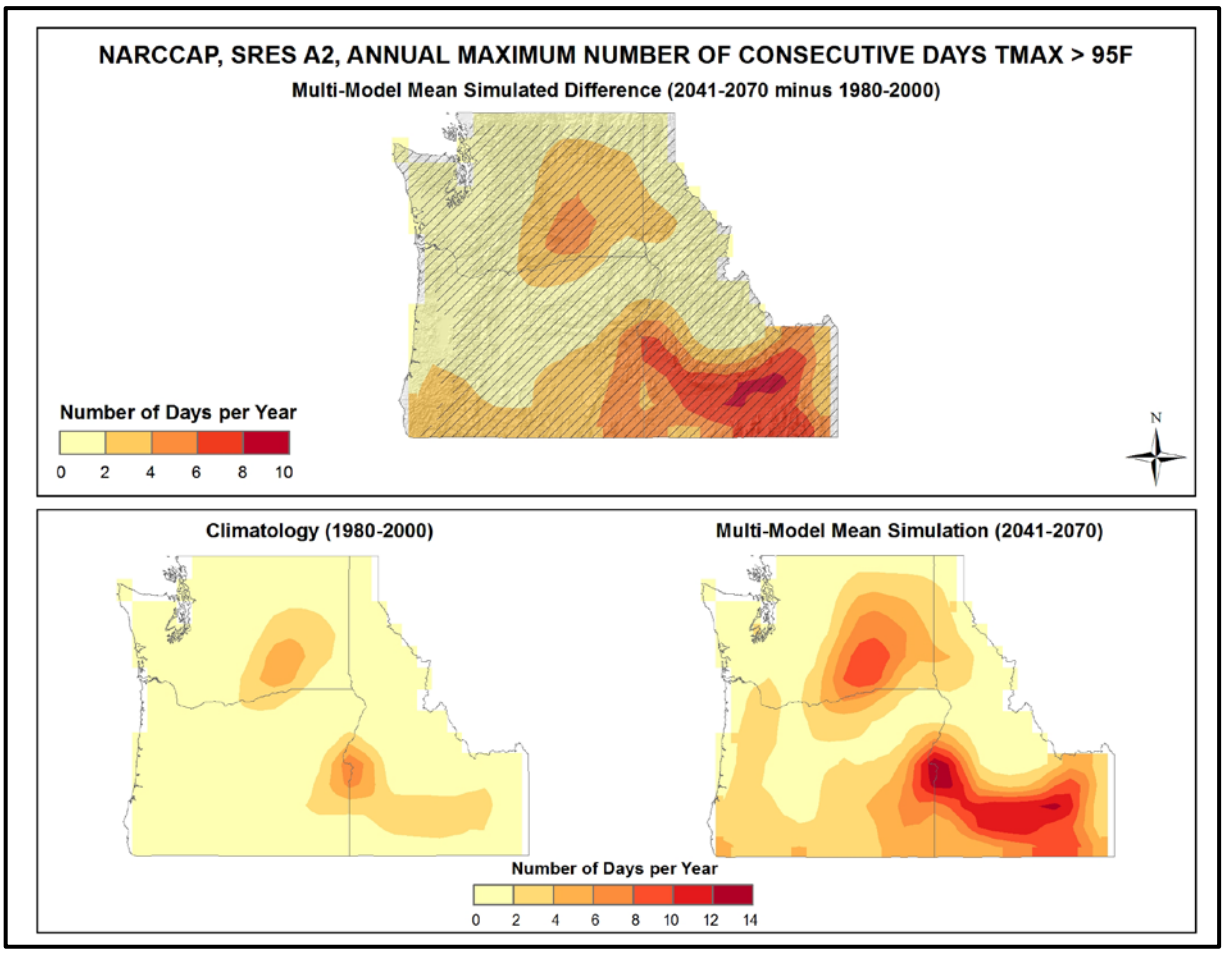

Figure 16. Simulated difference in the mean annual maximum number of consecutive days with a maximum temperature greater than 95°F (T_{max} > 95°F) for the Northwest region, for the 2041-2070 time period with respect to the reference period of 1980-2000 (top). Color only (category 1) indicates that less than 50% of the models show a statistically significant change in the number of consecutive days. Color with hatching (category 3) indicates that more than 50% of the models show a statistically significant change in the number of consecutive days, and more than 67% agree on the sign of the change (see text). Mean annual maximum number of consecutive days with T_{max} > 95°F for the 1980-2000 reference period (bottom left). Simulated mean annual maximum number of consecutive days with T_{max} > 95°F for the 2041-2070 future time period (bottom right). These are multi-model means from 8 NARCCAP regional climate simulations for the high (A2) emissions scenario. Note that top and bottom color scales are different. Increases are largest in the southeastern portion of the region.

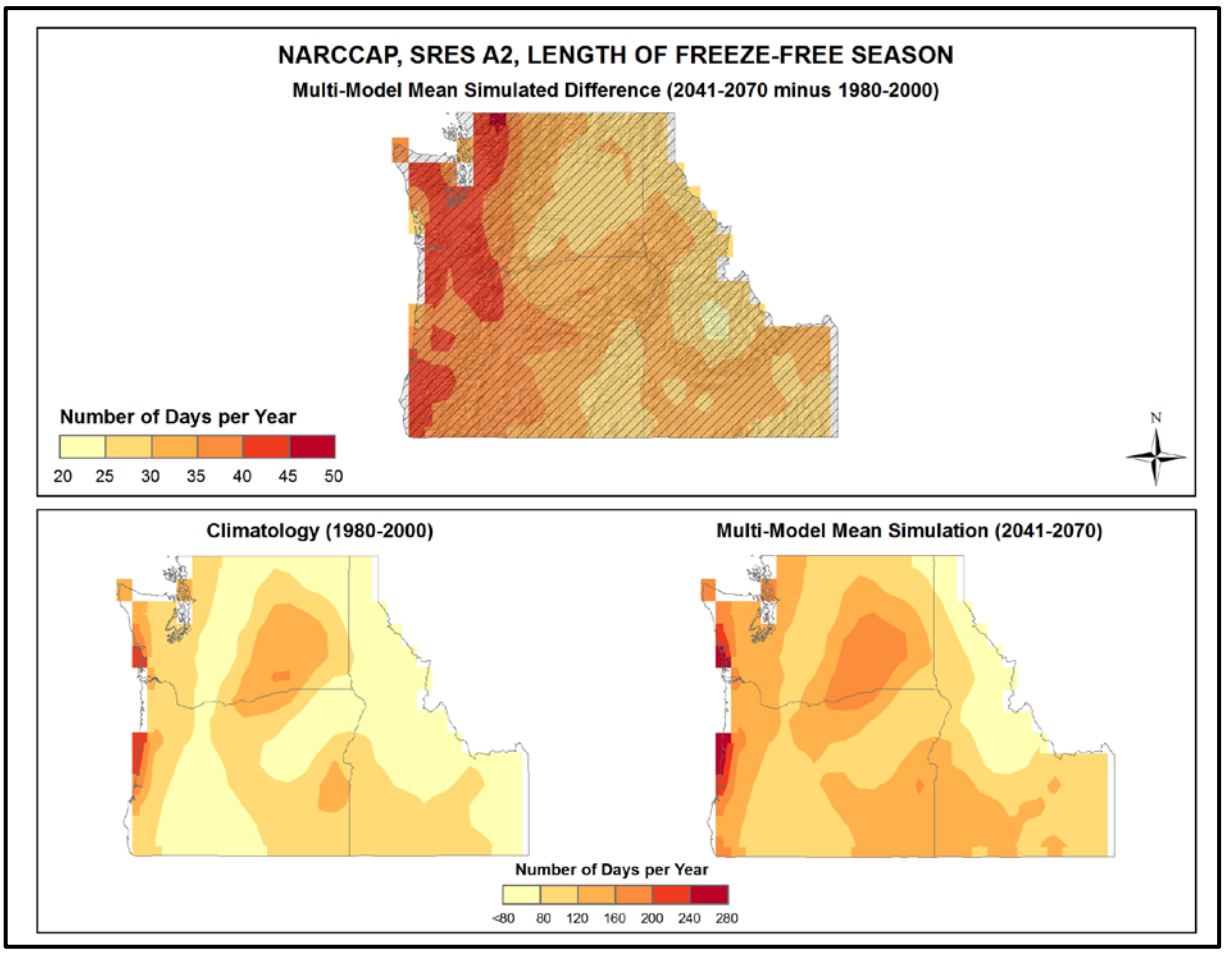

Figure 17. Simulated difference in the mean annual length of the freeze-free season for the Northwest region, for the 2041-2070 time period with respect to the reference period of 1980-2000 (top). Color with hatching (category 3) indicates that more than 50% of the models show a statistically significant change in the length of the freeze-free season, and more than 67% agree on the sign of the change (see text). Annual mean length of the freeze-free season for the 1980-2000 reference period (bottom left). Simulated mean annual length of the freeze-free season for the 2041-2070 future time period (bottom right). These are multi-model means from 8 NARCCAP regional climate simulations for the high (A2) emissions scenario. Note that top and bottom color scales are different. Simulated increases in the length of the freeze-free season are greatest in areas west of the Cascades.

Figure 18 shows the NARCCAP multi-model mean change in the average annual number of cooling degree days between 2055 and the model reference period of 1980-2000, for the high (A2) emissions scenario. In general, the simulated changes are quite closely related to mean temperature with the warmest (coolest) areas showing the largest (smallest) changes. All areas indicate an increase in the annual total cooling degree days (CDDs). The largest increases of up to 400 CDDs are simulated in southern Idaho. Increases of between 0 and 250 CDDs are seen across the majority of the region. The models indicate that the changes in cooling degree days across the Northwest are statistically significant. The models also agree on the sign of change, with all grid points satisfying category 3, i.e. the models are in agreement that the number of CDDs will increase throughout the region under this emissions scenario.

The NARCCAP multi-model mean change in the average annual number of heating degree days between 2055 and the model reference period of 1980-2000, for the high (A2) emissions scenario, is shown in Fig. 19. The majority of the region is simulated to experience a decrease of at least 1,000 heating degree days (HDDs) per year, with the exception of areas along the Oregon coast. The largest changes of up to 1,600 HDDs occur in central and eastern Idaho, where the number of HDDs is currently greatest. The models once again indicate that the changes across the entire Northwest are statistically significant. All grid points satisfy category 3, with the models also agreeing on the sign of change, i.e. the models are in agreement that the number of HDDs will decrease throughout the region under this emissions scenario.

3.6. Tabular Summary of Selected Temperature Variables

The mean changes for selected temperature-based derived variables from 8 NARCCAP simulations for 2055 with respect to the model reference period of 1971-2000, for the high (A2) emissions scenario, are summarized in Table 5. These were determined by first calculating the derived variable at each grid point. The spatially-averaged value of the variable was then calculated for the reference and future period. Finally, the difference or ratio between the two periods was calculated from the spatially-averaged values. In addition, these same variables were calculated from the 8 CMIP3 daily statistically-downscaled data set (Daily CMIP3) simulations for comparison.

For the NARCCAP simulations, the multi-model mean freeze-free period over the Northwest region is simulated to increase by 35 days, comparable to the 33 days calculated for the CMIP3 daily statistically-downscaled data. The number of days with daily maximum temperatures greater than 90°F, 95°F, and 100°F are simulated to increase by 8, 5, and 3 days, respectively, for the NARCCAP models. For the Daily CMIP3 data, corresponding increases are 18, 10, and 4, with the values decreasing by a greater amount as the thresholds become more extreme.

The number of days with minimum temperatures of less than 32°F, 10°F, and 0°F are simulated to decrease by 35, 15, and 8 days, respectively, for the NARCCAP models. Corresponding values for the Daily CMIP3 simulations are comparable decreases of 35, 9, and 4 days.

The multi-model mean annual maximum number of consecutive days exceeding 95°F and 100°F (our heat wave metric) are simulated to increase by 134% and 163%, respectively, for the NARCCAP data, a substantial increase in the length of such hot periods. These increases are even greater for the Daily CMIP3 simulations, with values of 225% and 439% for the 95°F and 100°F thresholds, respectively.

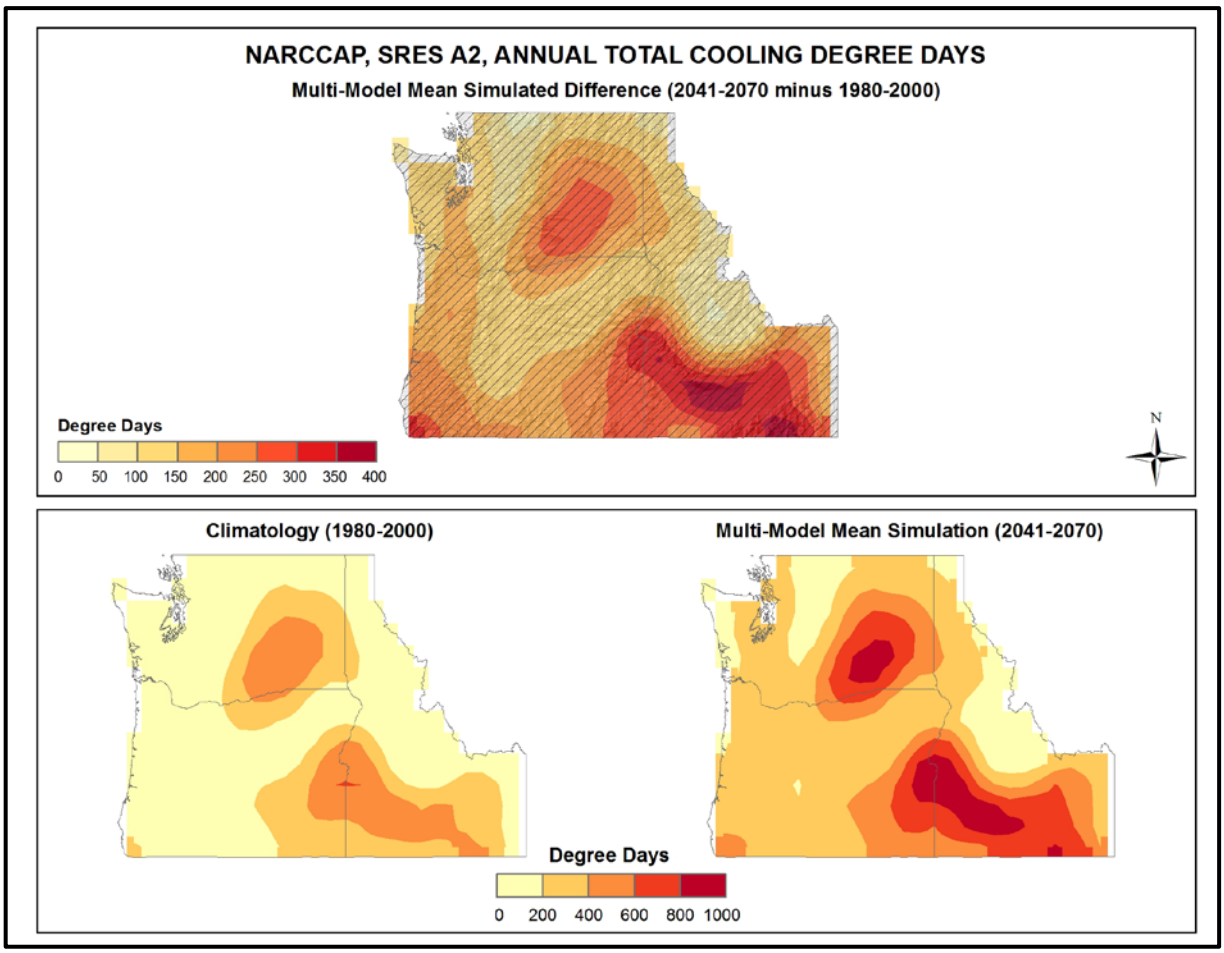

Figure 18. Simulated difference in the mean annual number of cooling degree days for the Northwest region, for the 2041-2070 time period with respect to the reference period of 1980-2000 (top). Color with hatching (category 3) indicates that more than 50% of the models show a statistically significant change in the number of cooling degree days, and more than 67% agree on the sign of the change (see text). Mean annual number of cooling degree days for the 1980-2000 reference period (bottom left). Simulated mean annual number of cooling degree days for the 2041-2070 future time period (bottom right). These are multi-model means from 8 NARCCAP regional climate simulations for the high (A2) emissions scenario. Note that top and bottom color scales are different. Increases are simulated everywhere, with the greatest increases occurring in southern Idaho and Oregon and southeastern Washington.

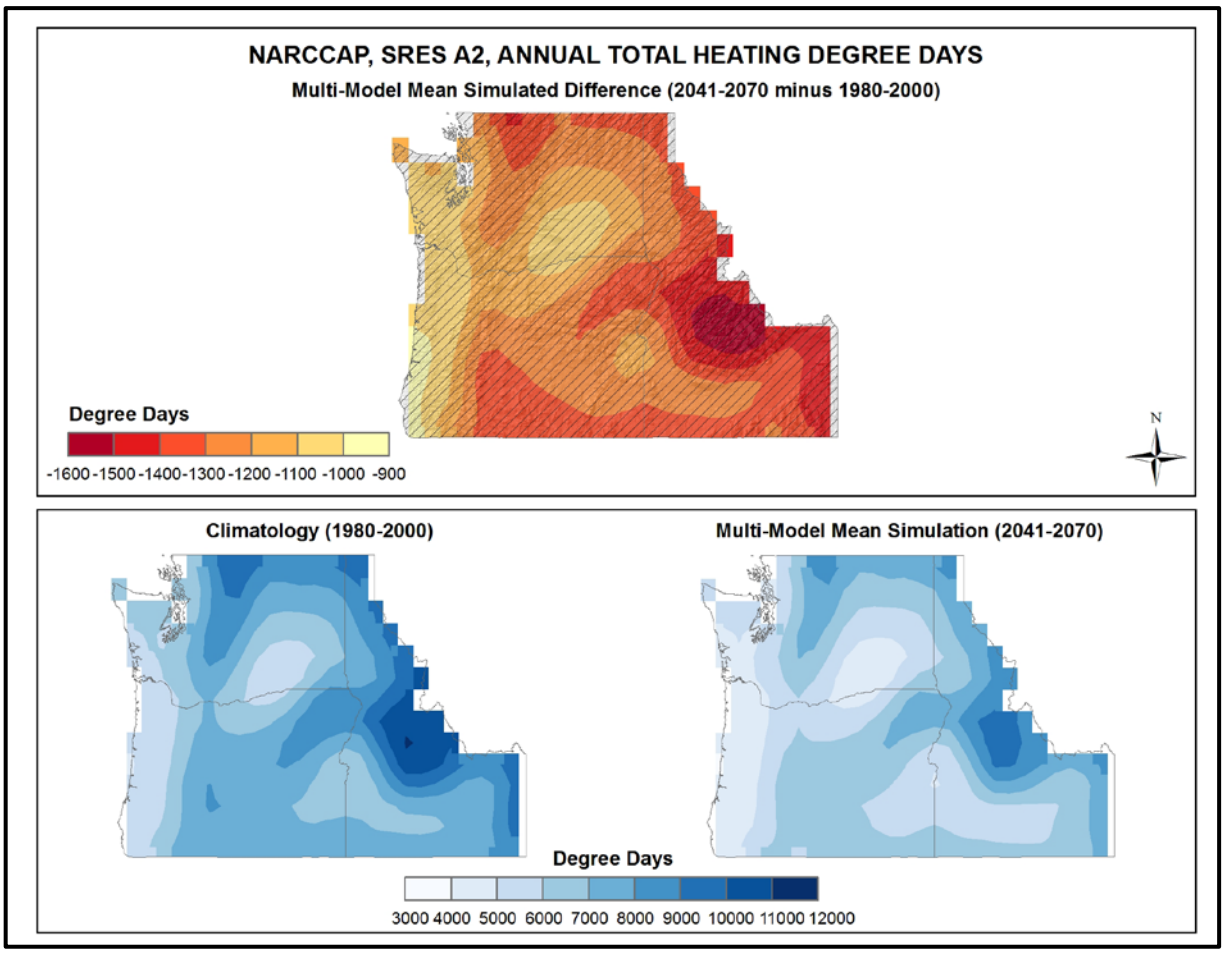

Figure 19. Simulated difference in the mean annual number of heating degree days for the Northwest region, for the 2041-2070 time period with respect to the reference period of 1980-2000 (top). Color with hatching (category 3) indicates that more than 50% of the models show a statistically significant change in in the number of heating degree days, and more than 67% agree on the sign of the change (see text). Mean annual number of heating degree days for the 1980-2000 reference period (bottom left). Simulated mean annual number of heating degree days for the 2041-2070 future time period (bottom right). These are multi-model means from 8 NARCCAP regional climate simulations for the high (A2) emissions scenario. The largest simulated increases are seen in southeastern Idaho, and the smallest increases, along the coast.

Table 5. Multi-model means and standard deviations of the simulated annual mean change in select temperature variables from 8 NARCCAP simulations for the Northwest region. Multi-model means from the 8 Daily_CMIP3 simulations are also shown for comparison. Analyses are for the 2041-2070 time period with respect to the reference period of 1971-2000, for the high (A2) emissions scenario.

Temperature Variable	**NARCCAP Mean**	**NARCCAP Standard Deviation**	**Daily_CMIP3 Mean**
Freeze-free period	+35 days	6 days	+33 days
#days T_{max} > 90°F	+8 days	7 days	+18 days
#days T_{max} > 95°F	+5 days	7 days	+10 days
#days T_{max} > 100°F	+3 days	6 days	+4 days
#days T_{min} < 32°F	-35 days	6 days	-35 days
#days T_{min} < 10°F	-15 days	7 days	-9 days
#days T_{min} < 0°F	-8 days	5 days	-4 days
Consecutive #days > 95°F	+134%	206%	+225%
Consecutive #days > 100°F	+163%	307%	+439%
Heating degree days	-15%	2%	-16%
Cooling degree days	+105%	98%	+147%
Growing degree days (base 50°F)	+51%	14%	+49%

Table 5 indicates that, for the high (A2) emissions scenario, the number of heating degree days are simulated by the NARCCAP simulations to decrease by 15% (16% for the Daily CMIP3), while the number of cooling degree days are simulated to increase by 105% (147% for the Daily CMIP3). The number of growing degree days are comparable for both data sets, increasing by 51% and 49%.

3.7. Mean Precipitation

Figure 20 shows the spatial distribution of the multi-model mean simulated differences in average annual precipitation, for the three future time periods (2035, 2055, 2085) with respect to 1971-1999, for both emissions scenarios, for the 14 (B1) or 15 (A2) CMIP3 models. The majority of the region is simulated to experience an increase in precipitation for all periods and scenarios. Generally, there is a north-south gradient in changes, with the largest increases seen in Washington. A slight decrease in precipitation is simulated for the southeastern and southwestern corners of the region in 2035 and 2055. The largest north-south differences are simulated for both emissions scenarios in 2085, varying from an increase of 0-3% in the southern corners of the region to 6-9% in the northwest. The smallest differences occur for the B1 scenario in 2035, with increases of between 0 and +3% across the entire region. The agreement between models was once again assessed using the three categories described in Fig. 9. It can be seen that for the 2035 time period the changes in precipitation are not statistically significant for most models (category 1) over all grid points. This means that most models are in agreement that any changes will be smaller than the normal year-to-year variations that occur. By 2085, most models simulate changes that are larger than these normal variations (category 3) across the majority of the region. For the low emissions scenario, the models are mostly in agreement that precipitation will increase throughout the Northwest. For the high emissions scenario, however, the models are in disagreement about the sign of the changes (category 2) in the southwest of the region.

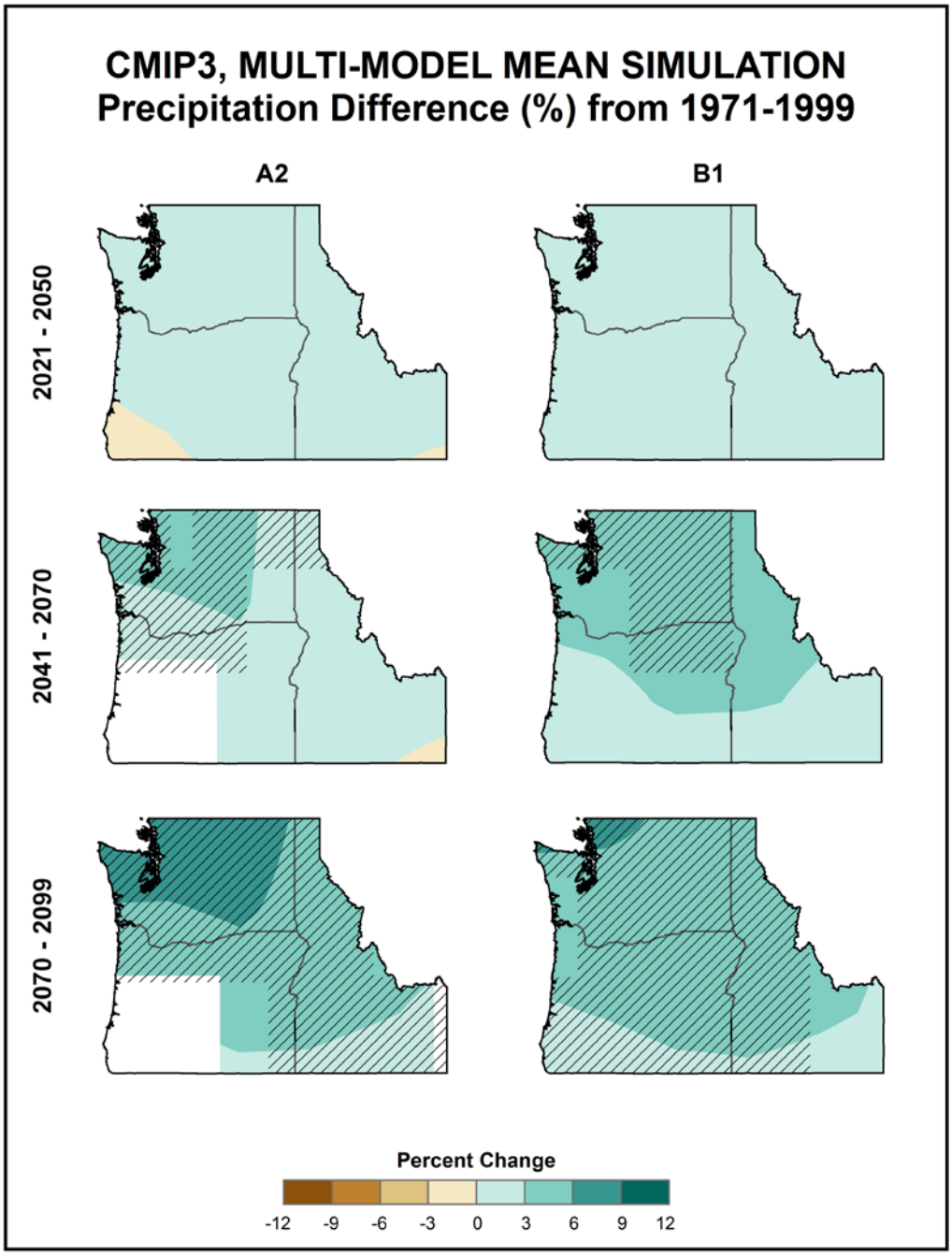

Figure 20. Simulated difference in annual mean precipitation (%) for the Northwest region, for each future time period (2021-2050, 2041-2070, and 2070-2099) with respect to the reference period of 1971-1999. These are multi-model means for the high (A2) and low (B1) emissions scenarios from the 14 (B1) or 15 (A2) CMIP3 global climate simulations. Color only (category 1) indicates that less than 50% of the models show a statistically significant change in precipitation. Color with hatching (category 3) indicates that more than 50% of the models show a statistically significant change in precipitation, and more than 67% agree on the sign of the change. Whited out areas (category 2) indicate that more than 50% of the models show a statistically significant change in precipitation, but less than 67% agree of the sign of the change (see text). Models simulate increases almost everywhere, and the changes generally become larger moving northward.

Table 6 shows the distribution of simulated changes in annual mean precipitation for each future time period with respect to 1971-1999, for both emissions scenarios, among the 14 (B1) or 15 (A2) CMIP3 models. The distribution of 9 NARCCAP simulations (for 2055, A2 scenario only) is also shown for comparison, with respect to 1971-2000. For all three time periods and both scenarios, the CMIP3 model simulations indicate both increases and decreases in precipitation. The inter-model range of changes in precipitation (i.e., the difference between the highest and lowest model values) varies from 10% to 27%. The NARCCAP simulated precipitation changes have a smaller range than the comparable CMIP3 simulations, varying from -5% to +7%. The interquartile range (the difference between the 75th and 25th percentiles) of precipitation changes across all the GCMs is less than 10% for all time periods, except 2085 for the A2 emissions scenario.

Table 6. Distribution of the simulated change in annual mean precipitation (%) from the 14 (B1) or 15 (A2) CMIP3 models for the Northwest region. The lowest, 25th percentile, median, 75th percentile and highest values are given for the high (A2) and low (B1) emissions scenarios, and for each future time period (2021-2050, 2041-2070, and 2070-2099) with respect to the reference period of 1971-1999. Also shown are values from the distribution of 9 NARCCAP models for 2041-2070, A2 only, with respect to 1971-2000.

Scenario	Period	Lowest	25th Percentile	Median	75th Percentile	Highest
A2	2021-2050	-5	-3	0	4	8
	2041-2070	-5	-3	3	6	11
	2070-2099	-7	-2	4	11	20
	NARCCAP (2041-2070)	*-5*	*-2*	*2*	*5*	*7*
B1	2021-2050	-4	1	3	4	6
	2041-2070	-4	-1	4	5	11
	2070-2099	-3	2	6	7	9

Figure 21 shows the multi-model mean annual and seasonal 30-year average precipitation change between 2041-2070 and 1971-2000 for the high (A2) emissions scenario, for 11 NARCCAP regional climate model simulations. The annual changes are mostly upward with the largest increases of 6-8% occurring in eastern Washington. However, decreases of up to 6% can also be seen in certain areas, such as parts of central Idaho and southwestern Oregon. Both increases and decreases in precipitation are simulated for all seasons, with an overall increase for winter, spring and fall. Simulated changes in the summer, however, are downward almost everywhere, with decreases of up to 20% in the south and east of the region. Spring and summer show a slightly larger spatial variability in precipitation change than is seen in fall and winter. The agreement between models was again assessed using the three categories described in Fig. 9. It can be seen that annually, and for all seasons, the simulated changes in precipitation are not statistically significant for most models over the majority of grid points (category 1). The models are in agreement (category 3), however, for an area of southwestern Oregon for the spring simulation, parts of Idaho and western Oregon for summer, and northern Washington and Idaho for fall. The models are in disagreement about the sign of change (category 2) for two small areas in northeastern Oregon for the annual simulation, as well as for portions of western Washington and Oregon for fall.

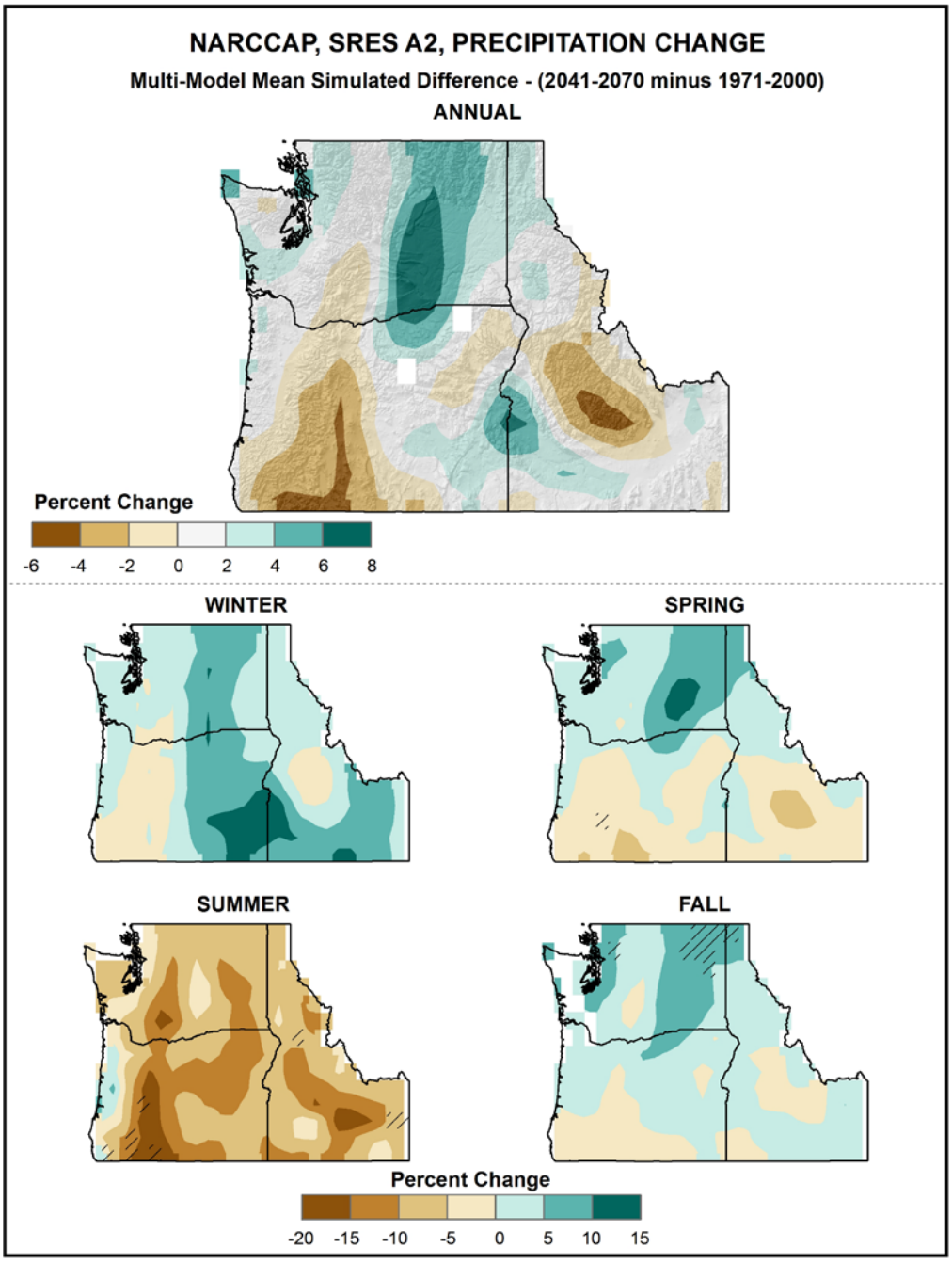

Figure 21. Simulated difference in annual and seasonal mean precipitation (%) for the Northwest region, for 2041-2070 with respect to the reference period of 1971-2000. These are multi-model means from 11 NARCCAP regional climate simulations for the high (A2) emissions scenario. Color only (category 1) indicates that less than 50% of the models show a statistically significant change in precipitation. Color with hatching (category 3) indicates that more than 50% of the models show a statistically significant change in precipitation, and more than 67% agree on the sign of the change. Whited out areas (category 2) indicate that more than 50% of the models show a statistically significant change in precipitation, but less than 67% agree of the sign of the change (see text). Note that the top and bottom color scales are unique, and different from that of Fig. 20. The simulated annual change is mostly upward, with drying seen in southwestern Oregon and central Idaho. Changes are mostly upward in winter, spring, and fall, and downward in summer.

Table 7 shows the distribution of simulated changes in seasonal mean precipitation among the 14 (B1) or 15 (A2) CMIP3 models, between 2070-2099 and 1971-1999 for both emissions scenarios. On a seasonal basis, the range of model-simulated changes is quite large. For example, in the high (A2) emissions scenario, the change in summer precipitation varies from a decrease of 51% to an increase of 10%. The majority of the models simulate increases in winter, spring, and fall precipitation, but decreases in summer precipitation. In the low (B1) emissions scenario, the range of changes in precipitation are generally smaller with a tendency towards somewhat wetter conditions. The central feature of the results in Table 7 is the large uncertainty in seasonal precipitation changes, with the interquartile range varying from 5 to 23%.

Table 7. Distribution of the simulated change in seasonal mean precipitation (%) from the 14 (B1) or 15 (A2) CMIP3 models for the Northwest region. The lowest, 25th percentile, median, 75th percentile and highest values are given for the high (A2) and low (B1) emissions scenarios, and for the 2070-2099 time period with respect to the reference period of 1971-1999.

Scenario	Period	Season	Lowest	25th Percentile	Median	75th Percentile	Highest
A2	2070-2099	DJF	-2	-5	9	18	44
		MAM	-3	-2	7	11	14
		JJA	-51	-34	-28	-11	10
		SON	-13	-4	3	18	42
B1	2070-2099	DJF	-1	5	8	12	26
		MAM	-7	3	6	8	11
		JJA	-30	-21	-11	-4	3
		SON	-3	0	3	9	29

Figure 22 shows the simulated change in annual mean precipitation for each future time period with respect to 1971-1999, for both emissions scenarios, averaged over the entire Northwest region for the individual 14 (B1) or 15 (A2) CMIP3 models. In addition, averages for 9 of the NARCCAP simulations (relative to 1971-2000) and the 4 GCMs used in the NARCCAP experiment are shown for 2055 (A2 scenario only). Both the multi-model mean and individual model values are shown. The mean simulated changes for the CMIP3 models are positive for all future time periods, for both scenarios, with values ranging from +1 to +4%. The multi-model mean of the NARCCAP simulations, an increase of just over +1%, is lower than the corresponding CMIP3 multi-model mean, but the mean of the 4 CMIP3 models used in the NARCCAP experiment is lower than the 15-model CMIP3 mean also. The inter-model range of changes in Fig. 22 is large compared to the differences in the multi-model means, as illustrated in Table 6. In fact, for both emissions scenarios, the individual model range is much larger than the differences in the CMIP3 multi-model means between time periods.

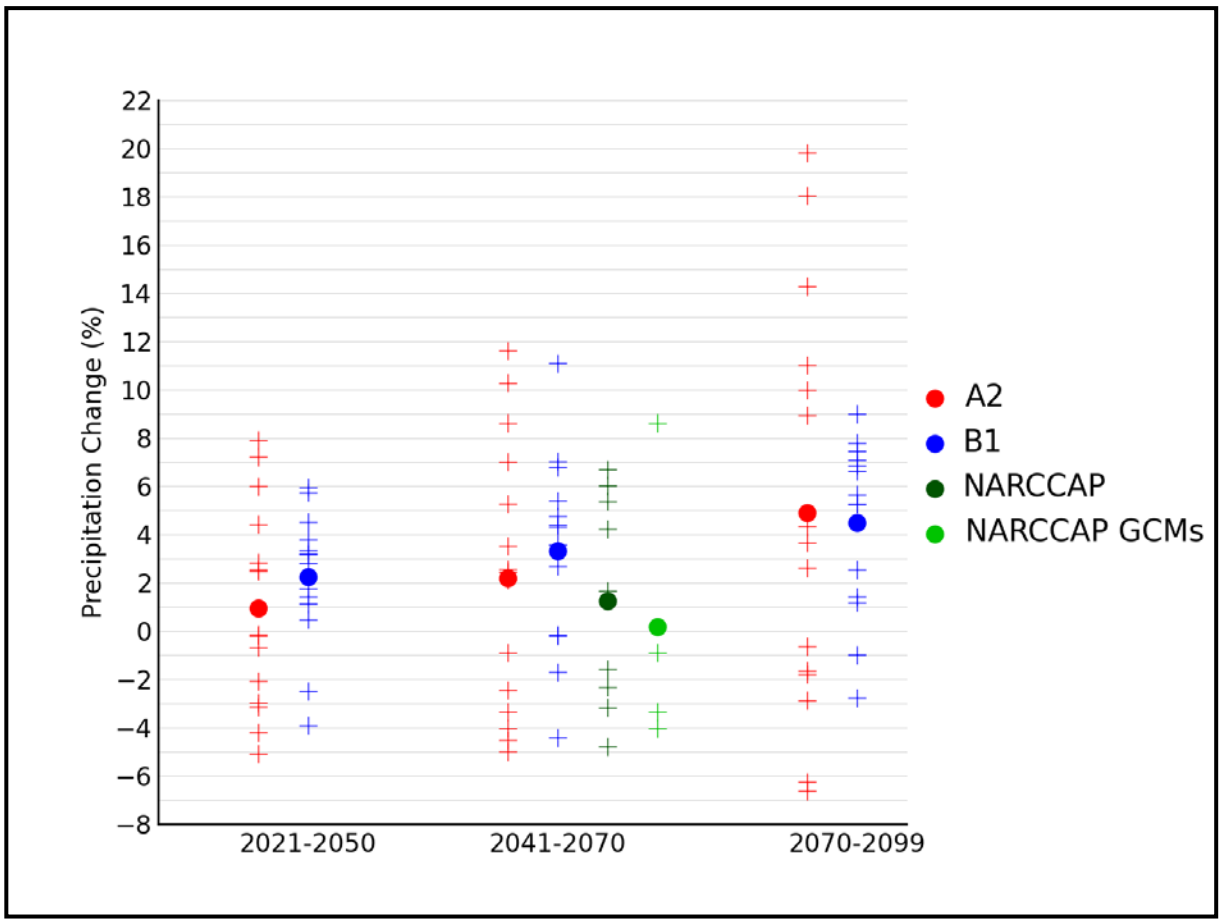

Figure 22. Simulated annual mean precipitation change (%) for the Northwest region, for each future time period (2021-2050, 2041-2070, and 2070-2099) with respect to the reference period of 1971-1999. Values are given for the high (A2) and low (B1) emissions scenarios for the 14 (B1) or 15 (A2) CMIP3 models. Also shown for 2041-2070 (high emissions scenario only) are values (relative to 1971-2000) for 9 NARCCAP models, as well as for the 4 GCMs used to drive the NARCCAP simulations. The small plus signs indicate each individual model and the circles depict the multi-model means. The ranges of model-simulated changes are very large compared to the mean changes and to differences between the A2 and B1 scenarios.

Figure 23 shows the simulated change in seasonal mean precipitation for each future time period with respect to 1971-1999, for the high (A2) emissions scenario, averaged over the entire Northwest region for the 15 CMIP3 models, as well as the NARCCAP models for 2055, relative to 1971-2000. Again, both the multi-model mean and individual model values are shown. The CMIP3 models simulate increases for winter, spring, and fall, but decreases for summer, for all three time periods. The changes is summer precipitation are large compared to those for the other seasons, ranging from around -12% in 2035 to -24% in 2085. The magnitudes of the NARCCAP multi-model mean values are similar to those of the CMIP3 models for three of the four seasons; for summer the NARCCAP mean is somewhat less negative than the CMIP3 mean. As was the case for the annual totals in Fig. 22, the model ranges in Fig. 23 are large compared to the multi-model mean differences. This illustrates the large uncertainty in the precipitation estimates using these simulations.

3.8. Extreme Precipitation

Figure 24 shows the spatial distribution of the multi-model mean change in the average annual number of days with precipitation exceeding 1 inch, for 8 NARCCAP regional climate model simulations. Again this is the difference between the period of 2041-2070 and the 1980-2000 model reference period, for the high (A2) emissions scenario. In addition to this difference map, maps of model simulations of the actual values for historical conditions (NARCCAP models driven by the NCEP Reanalysis II) and for the future are also displayed for comparison. Most areas exhibit increases, with the largest changes of more than 40% occurring east of the Cascades. These areas presently have less than 5 days per year with precipitation greater than 1 inch and would still have relatively few days by 2055. No overall trend in extreme precipitation events has been observed in the Northwest region over the past century (see Section 2.4.4). It can be seen that changes in days exceeding 1 inch are not statistically significant for most models (category 1) over the majority of grid points. This means that most models are in agreement that any changes will be smaller than the normal year-to-year variations that occur under this emissions scenario. In areas of eastern Washington and Oregon, and northern Idaho, however, most models indicate increases in days with precipitation of more than 1 inch that are larger than these normal variations (category 3).

Figure 25 shows the NARCCAP multi-model mean change in the average annual number of days with precipitation exceeding 0.3 inches between 2055 and the model reference period of 1980-2000, for the high (A2) emissions scenario. Most areas east of the Cascades exhibit increases, with the largest changes of more than 15% occurring in southeast Oregon. Most areas west of the Cascades and a small area of central Idaho have model-simulated decreases. In both cases (number days > 0.3 inches and > 1 inch), the changes are statistically significant (category 3) under this emissions scenario, only for small areas in central Washington and Oregon.

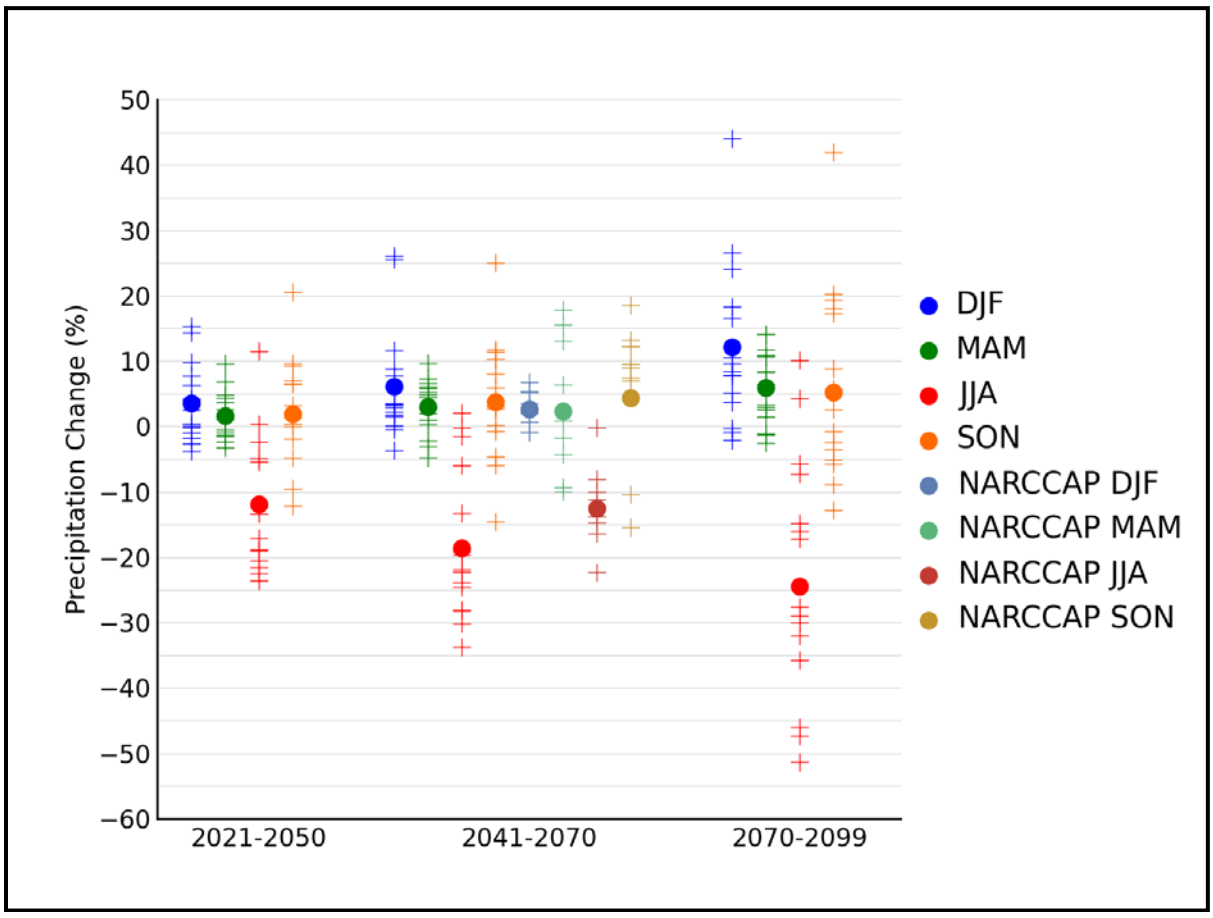

Figure 23. Simulated seasonal mean precipitation change (%) for the Northwest region, for each future time period (2021-2050, 2041-2070, and 2070-2099) with respect to the reference period of 1971-1999. Values are given for all 15 CMIP3 models for the high (A2) emissions scenario. Also shown are values (relative to 1971-2000) for 9 NARCCAP models for 2041-2070. The small plus signs indicate each individual model and the circles depict the multi-model means. Seasons are indicated as follows: winter (DJF, December-January-February), spring (MAM, March-April-May), summer (JJA, June-July-August), and fall (SON, September-October-November). The ranges of model-simulated changes are large compared to the mean changes and to differences between the seasons.

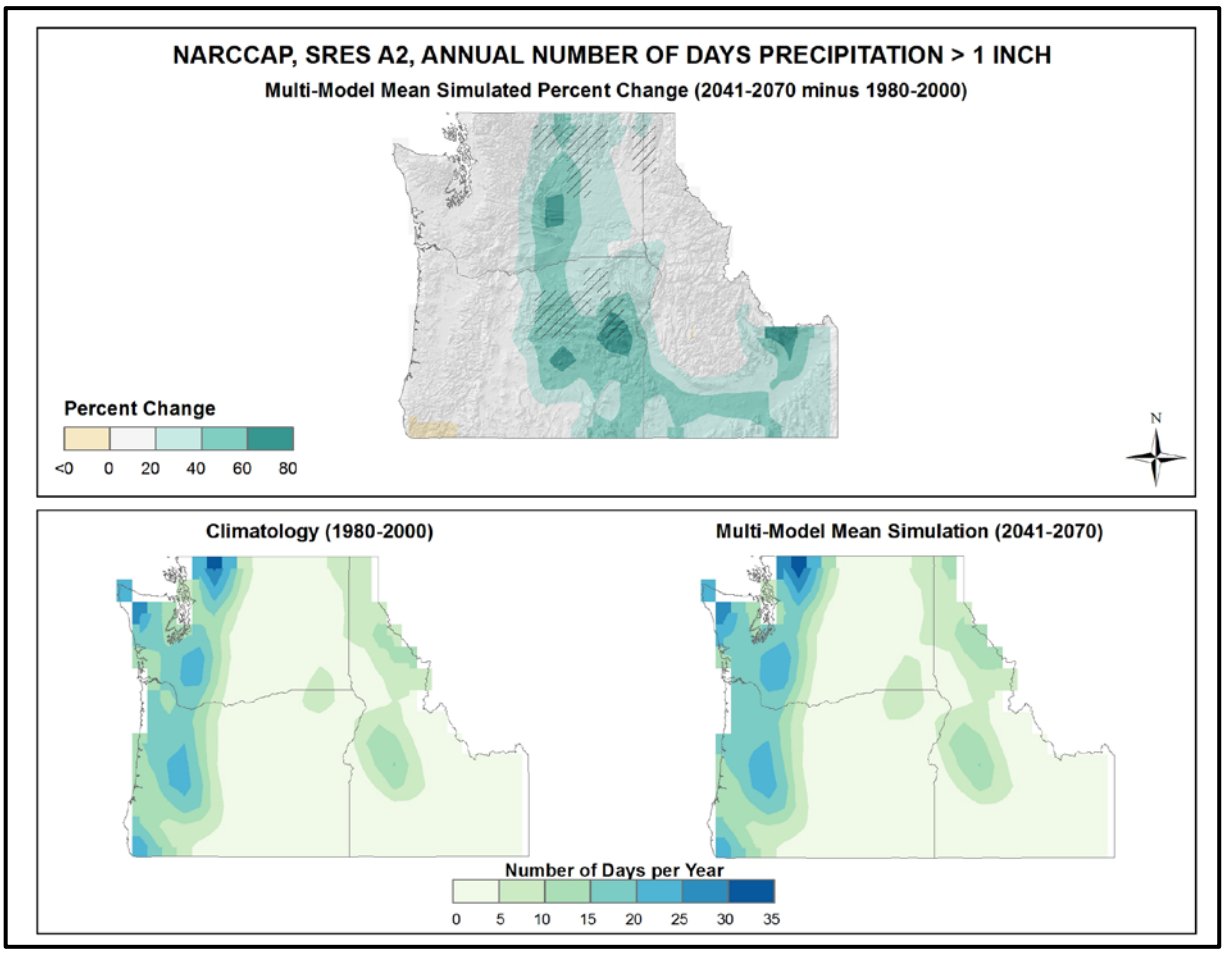

Figure 24. Simulated percentage difference in the mean annual number of days with precipitation of greater than one inch for the Northwest region, for the 2041-2070 time period with respect to the reference period of 1980-2000 (top). Color only (category 1) indicates that less than 50% of the models show a statistically significant change in the number of days. Color with hatching (category 3) indicates that more than 50% of the models show a statistically significant change in the number of days, and more than 67% agree on the sign of the change (see text). Mean annual number of days with precipitation of greater than one inch for the 1980-2000 reference period (bottom left). Simulated mean annual number of days with precipitation of greater than one inch for the 2041-2070 future time period (bottom right). These are multi-model means from 8 NARCCAP regional climate simulations for the high (A2) emissions scenario. The models simulate increases over most of the region.

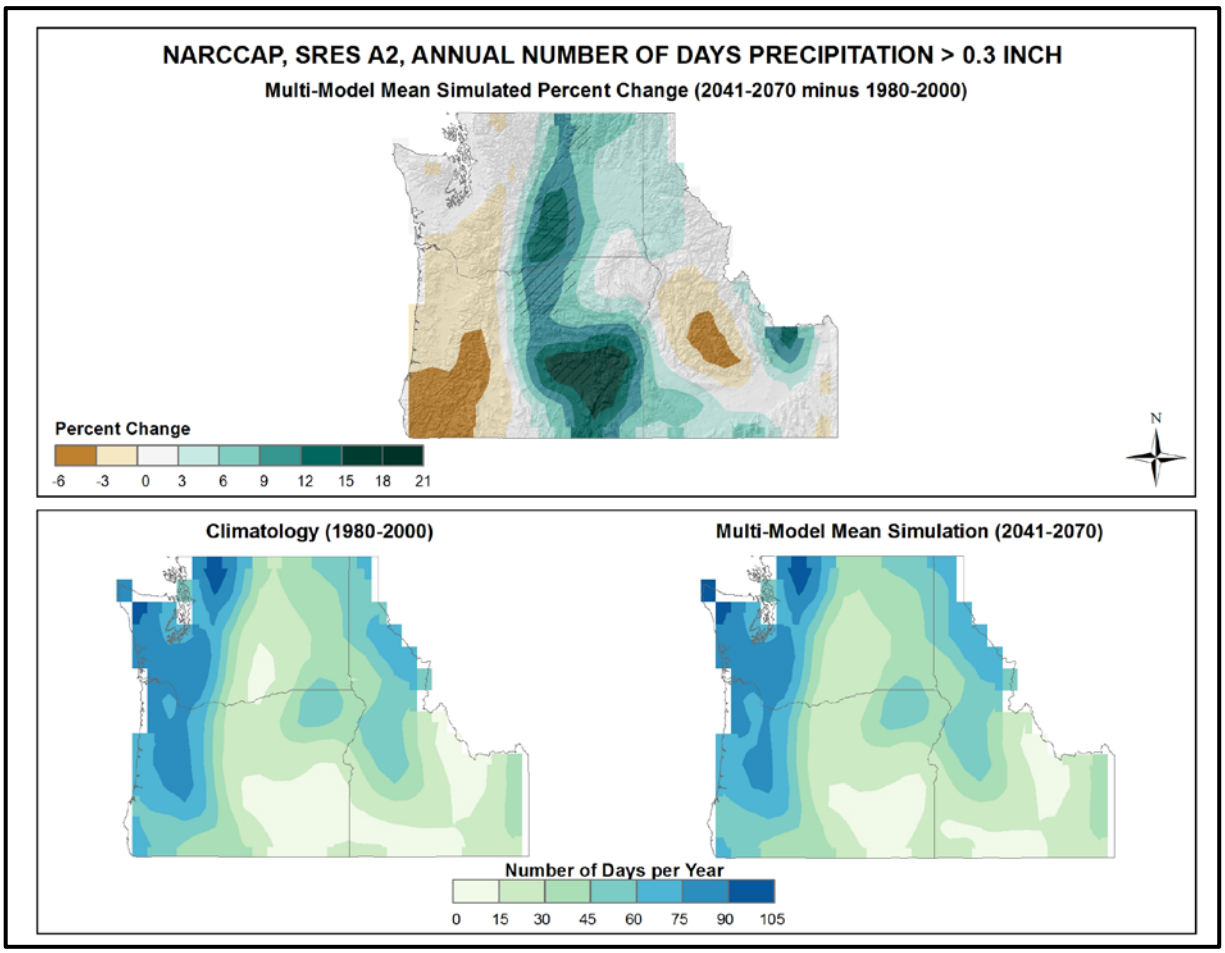

Figure 25. Simulated percentage difference in the mean annual number of days with precipitation of greater than 0.3 inches for the Northwest region, for the 2041-2070 time period with respect to the reference period of 1980-2000 (top). Color only (category 1) indicates that less than 50% of the models show a statistically significant change in the number of days. Color with hatching (category 3) indicates that more than 50% of the models show a statistically significant change in the number of days, and more than 67% agree on the sign of the change (see text). Mean annual number of days with precipitation of greater than 0.3 inches for the 1980-2000 reference period (bottom left). Simulated mean annual number of days with precipitation of greater than 0.3 inches for the 2041-2070 future time period (bottom right). These are multi-model means from 8 NARCCAP regional climate simulations for the high (A2) emissions scenario. The models simulated increases for the central part of the region, with the greatest increases occurring in southeastern Oregon. There are simulated decreases in the southwestern part of the region and in central Idaho.

Consecutive days with little or no precipitation reduce soil moisture levels and put stress on plants. Figure 26 shows the NARCCAP multi-model mean change in the average annual maximum number of consecutive days with precipitation less than 0.1 inches (3 mm) between 2055 and the model reference period of 1980-2000, for the high (A2) emissions scenario. All areas are simulated to see an increase in the maximum number of consecutive days with little or no precipitation, the greatest being up to 15 days in western Oregon. Most other areas are simulated to see annual increases of up to 12 days. For the majority of grid points most models indicate statistically significant changes in the number of consecutive days with precipitation of less than 0.1 inches (category 3). This means that most models are in agreement that any changes will be greater than the normal year-to-year variations that occur under this emissions scenario. Changes are not statistically significant for most models (category 1) in small areas of eastern Oregon. In a few small areas of southern Idaho the models are in disagreement about the sign of the changes (category 2).

3.9. Tabular Summary of Selected Precipitation Variables

The mean changes for select precipitation-based variables derived from 8 NARCCAP simulations for 2055 with respect to the model reference period of 1971-2000, for the high (A2) emissions scenario, are summarized in Table 8. The same variables from the 8 CMIP3 statistically-downscaled (Daily_CMIP3) simulations are also shown for comparison. These spatially-averaged values were calculated as described for Table 5.

Table 8. Multi-model means and standard deviations of the simulated mean annual change in select precipitation variables from 8 NARCCAP simulations for the Northwest region. Multi-model means from the 8 Daily_CMIP3 simulations are also shown for comparison. Analyses are for the 2041-2070 time period with respect to the reference period of 1971-2000, for the high (A2) emissions scenario.

Precipitation Variable	NARCCAP Mean	NARCCAP Standard Deviation	Daily_CMIP3 Mean
#days > 1 inch	+13%	7%	+19%
#days > 2 inches	+15%	14%	+29%
#days > 3 inches	+22%	22%	+36%
#days > 4 inches	+29%	40%	+43%
Consecutive #days < 0.1 inches	+6 days	+3 days	+8 days

For the NARCCAP data, the multi-model mean number of days with precipitation greater than certain thresholds increases for all threshold values (+13% for 1 inch, +15% for 2 inches, +22% for 3 inches, and +29% for 4 inches). The increases are higher for the more extreme thresholds. The average annual maximum number of consecutive days with precipitation less than 0.1 inches increases by 6 days. The multi-model means from the CMIP3 statistically-downscaled simulations are higher than their NARCCAP counterparts. The number of days with precipitation exceeding certain thresholds again increases for all 4 thresholds (+19% for 1 inch, +29% for 2 inches, +36% for 3 inches, and +43% for 4 inches). The average number of consecutive days with precipitation less than 0.1 inches increases by 10 days, compared to the NARCCAP value of 8 days.

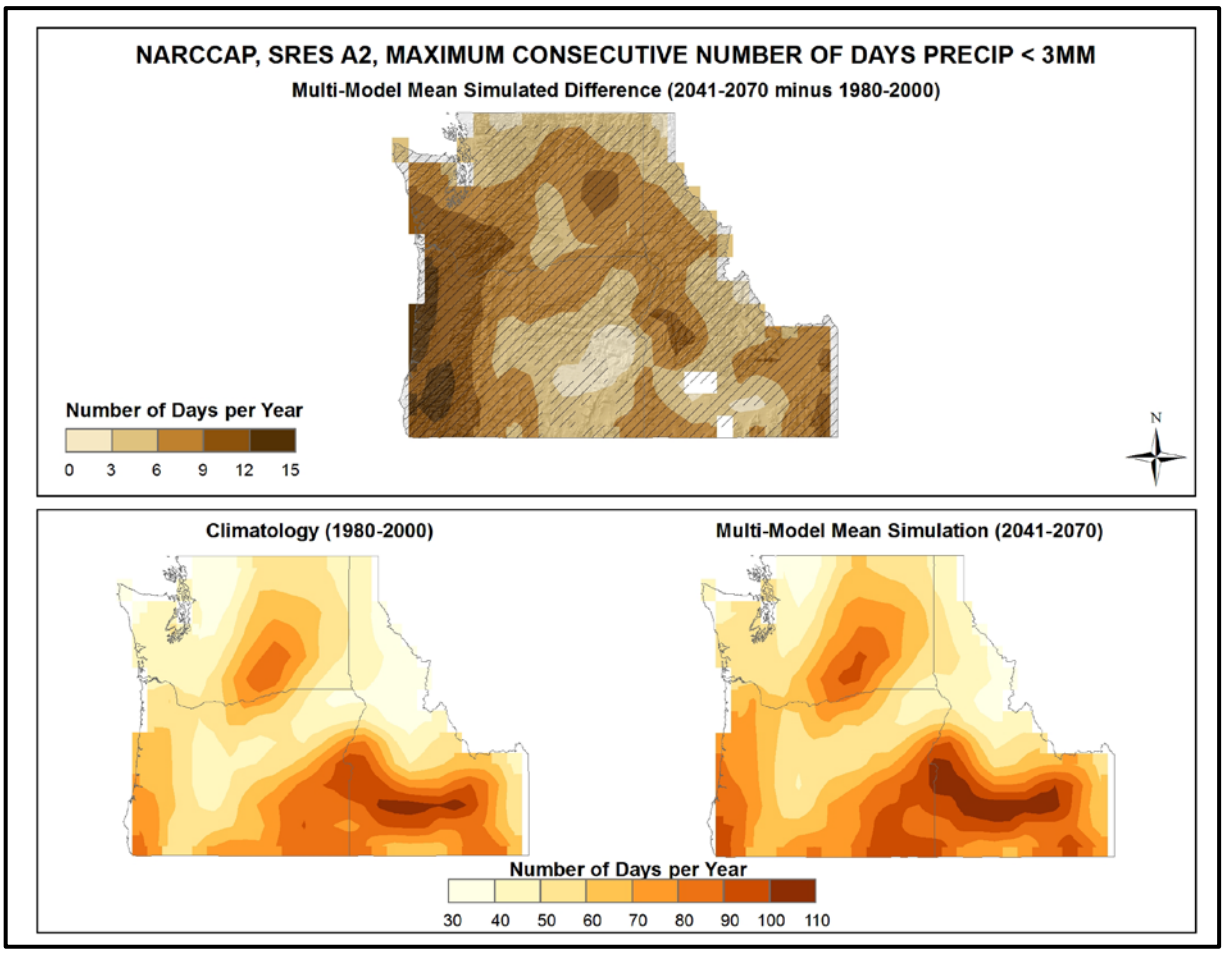

Figure 26. Simulated difference in the mean annual maximum number of consecutive days with precipitation of less than 0.1 inches/3 mm for the Northwest region, for the 2041-2070 time period with respect to the reference period of 1980-2000 (top). Color only (category 1) indicates that less than 50% of the models show a statistically significant change in the number of consecutive days. Color with hatching (category 3) indicates that more than 50% of the models show a statistically significant change in the number of consecutive days, and more than 67% agree on the sign of the change. Whited out areas (category 2) indicate that more than 50% of the models show a statistically significant change in the number of consecutive days, but less than 67% agree of the sign of the change (see text). Mean annual maximum number of consecutive days with precipitation of less than 0.1 inches/3 mm for the 1980-2000 reference period (bottom left). Simulated mean annual maximum number of consecutive days with precipitation of less than 0.1 inches/3 mm for the 2041-2070 future time period (bottom right). These are multi-model means from 8 NARCCAP regional climate simulations for the high (A2) emissions scenario. The models simulate increases throughout the region, with the greatest increases occurring in western Oregon.

3.10. Comparison Between Model Simulations and Observations

In this section, some selected comparisons between CMIP3 model simulations and observations are presented. These are limited to annual and seasonal temperature and precipitation. The model simulations of the 20th century that are shown herein are based on estimated historical forcings of the climate systems, including such factors as greenhouse gases, volcanic eruptions, solar variations, and aerosols. Also shown are the simulations of the 21st century for the high (A2) emissions scenario.

In these comparisons, both model and observational data are expressed as deviations from the 1901-1960 average. As explained in Section 2.4 (Climatic Trends), acceleration of the anthropogenic forcing occurs shortly after 1960. Thus, for the purposes of comparing net warming between periods of different anthropogenic forcing, 1960 is a rational choice for the ending date of a reference period. It is not practical to choose a beginning date earlier than about 1900 because many model simulations begin in 1900 or 1901 and the uncertainties in the observational time series increase substantially prior to 1900. Therefore, the choice of 1901-1960 as the reference period is well suited for this purpose (comparing the net warming between periods of different anthropogenic forcing). However, there are some uncertainties in the suitability of the 1901-1960 reference period for this purpose. Firstly, there is greater uncertainty in the natural climate forcings (e.g., solar variations) during this time period than in the latter half of the 20th century. If there are sizeable errors in the estimated natural forcings used in climate models, then the simulations will be affected; this type of error does not represent a model deficiency. Secondly, the 1930s "Dust Bowl" era is included in this period. The excessive temperatures experienced then, particularly during the summers, are believed to be caused partially by poor land management through its effects on the surface energy budget. Climate models do not incorporate land management changes and there is no expectation that models should simulate the effects of such. Thirdly, there are certain climate oscillations that occur over several decades. These oscillations have important effects on regional temperatures. A 60-year period is too short to sample entire cycles of some of these, and thus only represents a partial sampling of the true baseline climate.

Figure 27 shows observed (using the same data set as shown in Fig. 4) and simulated decadal mean annual temperature changes for the Northwest U.S. from 1900 to 2100, expressed as deviations from the 1901-1960 average. The observed rate of warming is similar to that of the models, with the overall amount of 20th century warming being contained within the envelope of modeled values.

For the spring and summer seasons (Fig. 28), observed temperatures for the 1930s are higher than any model simulation. The observed spring cooling from the 1940s to the 1950s is greater than simulated by any model. For the winter and fall seasons, the observed temperatures are lower than most model simulations during the 1910s to 20s. However, the overall warming for the entire observational record is within the range of model simulations for all seasons.

The 21st century portions of the time series indicate that the simulated future warming is much larger than the observed and simulated temperature changes for the 20th century.

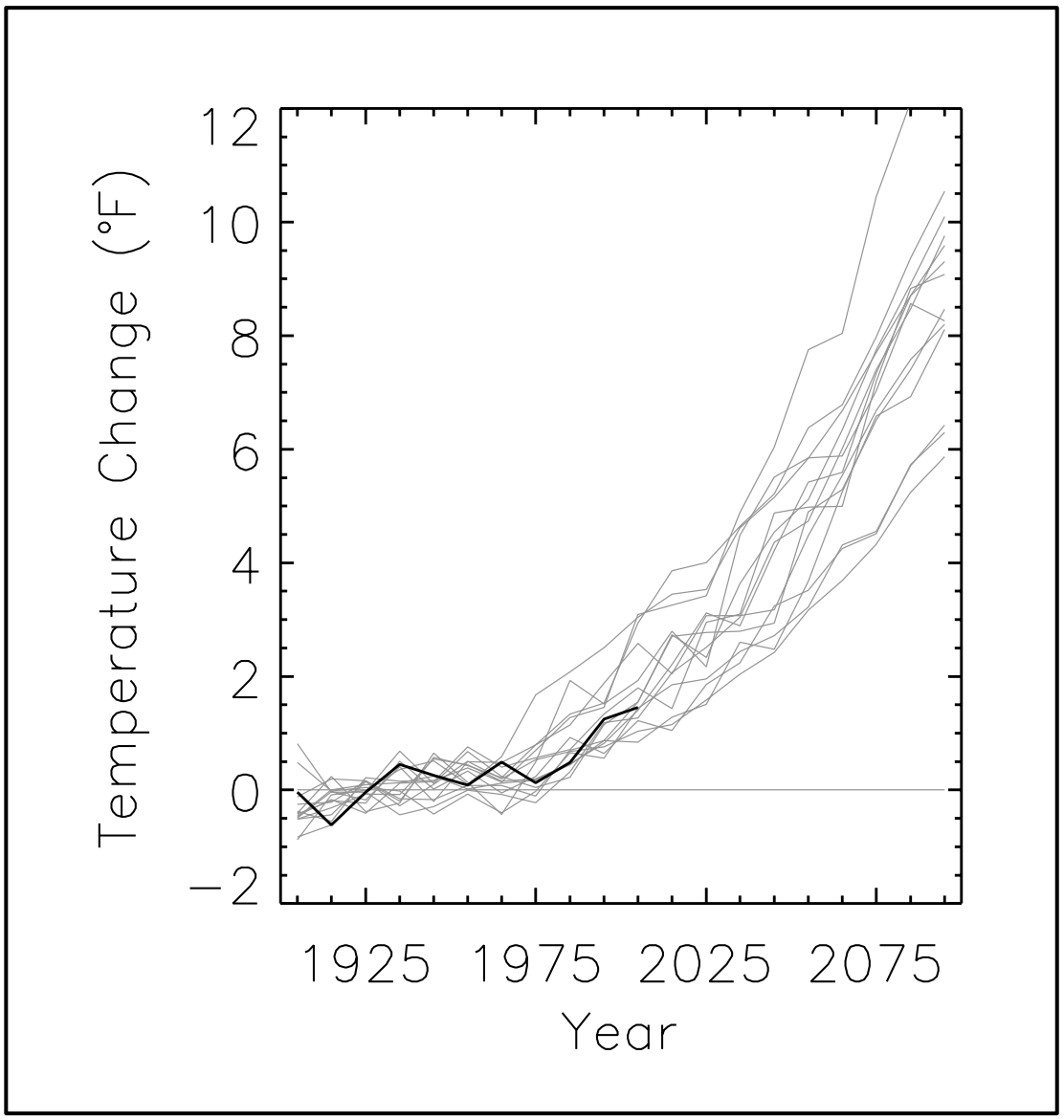

Figure 27. Observed decadal mean annual temperature change (deviations from the 1901-1960 average, °F) for the Northwest U.S. (black line). Based on a new gridded version of COOP data from the National Climatic Data Center, the CDDv2 data set (R. Vose, personal communication, July 27, 2012). Gray lines indicate the 20th and 21st century simulations from 15 CMIP3 models, for the high (A2) emissions scenario. The observed rate of warming is within the envelope of model simulations.

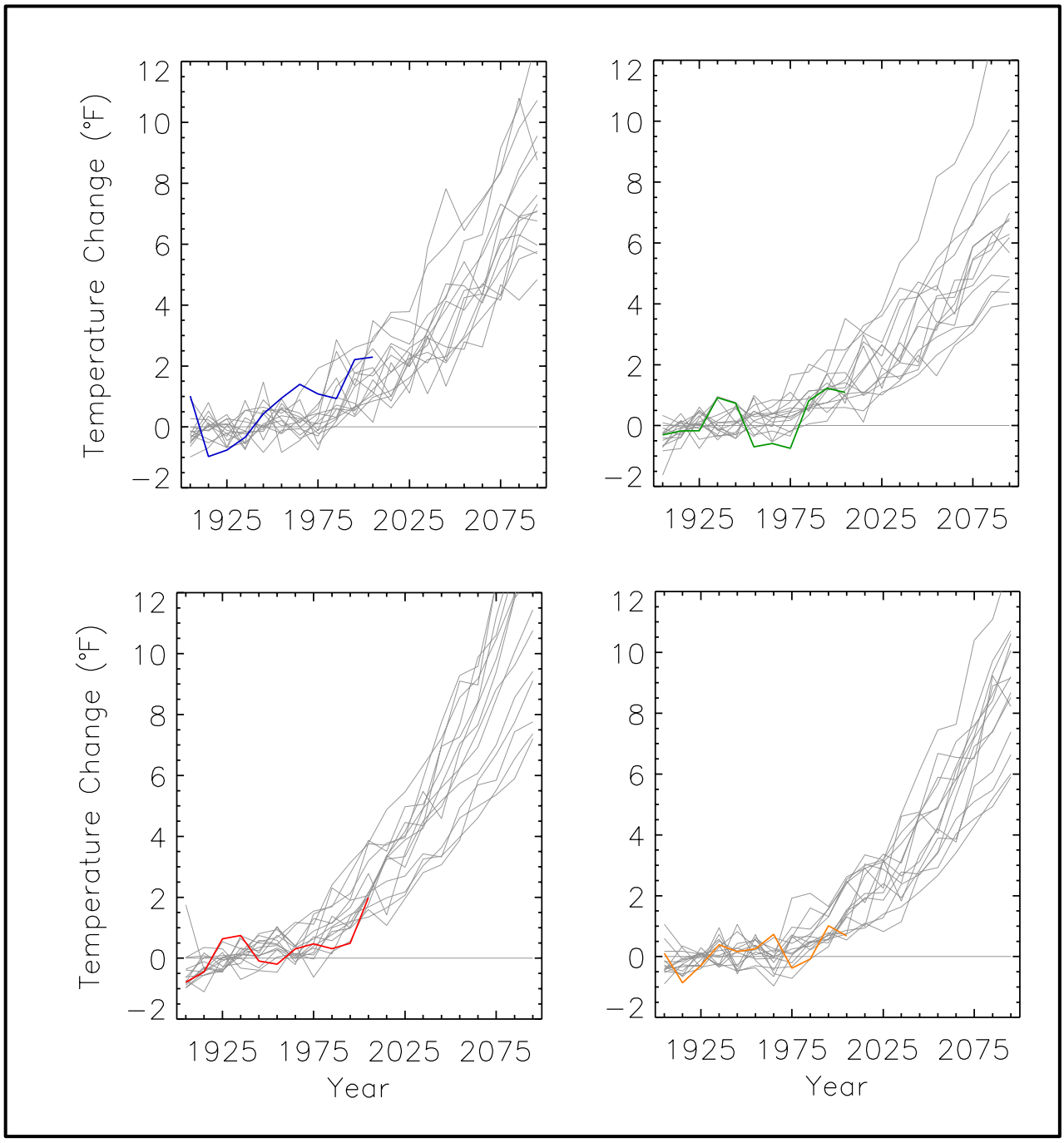

Figure 28. Observed decadal mean temperature change (deviations from the 1901-1960 average, °F) for the Northwest U.S. for winter (top left, blue line), spring (top right, green line), summer (bottom left red line), and fall (bottom right, orange line). Based on a new gridded version of COOP data from the National Climatic Data Center, the CDDv2 data set (R. Vose, personal communication, July 27, 2012). Gray lines indicate 20th and 21st century simulations from 15 CMIP3 models, for the high (A2) emissions scenario. The observed amount of 20th century warming is generally within the envelope of model simulations.

Observed and model-simulated decadal mean precipitation changes (using the same data set as shown in Fig. 5) can be seen in Fig. 29 for annual and Fig. 30 for seasonal values. The observed variability is generally greater than the model simulations. This leads to a number of individual observed decadal values being outside the envelope of the model simulations. This is particularly true of the summer where there are a few very large observed anomalies that are well outside the envelope of the model simulations. The 21st century portions of the time series show increased variability among the model simulations. It can be seen that the majority of the models simulate an overall increase in precipitation for winter and spring, and a decrease for the summer season.

The CMIP3 archive contains a total of 74 simulations of the 20th century, 40 simulations of the 21st century for the high (A2) emissions scenario, and 32 simulations of the 21st century for the low (B1) emissions scenario from a total of 23 different models (many models performed multiple simulations for these periods). An exploratory analysis of the entire archive was performed, limited to temperature and to the year as a whole. As before, the data were processed using 1901-1960 as the reference period to calculate anomalies.

Figure 31 compares observations of annual temperature with the entire suite of model simulations. For each model, the annual anomalies were first calculated using the 1901-1960 period as the reference. Then the mean 1901-1960 value from the observations was added to each annual anomaly, essentially removing the model mean bias. In this presentation, the multi-model mean and the 5th and 95th percentile bounds of the model simulations are shown. The mean and percentile values were calculated separately for each year. Then, the curves were smoothed with a 10-year moving boxcar average. The observational time series is not smoothed. During the first half of the 20th century, the observed annual values vary around the model mean because that is the common reference period. These values occasionally fall outside the 5th/95th percentile bounds for the model simulations, most noticeably in 1934. After about 1960, the observed values are generally within the 5th/95th percentile bounds but on the lower end of the distribution. The rate of observed warming after 1960 is similar to that of the multi-model mean, a similar result to that found in Fig. 27 for a subset of the CMIP3 models. A few values are below the 5th percentile bound while none are above the 95th percentile bound after 1960.

On decadal time scales, climate variations arising from natural factors can be comparable to or larger than changes arising from anthropogenic forcing. An analysis of change on such time scales was performed by examining the decadal changes simulated by the CMIP3 models with respect to the most recent historical decade of 2001-2010. Figure 32 shows the simulated change in decadal mean values of annual temperature for each future decadal time period with respect to the most recent historical decade of 2001-2010, averaged over the entire Northwest region for the 14 (B1) or 15 (A2) CMIP3 models. For the 2011-2020 decade, the temperature increases are not statistically significant relative to the 2001-2010 decade for most of the models. As the time period increases, more of the individual models simulate statistically significant temperature changes, with all being significant at the 95% confidence level by 2055 for the high emissions scenario (2065 for the low emissions scenario). By this point, all of the model decadal mean values lie outside the 10-90th percentile range of the historical annual temperature anomalies. As also shown in Fig. 27, the model simulations show increased variability over time, with the inter-model range of temperature changes for 2091-2100 being more than double that for 2061-2070 (for the high emissions scenario).

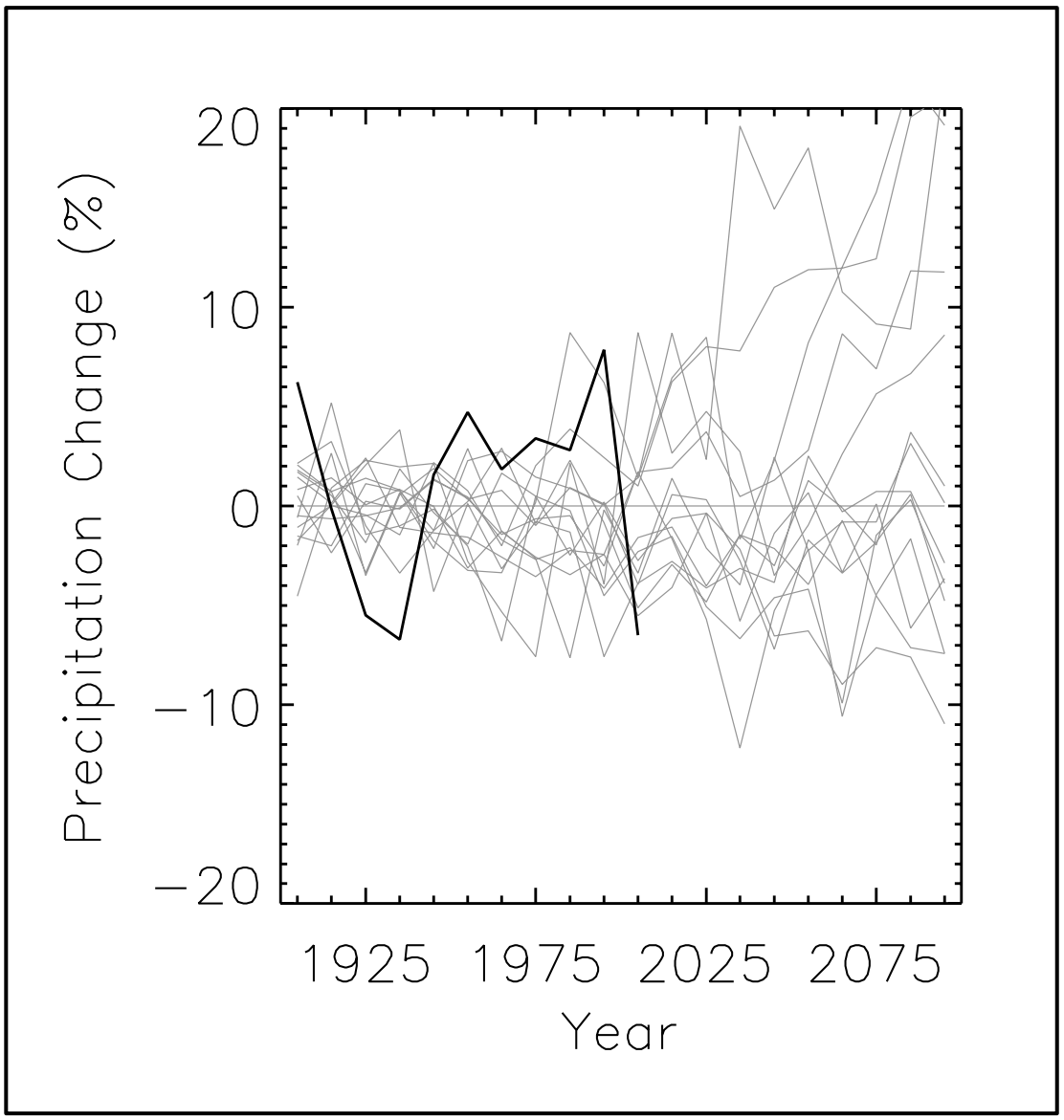

Figure 29. Observed decadal mean annual precipitation change (deviations from the 1901-1960 average, %) for the Northwest U.S. (black line). Based on a new gridded version of COOP data from the National Climatic Data Center, the CDDv2 data set (R. Vose, personal communication, July 27, 2012). Gray lines indicate the 20th and 21st century simulations from 15 CMIP3 models, for the high (A2) emissions scenario. Observed precipitation variations are greater than the variations in the model simulations.

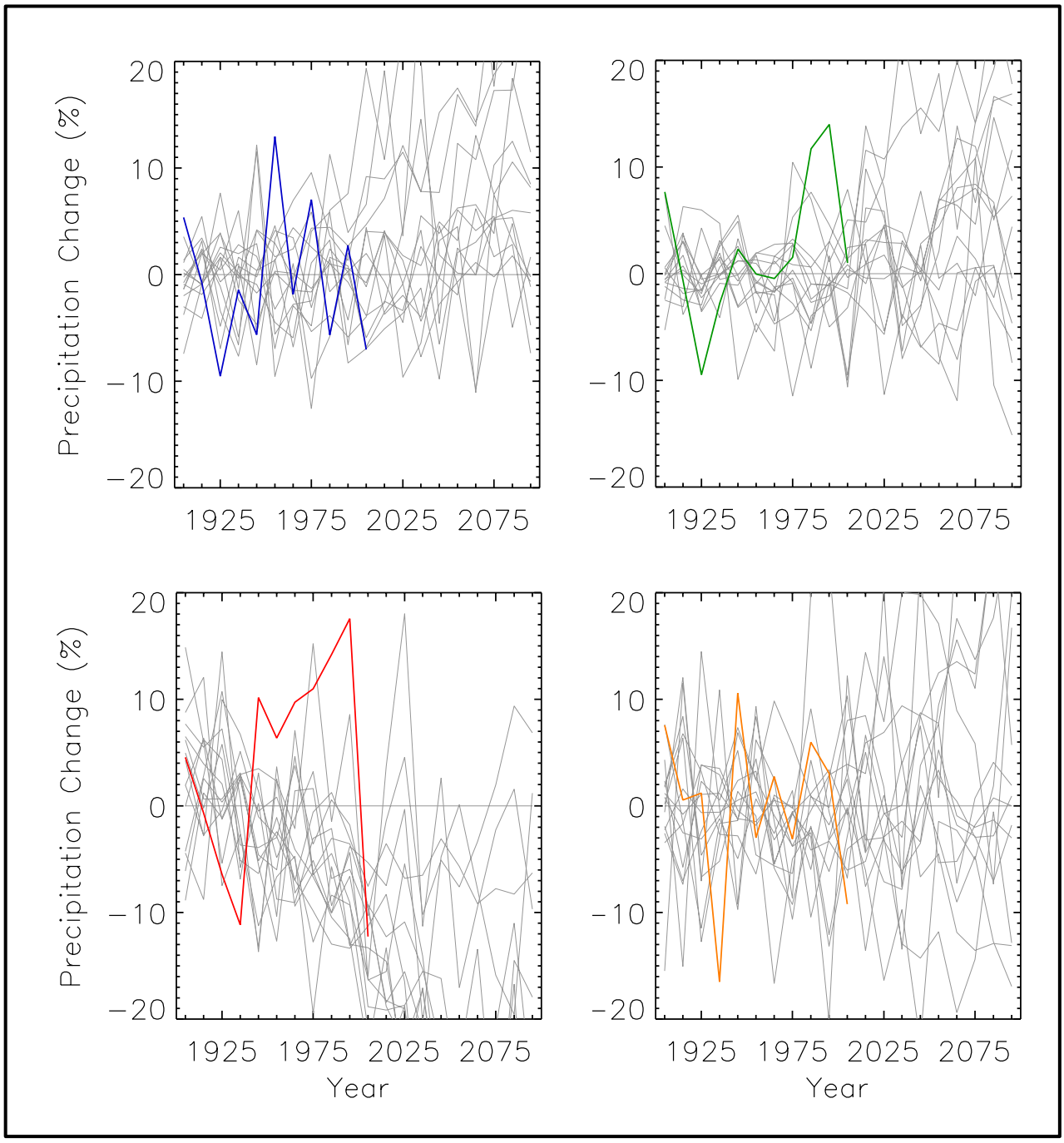

Figure 30. Observed decadal mean precipitation change (deviations from the 1901-1960 average, %) for the Northwest U.S. for winter (top left, blue line), spring (top right, green line), summer (bottom left red line), and fall (bottom right, orange line). Based on a new gridded version of COOP data from the National Climatic Data Center, the CDDv2 data set (R. Vose, personal communication, July 27, 2012). Gray lines indicate 20th and 21st century simulations from 15 CMIP3 models, for the high (A2) emissions scenario. Observed seasonal precipitation variations are greater than variations of the model simulations for all seasons.

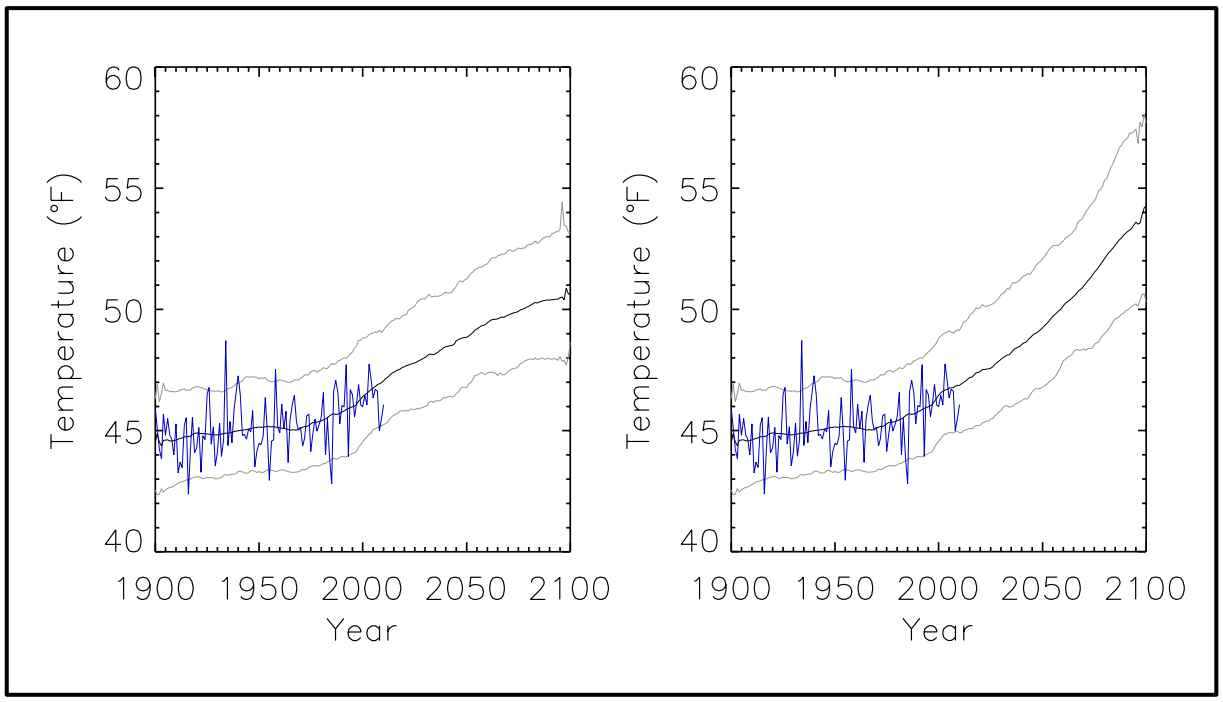

Figure 31. Time series of mean annual temperature for the Northwest region from observations (blue) and from all available CMIP3 global climate model simulations (black and grey). Black represents the mean and grey indicates the 5 and 95% limits of the model simulations. Model mean and percentile limits were calculated for each year separately and then smoothed. Results are shown for the low (B1) emissions scenario (left) and the high (A2) emissions scenario (right). A total of 74 simulations of the 20th century were used. For the 21st century, there were 40 simulations for the high emissions scenario and 32 for the low emissions scenario. For each model simulation, the annual temperature values were first transformed into anomalies by subtracting the simulation's 1901-1960 average from each annual value. Then, the mean bias between model and observations was removed by adding the observed 1901-1960 average to each annual anomaly value from the simulation. For each year, all available model simulations were used to calculate the multi-model mean and the 5th and 95th percentile bounds for that year. Then, the mean and 5th and 95th percentile values were smoothed with a 10-year moving boxcar average.

The corresponding simulated change in decadal mean values of annual precipitation can be seen in Fig. 33. Unlike for temperature, many of the model values of precipitation change are not statistically significant in all decades out to 2091-2099. For both emissions scenarios, positive changes in multi-model mean precipitation are simulated for almost the entire period. Little change in variability is seen over time for either scenario, with a large number of models lying outside the 10-90th percentile range for all time periods.

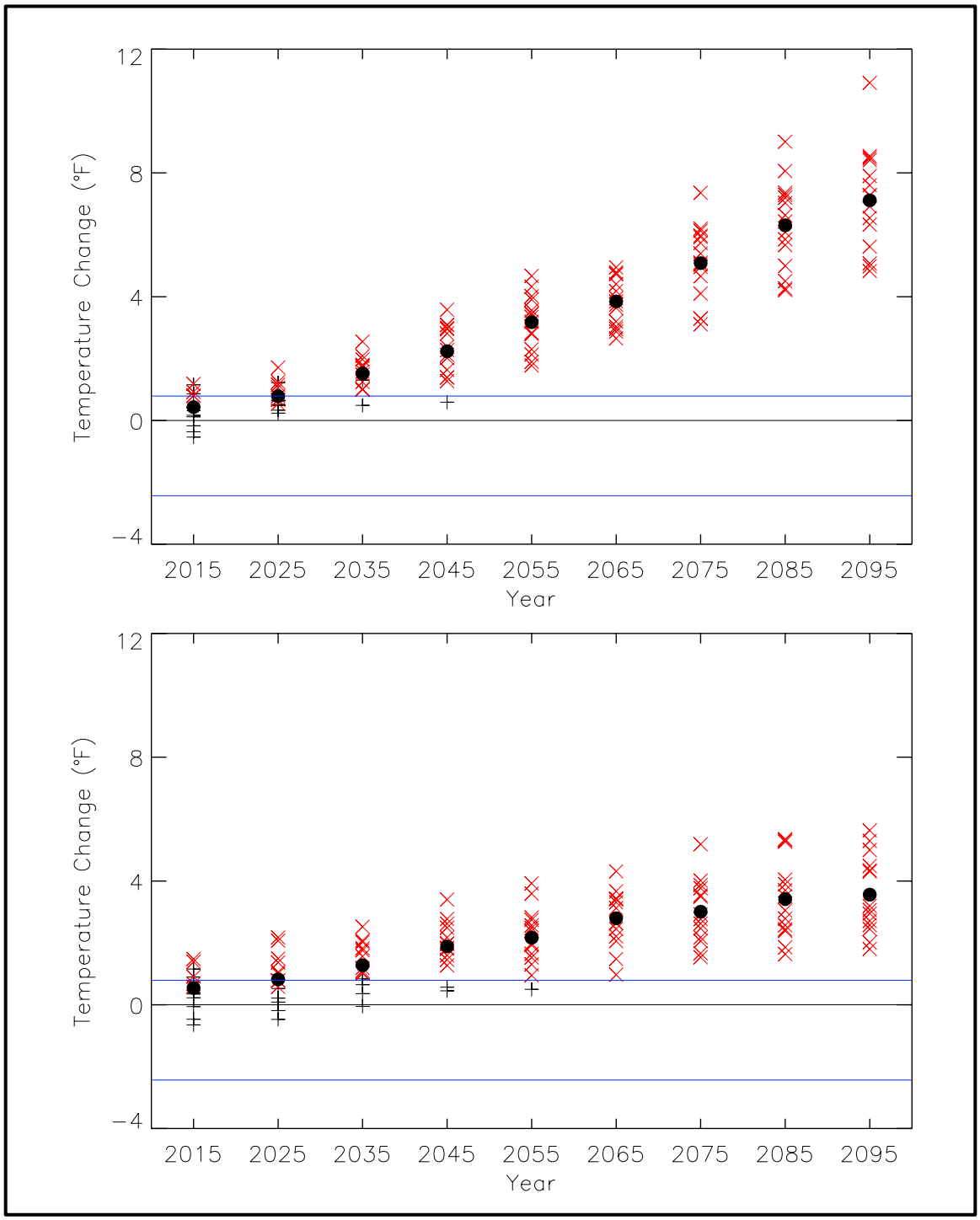

Figure 32. Simulated decadal mean change in annual temperature (°F) for the Northwest U.S. for each future decadal time period (represented by their approximate midpoints, e.g., 2015 = 2011-2020), with respect to the reference period of 2001-2010. Values are given for the high (A2, top) and low (B1, bottom) emissions scenarios for the 14 (B1) or 15 (A2) CMIP3 models. Large circles depict the multi-model means. Each individual model is represented by a black plus sign (+), or a red x if the value is statistically significant at the 95% confidence level. Blue lines indicate the 10th and 90th percentiles of 30 annual anomaly values from 1981-2010. The model simulated warming by 2015 is not statistically significant for many models but by mid-21st century, all models simulate statistically significant warming.

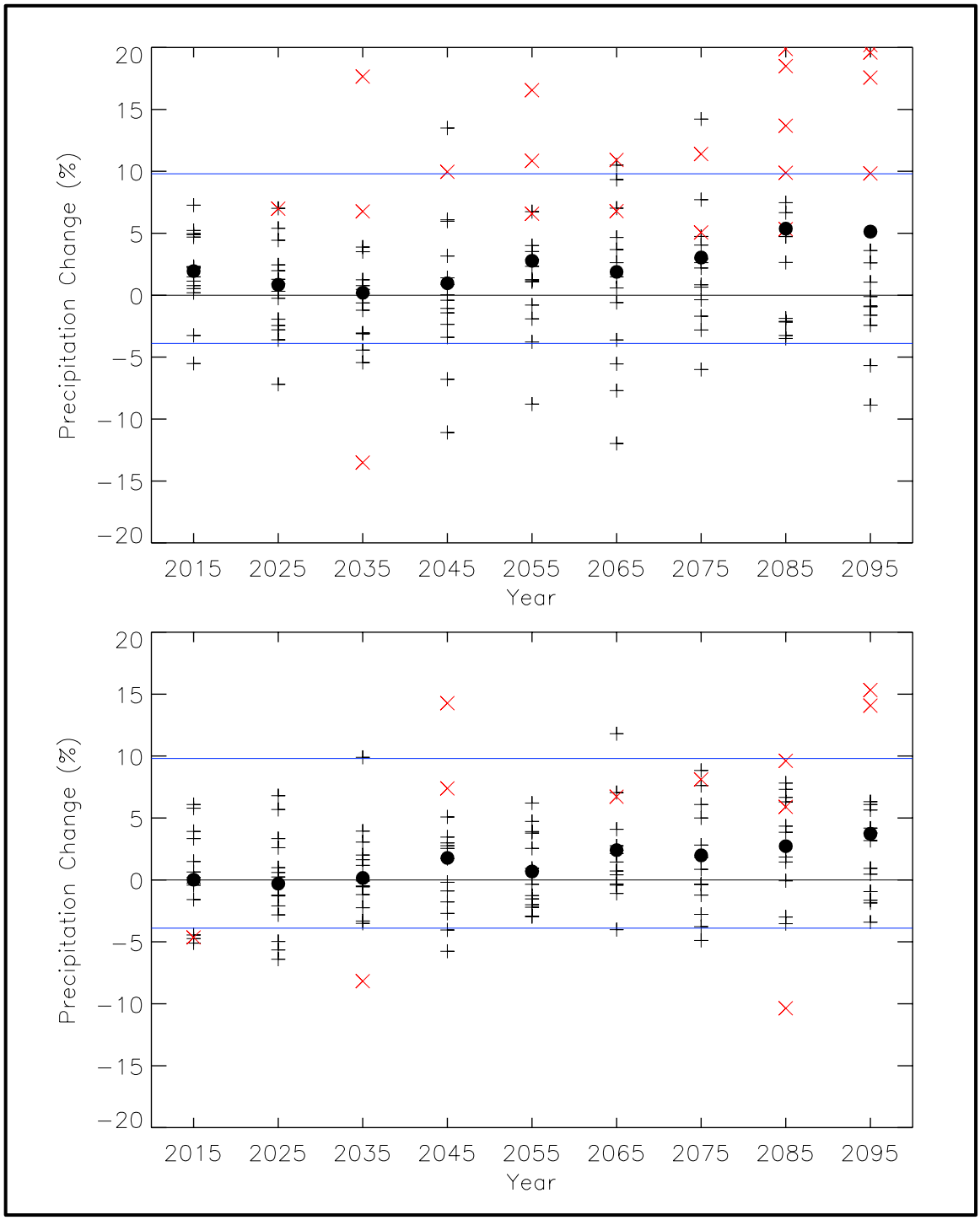

Figure 33. Simulated decadal mean change in annual precipitation (%) for the Northwest U.S. for each future decadal time period (represented by their approximate midpoints, e.g., 2015 = 2011-2020), with respect to the reference period of 2001-2010. Values are given for the high (A2, top) and low (B1, bottom) emissions scenarios for the 14 (B1) or 15 (A2) CMIP3 models. Large circles depict the multi-model means. Each individual model is represented by a black plus sign (+), or a red x if the value is statistically significant at the 95% confidence level. Blue lines indicate the 10th and 90th percentiles of the 30 annual anomaly values from 1981-2010. Many models simulate precipitation changes that are not statistically significant out to the end of the 21st century.

4. SUMMARY

The primary purpose of this document is to provide physical climate information for potential use by the authors of the 2013 National Climate Assessment report. The document contains two major sections. One section summarizes historical conditions in the U.S. Northwest and primarily focuses on trends in temperature and precipitation metrics that are important in the region. The core observational data set used is that of the National Weather Service's Cooperative Observer Network (COOP).

The second section summarizes climate model simulations for two scenarios of the future path of greenhouse gas emissions: the IPCC SRES high (A2) and low (B1) emissions scenarios. These simulations incorporate analyses from multiple sources, the core source being Coupled Model Intercomparison Project 3 (CMIP3) simulations. Additional sources consist of statistically- and dynamically-downscaled data sets, including simulations from the North American Regional Climate Change Assessment Program (NARCCAP). Analyses of the simulated future climate are provided for the periods of 2021-2050, 2041-2070, and 2070-2099), with changes calculated with respect to an historical climate reference period (1971-1999, 1971-2000, or 1980-2000). The resulting climate conditions are to be viewed as scenarios, not forecasts, and there are no explicit or implicit assumptions about the probability of occurrence of either scenario. The basis for these climate scenarios (emissions scenarios and sources of climate information) were considered and approved by the National Climate Assessment Development and Advisory Committee.

Some key characteristics of the historical climate include:

- Climatic phenomena that have major impacts on the Northwest include winter storms, flood-producing extreme precipitation, drought, heat and cold waves, and sea-level rise.
- Temperatures have generally been above the 1901-1960 average for the last 25 years, both annually and for all seasons. Temperature trends are statistically significant (at the 95% level) for all seasons and the year as a whole, ranging from +0.10 to +0.20°F per decade.
- Annual precipitation has exhibited very high variability since 1976, compared to the previous 75 years. Though the recent 35 years have seen a few very wet years – including the wettest on record, 1996 – the majority have been below the 1901-1960 average. Seasonal averages are similar, with winter having notably high variability.
- The frequency of cold waves has been generally low since 1990, with the exception of a few years (1996, 1998, and 2009). The occurrence of heat waves has been high in the last 20 years – about 70% above the long-term average.
- The 1990s saw a high frequency of extreme precipitation events, but since then, the numbers have been about the same as the prior records. There is no evidence of an overall trend.
- Freeze-free season length was short in the early 20th century, long in the 1930s, moderately short from the 1950s through the 1980s, and long since about 1990. Freeze-free season lengths during 1991-2010 average about 11 days longer than during 1961-1990.

The climate characteristics simulated by climate models for the two emissions scenarios have the following key features:

- CMIP3 models indicate that temperature changes across the Northwest are statistically significant for all three future time periods and both emissions scenarios. Increases in temperature show relatively little spatial variation for all three future time periods, although increases along the coast are generally less than those inland.
- Overall temperature increases are simulated to be similar in magnitude for the high and low emissions scenarios for the near future, whereas late in the 21st century, the high emissions scenario indicates about twice the amount of warming. Seasonal warming shows similar patterns in all seasons, with the greatest warming simulated in summer and winter.
- The range of model-simulated temperature changes is substantial, indicating substantial uncertainty in the magnitude of warming associated with each scenario. However, in each model simulation, the warming is unequivocal and large compared to historical variations. This is also true for all of the derived temperature variables described below.
- The number of days with a maximum temperature exceeding 95°F is simulated to increase the most (more than 12 days) in the southeast of the region. The average annual longest string of days with such high temperatures increases by up to 10 days in southern Idaho, and generally 0-4 days in the rest of the region (for the A2 scenario at mid-century).
- The number of days with a minimum temperature below 10°F is simulated to decrease by 10-30 days in inland regions (for the A2 scenario at mid-century). There is little or no change in coastal regions because they are currently very rare in those areas. Decreases in the number of days with a minimum temperature below 32 °F are more than 30 days in much of the central and eastern portions of the region. The greatest decreases (more than 40 days) occur in high elevation areas.
- The freeze-free period throughout the Northwest region is simulated to increase by 25-35 days across much of the region (for the A2 scenario at mid-century). The largest increases (more than 40 days) occur west of the Cascade Mountains.
- Annual cooling degree days are simulated to increase throughout the region, with the largest increases (up to 400) occurring in southern Idaho (for the A2 scenario at mid-century). Increases of 100-300 cooling degree days are expected across the majority of the rest of the region. Annual heating degree days are simulated to decrease by at least 1,000 across the majority of the region, with the exception of areas along the Oregon coast. The largest decreases (up to 1,600) occur in central and eastern Idaho.
- The majority of the region is simulated to experience an increase in average annual precipitation for all three future time periods and both emissions scenarios. The largest increases are expected in Washington and northern Idaho and Oregon. Models are mostly in agreement that precipitation will increase under the low (B1) emissions scenario; however, they do not agree on the sign of the changes in the southwest under the high (A2) emissions scenario.
- The majority of models simulate increases in winter and fall precipitation, but decreases in summer precipitation. In spring, the majority indicate a decrease for the high (A2) emissions scenario, but an increase for the low (B1) scenario. However, the range of model-simulated precipitation changes is considerably larger than the multi-model mean change. Thus, there is great uncertainty associated with future precipitation changes in these scenarios.

- Increases in the average annual number of days with precipitation exceeding 1 inch are simulated for most regions, with the greatest increases (greater than 40%) occurring east of the Cascade Mountains (for the A2 scenario at mid-century). Changes are statistically significant only for small areas in central Washington and Oregon.
- All areas are simulated to see an increase in the maximum number of consecutive days with little or no precipitation (less than 0.1 inches), the greatest being up to 15 days in western Oregon (for the A2 scenario at mid-century). Most other areas are expected to see annual increases of up to 9 days. These increases are statistically significant in most areas.
- Most models do not indicate a statistically significant change in decadal-average temperature (with respect to 2001-2010) for the near future; however, as the time period increases, a greater number of models simulate statistically significant temperature changes, with all being significant at the 95% confidence level by 2055 (for the high emissions scenario).
- Most of the modeled values of decadal precipitation change are not statistically significant, with respect to 2001-2010, out to 2091-2099.

A comparison of model simulations of the 20th century with observations indicates the following:

- The overall observed rate of warming is simulated rather well by the CMIP3 models for annual temperature. For seasonal temperatures, there are a few periods when observed temperatures are outside the range of the model simulations. However, even for seasonal temperatures, the overall observed rate of warming is simulated rather well by the CMIP3 models. Simulations of temperature in the 21st century indicate that future warming is much larger than the observed and simulated values for the 20th century.
- The variability in observed precipitation change tends to be somewhat higher than that of the models.

5. REFERENCES

AchutaRao, K., and K.R. Sperber, 2002: Simulation of the El Niño Southern Oscillation: Results from the Coupled Model Intercomparison Project. *Clim. Dyn.*, **19,** 191–209.

Allan, J., and P. Komar, 2006: Climate controls on US West Coast erosion processes. *J. Coastal Res.*, **22,** 511-529.

Arakawa, A., 2004: The cumulus parameterization problem: Past, present, and future. *J. Climate,* **17**, 2493-2525.

Bader D. C., C. Covey, W. J. Gutowski Jr., I. M. Held, K. E. Kunkel, R. L. Miller, R. T. Tokmakian, and M. H. Zhang, 2008: *Climate models: An Assessment of Strengths and Limitations*. U.S. Climate Change Science Program Synthesis and Assessment Product 3.1. Department of Energy, Office of Biological and Environmental Research, 124 pp.

Bumbaco, K. A., and P. W. Mote, 2010: Three recent flavors of drought in the Pacific Northwest. *J. Appl. Meteorol. Climatol.*, **49,** 2058-2068.

Daly, C., W. P. Gibson, G. H. Taylor, G. L. Johnson, and P. Pasteris, 2002: A knowledge-based approach to the statistical mapping of climate. *Clim. Res.*, **22,** 99-113.

Dufresne, J.-L., and S. Bony. 2008: An assessment of the primary sources of spread of global warming estimates from coupled ocean–atmosphere models. *J. Climate*, **21**, 5135-5144.

Fall, S., A. Watts, J. Nielsen-Gammon, E. Jones, D. Niyogi, J. R. Christy, and R. A. Pielke Sr, 2011: Analysis of the impacts of station exposure on the US Historical Climatology Network temperatures and temperature trends. *J. Geophys. Res.*, **116,** D14120.

Gedalof, Z., D. L. Peterson, and N. J. Mantua, 2004: Columbia River flow and drought since 1750. *J. Am. Water Resour. As.*, **40,** 1579-1592.

Hayhoe, K., and Coauthors, 2004: Emission pathways, climate change, and impacts on California. *P. Natl. Acad. Sci. USA*, **101,** 12422-12427.

Hayhoe, K., and Coauthors, 2008: Regional climate change projections for the Northeast USA. *Mitig. Adapt. Strateg. Glob. Change*, **13,** 425-436.

Hayhoe, K. A., 2010: A standardized framework for evaluating the skill of regional climate downscaling techniques. Ph.D. thesis, University of Illinois, 153 pp. [Available online at https://www.ideals.illinois.edu/handle/2142/16044.]

Hubbard, K., and X. Lin, 2006: Reexamination of instrument change effects in the US Historical Climatology Network. *Geophys. Res. Lett.*, **33,** L15710.

IPCC, 2000: *Special Report on Emissions Scenarios: A Special Report of Working Group III of the Intergovernmental Panel on Climate Change*, N. Nakicenovic, and R. Swart, Eds., Cambridge University Press, 570 pp.

——, 2007: *Climate Change 2007: Synthesis Report. Contribution of Working Groups I, II and III to the Fourth Assessment Report of the Intergovernmental Panel on Climate Change*, Pachauri, R. K, and Reisinger, A., Eds., IPCC, 104 pp.

——, cited 2012: IPCC Data Distribution Centre. [Available online at http://www.ipcc-data.org/ddc_co2.html.]

Jones, P. D., P. Y. Groisman, M. Coughlan, N. Plummer, W. C. Wang, and T. R. Karl, 1990: Assessment of urbanization effects in time series of surface air temperature over land. *Nature*, **347,** 169-172.

Karl, T. R., C. N. Williams Jr, P. J. Young, and W. M. Wendland, 1986: A model to estimate the time of observation bias associated with monthly mean maximum, minimum and mean temperatures for the United States. *J. Appl. Meteorol.*, **25,** 145-160.

Karl, T. R., H. F. Diaz, and G. Kukla, 1988: Urbanization: Its detection and effect in the United States climate record. *J. Climate*, **1,** 1099-1123.

Karl, T. R., J. M. Melillo, and T. C. Peterson, Eds, 2009: *Global Climate Change Impacts in the United States.* Cambridge University Press, 188 pp.

Knutti, R., 2010: The end of model democracy? *Climatic Change*, **102,** 395-404.

Komar, P. D., and S. M. Shih, 1993: Cliff erosion along the Oregon Coast: A tectonic-sea level imprint plus local controls by beach processes. *J. Coastal Res.***,** 747-765.

LSU, cited 2012: Climate Trends. [Available online at http://charts.srcc.lsu.edu/trends/.]

Mass, C., 2008: *The weather of the Pacific Northwest.* Univ of Washington Press, 281 pp.

Maurer, E. P., A. W. Wood, J. C. Adam, D. P. Lettenmaier, and B. Nijssen, 2002: A long-term hydrologically based dataset of land surface fluxes and states for the conterminous United States. *J. Climate*, **15,** 3237–3251.

Meehl, G. A., W. M. Washington, T. M. L. Wigley, J. M. Arblaster, and A. Dai, 2003: Solar and greenhouse gas forcing and climate response in the twentieth century. *J. Climate*, **16,** 426-444.

Meehl, G. A., and Coauthors, 2007: Global climate projections. *Climate Change 2007: The Physical Basis. Contribution of Working Group I to the Fourth Assessment Report of the Intergovernmental Panel on Climate Change*, Solomon, S., D. Qin, M. Manning, Z. Chen, M. Marquis, K.B. Averyt, M. Tignor, and H.L. Miller, Eds., Cambridge University Press, 747-845.

Menne, M. J., C. N. Williams, and R. S. Vose, 2009: The US Historical Climatology Network monthly temperature data, version 2. *Bull. Am. Meteorol. Soc.*, **90,** 993-1007.

Menne, M. J., C. N. Williams, and M. A. Palecki, 2010: On the reliability of the U.S. surface temperature record. *J. Geophys. Res.*, **115,** D11108.

Monahan, A.H., and A. Dai, 2004: The spatial and temporal structure of ENSO nonlinearity. *J. Climate*, **17,** 3026–3036.

NARCCAP, cited 2012: North American Regional Climate Change Assessment Program. [Available online at http://www.narccap.ucar.edu/.]

NCDC, cited 2012a: NCDC Palmer Drought Indices. [Available online at www.ncdc.noaa.gov/temp-and-precip/drought/historical-palmers.php.]

——, cited 2012b: NOAA's 1980-2010 Climate Normals. [Available online at http://www.ncdc.noaa.gov/oa/climate/normals/usnormals.html.]

Neiman, P. J., F. M. Ralph, G. A. Wick, J. D. Lundquist, and M. D. Dettinger, 2008: Meteorological characteristics and overland precipitation impacts of atmospheric rivers affecting the west

coast of North America based on eight years of SSM/I satellite observations. *J. Hydrometeorol.*, **9,** 22-47.

NOAA, cited 2012a: Cooperative Observer Program. [Available online at http://www.nws.noaa.gov/om/coop/.]

——, cited 2012b: NCEP/DOE AMIP-II Reanalysis. [Available online at http://www.cpc.ncep.noaa.gov/products/wesley/reanalysis2/.]

Norton, C. W., P.-S. Chu, and T. A. Schroeder, 2011: Projecting changes in future heavy rainfall events for Oahu, Hawaii: A statistical downscaling approach. *J. Geophys. Res.*, **116,** D17110.

NRC, 2004: *Endangered and Threatened Fishes in the Klamath River Basin: Causes of Decline and Strategies for Recovery.* National Academies Press, 398 pp.

——, 2008: *Hydrology, Ecology, and Fishes of the Klamath River Basin.* National Academies Press, 272 pp.

NWS, 1993: Cooperative Program Operations. National Weather Service Observing Handbook No. 6, 56 pp. [Available online at http://www.srh.noaa.gov/srh/dad/coop/coophb6.pdf.]

Overland, J. E., M. Wang, N. A. Bond, J. E. Walsh, V. M. Kattsov, and W. L. Chapman, 2011: Considerations in the selection of global climate models for regional climate projections: The Arctic as a case study. *J. Climate*, **24,** 1583-1597.

PCMDI, cited 2012: CMIP3 Climate Model Documentation, References, and Links. [Available online at http://www-pcmdi.llnl.gov/ipcc/model_documentation/ipcc_model_documentation.php.]

PNRBC, 1969: *Climatological Handbook. Columbia Basin States: Temperature.* Pacific Northwest River Basins Commission, 540 pp.

PRISM: Parameter Regression on Independent Slopes Method. 30-year means. [Available online at www.prism.oregonstate.edu/.]

Quayle, R. G., D. R. Easterling, T. R. Karl, and P. Y. Hughes, 1991: Effects of recent thermometer changes in the cooperative station network. *Bull. Am. Meteorol. Soc.*, **72,** 1718-1723.

Randall, D.A., and Coauthors, 2007: Climate models and their evaluation. *Climate Change 2007: The Physical Basis. Contribution of Working Group I to the Fourth Assessment Report of the Intergovernmental Panel on Climate Change*, Solomon, S., D. Qin, M. Manning, Z. Chen, M. Marquis, K.B. Averyt, M. Tignor, and H.L. Miller, Eds., Cambridge University Press, 590-662.

Schoonmaker, P. K., B. Von Hagen, and E. C. Wolf, 1997: *The Rain Forests of Home: Profile of a North American Bioregion.* Island Press, 447 pp.

Taylor, G. H., and C. Hannan, 1999: *The Climate of Oregon: From Rain Forest to Desert.* Oregon State University Press, 224 pp.

Taylor, G. H., and R. R. Hatton, 1999: *The Oregon Weather Book: A State of Extremes.* Oregon State University Press, 256 pp.

Tebaldi, C., J. M. Arblaster, and R. Knutti, 2011: Mapping model agreement on future climate projections. *Geophys. Res. Lett.*, **38,** L23701.

U.S. Census Bureau, cited 2011: Metropolitan and Micropolitan Statistical Areas. [Available online at http://www.census.gov/popest/data/metro/totals/2011/.]

Vose, R. S., C. N. Williams, Jr., T. C. Peterson, T. R. Karl, and D. R. Easterling, 2003: An evaluation of the time of observation bias adjustment in the U.S. Historical Climatology Network. *Geophys. Res. Lett.*, **30,** 2046.

Wilby, R. L., and T. Wigley, 1997: Downscaling general circulation model output: a review of methods and limitations. *Prog. Phys. Geog.*, **21,** 530.

Williams, C. N., M. J. Menne, and P. W. Thorne, 2011: Benchmarking the performance of pairwise homogenization of surface temperatures in the United States. *J. Geophys. Res.*, **52,** 154-163.

6. ACKNOWLEDGEMENTS

6.1. Regional Climate Trends and Important Climate Factors

Document and graphics support was provided by Brooke Stewart of the Cooperative Institute for Climate and Satellites (CICS), and by Fred Burnett and Clark Lind of TBG Inc. Analysis support was provided by Russell Vose of NOAA's National Climatic Data Center (NCDC).

6.2. Future Regional Climate Scenarios

We acknowledge the modeling groups, the Program for Climate Model Diagnosis and Intercomparison (PCMDI) and the WCRP's Working Group on Coupled Modelling (WGCM) for their roles in making available the WCRP CMIP3 multi-model dataset. Support of this dataset is provided by the Office of Science, U.S. Department of Energy. Analysis of the CMIP3 GCM simulations was provided by Michael Wehner of the Lawrence Berkeley National Laboratory, and by Jay Hnilo of CICS. Analysis of the NARCCAP simulations was provided by Linda Mearns and Seth McGinnis of the National Center for Atmospheric Research, and by Art DeGaetano and William Noon of the Northeast Regional Climate Center. Additional programming and graphical support was provided by Byron Gleason of NCDC, and by Andrew Buddenberg of CICS.

A partial listing of reports appears below:

NESDIS 102 **NOAA Operational Sounding Products From Advanced-TOVS Polar Orbiting Environmental Satellites. Anthony L. Reale, August 2001.**

NESDIS 103 **GOES-11 Imager and Sounder Radiance and Product Validations for the GOES-11 Science Test. Jaime M. Daniels and Timothy J. Schmit, August 2001.**

NESDIS 104 **Summary of the NOAA/NESDIS Workshop on Development of a Coordinated Coral Reef Research and Monitoring Program. Jill E. Meyer and H. Lee Dantzler, August 2001.**

NESDIS 105 **Validation of SSM/I and AMSU Derived Tropical Rainfall Potential (TRaP) During the 2001 Atlantic Hurricane Season. Ralph Ferraro, Paul Pellegrino, Sheldon Kusselson, Michael Turk, and Stan Kidder, August 2002.**

NESDIS 106 **Calibration of the Advanced Microwave Sounding Unit-A Radiometers for NOAA-N and NOAA-N=. Tsan Mo, September 2002.**

NESDIS 107 **NOAA Operational Sounding Products for Advanced-TOVS: 2002. Anthony L. Reale, Michael W. Chalfant, Americo S. Allegrino, Franklin H. Tilley, Michael P. Ferguson, and Michael E. Pettey, December 2002.**

NESDIS 108 **Analytic Formulas for the Aliasing of Sea Level Sampled by a Single Exact-Repeat Altimetric Satellite or a Coordinated Constellation of Satellites. Chang-Kou Tai, November 2002.**

NESDIS 109 **Description of the System to Nowcast Salinity, Temperature and Sea nettle (*Chrysaora quinquecirrha*) Presence in Chesapeake Bay Using the Curvilinear Hydrodynamics in3-Dimensions (CH3D) Model. Zhen Li, Thomas F. Gross, and Christopher W. Brown, December 2002.**

NESDIS 110 **An Algorithm for Correction of Navigation Errors in AMSU-A Data. Seiichiro Kigawa and Michael P. Weinreb, December 2002.**

NESDIS 111 **An Algorithm for Correction of Lunar Contamination in AMSU-A Data. Seiichiro Kigawa and Tsan Mo, December 2002.**

NESDIS 112 **Sampling Errors of the Global Mean Sea Level Derived from Topex/Poseidon Altimetry. Chang-Kou Tai and Carl Wagner, December 2002.**

NESDIS 113 **Proceedings of the International GODAR Review Meeting: Abstracts. Sponsors: Intergovernmental Oceanographic Commission, U.S. National Oceanic and Atmospheric Administration, and the European Community, May 2003.**

NESDIS 114 **Satellite Rainfall Estimation Over South America: Evaluation of Two Major Events. Daniel A. Vila, Roderick A. Scofield, Robert J. Kuligowski, and J. Clay Davenport, May 2003.**

NESDIS 115 **Imager and Sounder Radiance and Product Validations for the GOES-12 Science Test. Donald W. Hillger, Timothy J. Schmit, and Jamie M. Daniels, September 2003.**

NESDIS 116 **Microwave Humidity Sounder Calibration Algorithm. Tsan Mo and Kenneth Jarva, October 2004.**

NESDIS 117 **Building Profile Plankton Databases for Climate and EcoSystem Research. Sydney Levitus, Satoshi Sato, Catherine Maillard, Nick Mikhailov, Pat Cadwell, Harry Dooley, June 2005.**

NESDIS 118 **Simultaneous Nadir Overpasses for NOAA-6 to NOAA-17 Satellites from 1980 and 2003 for the Intersatellite Calibration of Radiometers. Changyong Cao, Pubu Ciren, August 2005.**

NESDIS 119 **Calibration and Validation of NOAA 18 Instruments. Fuzhong Weng and Tsan Mo, December 2005.**

NESDIS 120 **The NOAA/NESDIS/ORA Windsat Calibration/Validation Collocation Database. Laurence Connor, February 2006.**

NESDIS 121 **Calibration of the Advanced Microwave Sounding Unit-A Radiometer for METOP-A. Tsan Mo, August 2006.**

NESDIS 122 JCSDA Community Radiative Transfer Model (CRTM). Yong Han, Paul van Delst, Quanhua Liu, Fuzhong Weng, Banghua Yan, Russ Treadon, and John Derber, December 2005.

NESDIS 123 Comparing Two Sets of Noisy Measurements. Lawrence E. Flynn, April 2007.

NESDIS 124 Calibration of the Advanced Microwave Sounding Unit-A for NOAA-N'. Tsan Mo, September 2007.

NESDIS 125 The GOES-13 Science Test: Imager and Sounder Radiance and Product Validations. Donald W. Hillger, Timothy J. Schmit, September 2007.

NESDIS 126 A QA/QC Manual of the Cooperative Summary of the Day Processing System. William E. Angel, January 2008.

NESDIS 127 The Easter Freeze of April 2007: A Climatological Perspective and Assessment of Impacts and Services. Ray Wolf, Jay Lawrimore, April 2008.

NESDIS 128 Influence of the ozone and water vapor on the GOES Aerosol and Smoke Product (GASP) retrieval. Hai Zhang, Raymond Hoff, Kevin McCann, Pubu Ciren, Shobha Kondragunta, and Ana Prados, May 2008.

NESDIS 129 Calibration and Validation of NOAA-19 Instruments. Tsan Mo and Fuzhong Weng, editors, July 2009.

NESDIS 130 Calibration of the Advanced Microwave Sounding Unit-A Radiometer for METOP-B. Tsan Mo, August 2010.

NESDIS 131 The GOES-14 Science Test: Imager and Sounder Radiance and Product Validations. Donald W. Hillger and Timothy J. Schmit, August 2010.

NESDIS 132 Assessing Errors in Altimetric and Other Bathymetry Grids. Karen M. Marks and Walter H.F. Smith, January 2011.

NESDIS 133 The NOAA/NESDIS Near Real Time CrIS Channel Selection for Data Assimilation and Retrieval Purposes. Antonia Gambacorta, Chris Barnet, Walter Wolf, Thomas King, Eric Maddy, Murty Divakarla, Mitch Goldberg, April 2011.

NESDIS 134 Report from the Workshop on Continuity of Earth Radiation Budget (CERB) Observations: Post-CERES Requirements. John J. Bates and Xuepeng Zhao, May 2011.

NESDIS 135 Averaging along-track altimeter data between crossover points onto the midpoint gird: Analytic formulas to describe the resolution and aliasing of the filtered results. Chang-Kou Tai, August 2011.

NESDIS 136 Separating the Standing and Net Traveling Spectral Components in the Zonal-Wavenumber and Frequency Spectra to Better Describe Propagating Features in Satellite Altimetry. Chang-Kou Tai, August 2011.

NESDIS 137 Water Vapor Eye Temperature vs. Tropical Cyclone Intensity. Roger B. Weldon, August 2011.

NESDIS 138 Changes in Tropical Cyclone Behavior Related to Changes in the Upper Air Environment. Roger B. Weldon, August 2011.

NESDIS 139 Computing Applications for Satellite Temperature Datasets: A Performance Evaluation of Graphics Processing Units. Timothy F.R. Burgess and Scott F. Heron, December 2011.

NESDIS 140 Microburst Nowcasting Applications of GOES. Kenneth L. Pryor, September 2011.

NESDIS 141 The GOES-15 Science Test: Imager and Sounder Radiance and Product Validations. Donald W. Hillger and Timothy J. Schmit, November 2011.

NOAA SCIENTIFIC AND TECHNICAL PUBLICATIONS

The National Oceanic and Atmospheric Administration **was established as part of the Department of Commerce on October 3, 1970. The mission responsibilities of NOAA are to assess the socioeconomic impact of natural and technological changes in the environment and to monitor and predict the state of the solid Earth, the oceans and their living resources, the atmosphere, and the space environment of the Earth.**

The major components of NOAA regularly produce various types of scientific and technical information in the following types of publications

PROFESSIONAL PAPERS – Important definitive research results, major techniques, and special investigations.

CONTRACT AND GRANT REPORTS – Reports prepared by contractors or grantees under NOAA sponsorship.

ATLAS – Presentation of analyzed data generally in the form of maps showing distribution of rainfall, chemical and physical conditions of oceans and atmosphere, distribution of fishes and marine mammals, ionospheric conditions, etc.

TECHNICAL SERVICE PUBLICATIONS – Reports containing data, observations, instructions, etc. A partial listing includes data serials; prediction and outlook periodicals; technical manuals, training papers, planning reports, and information serials; and miscellaneous technical publications.

TECHNICAL REPORTS – Journal quality with extensive details, mathematical developments, or data listings.

TECHNICAL MEMORANDUMS – Reports of preliminary, partial, or negative research or technology results, interim instructions, and the like.

U.S. DEPARTMENT OF COMMERCE
National Oceanic and Atmospheric Administration
National Environmental Satellite, Data, and Information Service
Washington, D.C. 20233